Atomic Data and Nuclear Data Tables 157 (2024) 101636

Contents lists available at ScienceDirect

Atomic Data and Nuclear Data Tables

journal homepage: www.elsevier.com/locate/adt

Radiative decay rates for electric dipole transitions in doubly-, trebly- and quadruply-charged rhenium ions (Re III – V) of interest to nuclear fusion research and astrophysical spectra analyses

Maxime Brasseur [a], Sébastien Gamrath [a], Pascal Quinet [a,b,*]

[a] Physique Atomique et Astrophysique, Université de Mons, B-7000 Mons, Belgium
[b] IPNAS, Université de Liège, B-4000 Liège, Belgium

A B S T R A C T

A new set of radiative parameters (oscillator strengths and transition probabilities) was obtained for the most intense spectral lines in Re III, Re IV and Re V ions. These parameters were calculated using two independent methods, namely the pseudo-relativistic Hartree–Fock approach including core-polarization effects (HFR+CPOL) and the fully relativistic multiconfiguration Dirac–Hartree–Fock (MCDHF) approach. Detailed comparisons between the results obtained from these two methods as well as with the few data available in the literature allowed us to estimate the precision of the calculations carried out. The radiative parameters reported in the present paper concern a total of 368 electric dipole (E1) transitions in Re III, Re IV and Re V covering the ultraviolet spectral region from 655 to 2135 Å. These are of great interest for the analysis of spectra emitted by plasmas in nuclear fusion reactors, such as ITER where rhenium can be produced by neutron bombardment of the tungsten divertor wall, as well as for the investigation of astrophysical spectra observed from chemically peculiar stars or from kilonovae where rhenium can be produced by the nucleosynthesis r-process.

* Corresponding author at: Physique Atomique et Astrophysique, Université de Mons, B-7000 Mons, Belgium.
E-mail address: pascal.quinet@umons.ac.be (P. Quinet).

https://doi.org/10.1016/j.adt.2024.101636
Received 30 November 2023; Received in revised form 26 January 2024; Accepted 26 January 2024
Available online 13 February 2024

Contents

1. Introduction

It is now well established that, due to its high melting point, its low sputtering rate and its strength at high temperatures, tungsten will be one of the main divertor components of the ITER nuclear fusion reactor, see e.g. [1–3]. When deuterium–tritium fusion will take place, tungsten atoms will be torn from the reactor wall and will penetrate the plasma where they will contribute to the radiation emission. In addition, very energetic neutrons will strike the walls of the reactor and cause the transmutation of tungsten atoms by irradiation, from which the primary transmutation products will be rhenium, osmium and tantalum. In particular, simulations revealed that, after 5-year irradiation under first wall fusion power-plant conditions in ITER, Re, Os and Ta would reach concentrations of 3.8 × 10^4 appm (3.8 at.%), 1.38 × 10^4 appm (1.4 at.%) and 8.09 × 10^3 appm (0.81 at.%), respectively [4]. As with tungsten, during fusion operations, Re, Os and Ta atoms will be torn from the reactor wall and enter the plasma where they will constitute impurities contributing also to the energy loss by radiation. However, the electromagnetic light emitted by these elements can be used as well for plasma temperature and density diagnostics from the analysis of their spectra in all ionization stages. Therefore the radiative properties of these ions have potential important applications in this field of research.

If the spectroscopic data of tungsten ions have already been the subject of many studies, much less work was carried out with regard to rhenium, osmium and tantalum ions. So for example, if we are only interested in radiative decay parameters of the first five charge states (I–V), we can note that the NIST atomic transition probability bibliographic database [5] contains 53 references for W I–V ions, 24 references for Re I–V ions, 24 references for Os I–V ions, and 31 references for Ta I–V ions. Moreover, when looking into more details, we notice that the radiative properties of III–V spectra have been less investigated than those of I–II spectra in the case of rheniumn osmium and tantalum elements, the only transition rates available being published by Azarov and Gayasov [6] for Re III, Azarov and Gayasov [7] for Re IV, Azarov and Gayasov [8] for Re V, Azarov [9] and Azarov et al. [10] for Os III, Ryabtsev et al. [11] for Os IV, Azarov et al. [12] for Os V, Azarov et al. [13] and Fivet et al. [14] for Ta III, Migdalek and Baylis [15] and Safronova et al. [16] for Ta IV, and Migdalek and Siegel [17,18] for Ta V.

The main goal of the present work is to provide new radiative data for Re III–V ions for which recent analyses of the energy level structures have been published [6–8] thus allowing us to perform semi-empirical calculations based on the pseudo-relativistic Hartree–Fock (HFR) method including core-polarization effects, giving rise to the HFR+CPOL approach. In order to estimate the precision of the HFR+CPOL results obtained, the latter were compared to calculations carried out using the purely relativistic Multiconfiguration Dirac–Hartree–Fock (MCDHF) method. This led us to obtain a consistent set of transition probabilities and oscillator strengths for the most intense electric dipole lines in doubly-, trebly-, and quadruply-ionized rhenium that can be used for the diagnosis of plasmas produced in future nuclear fusion reactors. From an astrophysical point of view, Re ions are also of great interest as they are among the chemical species abundantly produced in kilonovae following neutron star mergers. It was indeed shown that elements with an open d-subshell, as is the case for Re III–V ions, have the second largest contributions to kilonova opacities after the open-f subshell elements, see e.g. [19,20]. In addition, rhenium ions were also observed in the spectra of chemically peculiar stars in which such heavy elements are produced by nucleosynthesis processes [21–23].

2. Available atomic data

A few years ago, detailed and comprehensive investigations of Re III, Re IV and Re V spectra were published by Azarov and Gayasov in three different papers [6–8]. In these works, new spectrograms were photographed in the wavelength range between 500 and 2100 Å at the Troitsk Institute of Spectroscopy in Russia. The spectra of rhenium in different ionization stages were obtained on a 6.65 m normal incidence spectrograph with a plate factor of 1.25 Å/mm. The sources used were vacuum triggered and sliding sparks with operating voltage of 4.0–4.5 kV. The sparks were fed from a low-inductance 10 μF capacitor. The photographic plates were analyzed using a comparator controlled by the system for automatic processing of photo-spectrograms [24] while impurity lines of oxygen, carbon, nitrogen, aluminum and silicon present in the spectrograms were used as standards in the initial wavelength interpolation procedure [25].

More specifically, if we look at rhenium ions individually, the works of Azarov and Gayasov led to the following results. For Re III [6], 1305 spectral lines were classified in the 1017–2074 Å wavelength region allowing the identification of 70 energy levels in the $5d^5$ and $5d^46s$ even configurations, and 161 levels in the $5d^46p$ and $5d^36s6p$ odd configurations. For Re IV [7], 975 lines were identified between 786 and 2063 Å as being due to transitions involving 65 levels of the ($5d^4 + 5d^36s$) even configuration system and 95 levels of the $5d^36p$ odd configuration. In the case of Re V [8], 398 lines were observed in the 597–2053 Å spectral range leading to the determination of 34 and 45 energy levels belonging to the $5d^3$, $5d^26s$ even configurations and to the $5d^26p$ odd configuration, respectively. Moreover, in all these studies, the orthogonal operators technique in which the radial parameters were determined by the least-squares fit to the observed levels, was used to calculate the level structure, the LS-coupling compositions as well as transition probabilities for all the experimentally classified lines.

3. HFR+CPOL calculations

The first computational procedure used in the present work was based on the pseudo-relativistic Hartree–Fock (HFR) approach, initially introduced by Cowan [26] in which the core-polarization effects were included, giving rise to the HFR+CPOL method, as developed by the Atomic and Astrophysics group at Mons University (see e.g. [27,28]). The physical models adopted for the atomic structure calculations in Re III, Re IV and Re V ions were similar to those considered in our previous studies focused on the isoelectronic tungsten ions, namely W II [29], W III [30], and W IV [31], respectively.

More precisely, for Re III, the valence–valence interactions were taken into account by explicitly including the following configurations in the calculations : $5d^5$, $5d^46s$, $5d^47s$, $5d^48s$, $5d^36s^2$, $5d^36s7s$, $5d^36s8s$, $5d^46d$, $5d^36s6d$, $5d^26s^26d$, $5d^36p^2$ for the even parity, and $5d^46p$, $5d^47p$, $5d^48p$, $5d^36s6p$, $5d^36s7p$, $5d^36s8p$, $5d^26s^26p$, $5d^26p^3$ for the odd parity. The core-polarization corrections were estimated by considering a $4f^{14}5d^2$ Yb-like ionic core surrounded by 3 electrons. This led us to use a value of the dipole polarizability corresponding to Re VI, i.e. α_d = 3.80 $a_0{}^3$ according to an extrapolation performed using the data reported by Fraga et al. [32] for the first ions along the Yb isoelectronic sequence and a cut-off radius, r_c, equals to 1.66 a_0, as deduced from our HFR calculations for the average value $<r_{5d}>$ of the outermost core orbital.

In the case of Re IV, the $5d^4$, $5d^36s$, $5d^37s$, $5d^38s$, $5d^26s^2$, $5d^26s7s$, $5d^26s8s$, $5d^36d$, $5d^26s6d$, $5d6s^26d$, $5d^26p^2$ even-parity, and the $5d^36p$, $5d^37p$, $5d^38p$, $5d^26s6p$, $5d^26s7p$, $5d^26s8p$, $5d6s^26p$ odd-parity configurations were included in the HFR model. The $4f^{14}5d$ Tm-like ionic core-polarization effects were then computed using α_d = 3.50 a_0^3 deduced from an extrapolation of the data published in [32] for the first ions along the Tm isoelectronic sequence and $r_c = < r_{5d} >$ = 1.59 a_0.

Finally, for Re V, we considered for the core-polarization potential a $4f^{14}$ erbium-like Re VIII ionic core surrounded by three valence electrons whose correlations were explicitly introduced by the following interacting configurations: $5d^3$, $5d^26s$, $5d6s^2$, $5d^26d$, $5d6p^2$, $5d6d^2$, $5d5f^2$, $5d6f^2$, 5d6s6d, 5d6p5f, 5d6p6f, 5d5f6f, $6s^26d$, $6s6p^2$, $6p^26d$, $6s6d^2$, $6d^3$, $6s5f^2$, $6d5f^2$, $6s6f^2$, $6d6f^2$ (even parity) and $5d^26p$, $5d^25f$, $5d^26f$, 5d6s6p, 5d6s5f, 5d6s6f, 5d6p6d, 5d6d5f, 5d6d6f, $6s^26p$, $6s^25f$, $6s^26f$, $6p^25f$, $6p^26f$, $6p^3$, $6p6d^2$, $6d^25f$, $6d^26f$, $6p5f^2$, $6p6f^2$, $5f^26f$, $5f6f^2$ (odd parity). The core-polarization parameters were chosen such that α_d = 2.30 a_0^3 and $r_c = < r_{5p} >$ = 1.17 a_0, the dipole polarizability being deduced from an extrapolation of the values given in [32] for the first ions of the Er isoelectronic sequence.

For each rhenium ion considered, a semi-empirical adjustment of radial parameters was performed in order to reduce as much as possible the differences between the HFR+CPOL calculated energy levels and available experimental data. In particular, all the energy levels established by Azarov and Gayasov within the $5d^5$, $5d^46s$, $5d^46p$, $5d^36s6p$ configurations of Re III [6], within the $5d^4$, $5d^36s$, $5d^36p$ configurations of Re IV [7], and within the $5d^3$, $5d^26s$, $5d^26p$ configurations of Re V [8] were used to fit the average energies (E_{av}), the electrostatic Slater integrals (F^k, G^k), the spin–orbit parameters (ζ_{nl}) and some configuration interaction integrals (R^k) characterizing these configurations. In addition, the quality of the fit was improved by the use of the effective operators parameters α and β, representing corrections to both electrostatic and magnetic single-configuration effects within nd^k subshells, as described by Cowan [26]. Let us also mention that all the F^k, G^k, R^k electrostatic parameters not fitted in the semi-empirical procedure were scaled down by a factor 0.90 while the ζ_{nl} spin–orbit parameters were kept to their *ab initio* values, as also suggested by Cowan [26]. The fitted values of the radial parameters obtained in the present work are given in Tables 1, 2 and 3 for Re III, Re IV and Re V ions, respectively. Using these parameters, the standard deviations between calculated and experimental levels were found to be 64 cm^{-1} (even parity) and 195 cm^{-1} (odd parity) in Re III, 50 cm^{-1} (even parity) and 190 cm^{-1} (odd parity) in Re IV, 42 cm^{-1} (even parity) and 139 cm^{-1} (odd parity) in Re V. It should be noted that these standard deviations are larger than those obtained from the fits carried out in the same ions by Azarov and Gayasov [6–8], i.e. 32, 55, 18, 40, 13, and 101 cm^{-1}, respectively. This can be explained by the fact that, on top of using additional orthogonal radial parameters, the latter authors used much more limited physical models, including only the $5d^k$, $5d^{k-1}6s$, $5d^{k-2}6s^2$ even- and $5d^{k-1}6p$, $5d^{k-2}6s6p$, $5d^{k-3}6s^26p$ odd-parity configurations (with k = 5,4,3 for Re III, Re IV, Re V) in their semi-empirical HFR calculations, in comparison with the more elaborated configuration interaction models considered in the present work, which generally makes a very precise fit more complicated to achieve. Nevertheless, the accuracy of our least-squares optimization can be considered as very good because the standard deviations obtained do not exceed 0.10% of the energy range covered by the fitted levels, which is well below the upper limit of 1% recommended by Cowan [26].

In Tables 4, 5 and 6, we show the comparison between our HFR+CPOL computed levels and the experimental values taken from the measurements carried out by Azarov and Gayasov for Re III [6], Re IV [7], and Re V [8], respectively. The first three components in LS coupling are also given in these tables. It is worth emphasizing that the eigenvector compositions obtained in the present work, although deduced from more extensive physical models, are very similar to those calculated using the rather limited HFR computational approach used in [6–8]. It should also be noted that most of the levels listed in Tables 4–6 are extremely mixed, these mixtures being systematically much greater in the odd parity than in even parity with average LS-purities of 44% (even) and 27% (odd) for Re III, 60% (even) and 37% (odd) for Re IV and 75% (even) and 46% (odd) for Re V. These strong mixings obviously make the accurate calculation of the radiative transition rates between the states involved extremely complicated, in particular for weak transitions.

4. MCDHF calculations

A second theoretical method used for computing the atomic parameters in Re III–IV ions was the one based on the fully relativistic Dirac–Hartree–Fock (MCDHF) approach [33,34], as implemented in the GRASP2018 code [35], which is the latest version of the General Relativistic Atomic Structure Program (GRASP). High-order relativistic

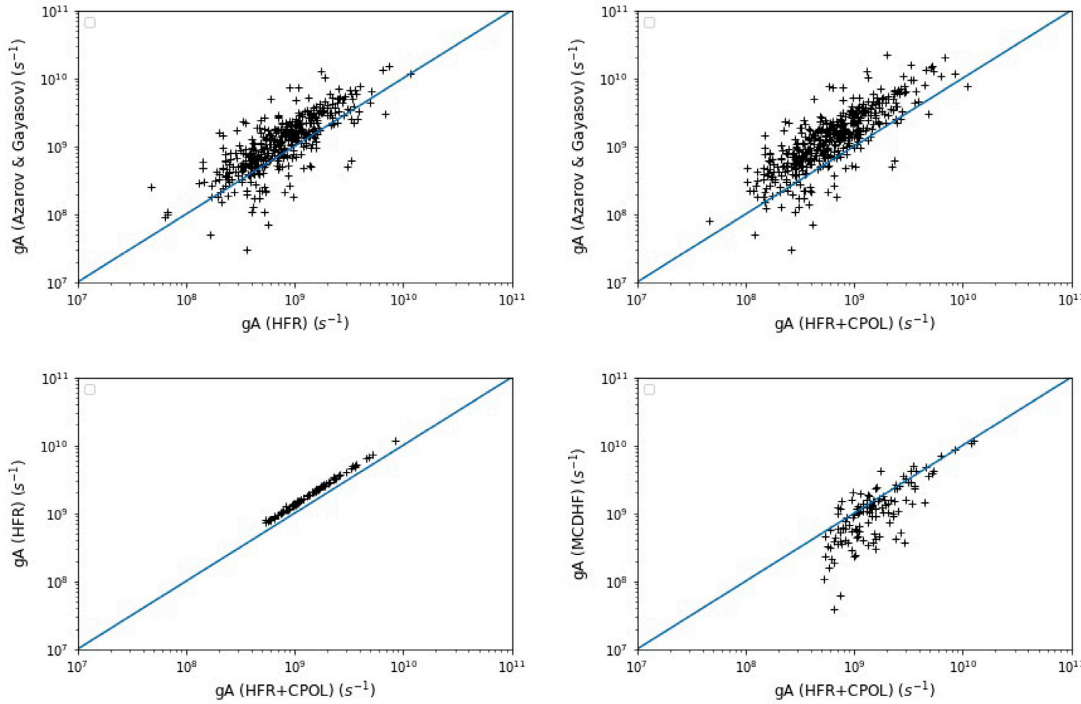

Fig. 1. Comparison between the transition probabilities obtained from different calculations in Re III.

effects, i.e. the Breit interaction, QED self-energy, and vacuum polarization effects were incorporated in the relativistic configuration interaction (RCI) step of the GRASP2018 package. For each rhenium ion, different physical models were applied in order to optimize the wave functions and the atomic structures by gradually increasing the basis of configuration state functions (CSFs), and thus taking more correlations into account.

Valence–valence (VV) models were first elaborated by considering single and double (SD) excitations of valence electrons from a multireference (MR) to a set of active orbitals denoted {*n*s, *n*'p, *n*"d, . . . } where *n*, *n*', *n*", . . . are the maximum principal quantum numbers corresponding to each azimuthal quantum number *l*. More precisely, the MR consisted in $5d^k$, $5d^{k-1}6s$, $5d^{k-2}6s^2$, $5d^{k-1}6p$ and $5d^{k-2}6s6p$ with $k = 5, 4, 3$ for Re III, Re IV, and Re V, respectively. The orbitals 1s–6p were optimized on all the configurations included in the MR. Different VV models were then built by adding SD excitations from the MR to the {6s, 6p, 6d, 6f}, {7s, 7p, 7d, 7f} and {8s, 8p, 8d, 8f} active sets, giving rise to the VV1, VV2 and VV3 models, respectively. In each of these VV models, only the new orbitals were optimized, the other ones being kept to their values obtained before. A VV3+CV model was then built by considering SD excitations from 4f, 5s and 5p core-orbitals to the MR configurations. This gave rise to atomic structure calculations involving a total number of 307 536 CSFs in Re III, 93 819 CSFs in Re IV, and 84 673 CSFs in Re V.

It was verified that the MCDHF energy levels finally obtained in the VV3+CV model were in good agreement with the experimental values, the mean deviation $\Delta E = E_{Exp}$ - E_{MCDHF} being found to be equal to 24 cm^{-1} for Re III, 1763 cm^{-1} for Re IV, and 986 cm^{-1} for Re V. These values represent 0.02%, 1.1% and 0.5% of the energy ranges considered for each ion, respectively. The comparisons between the MCDHF energy levels and the available experimental data taken from [6–8] are given in Tables 7, 8 and 9 in the case of Re III, Re IV and Re V, respectively. In these tables, we also report the HFR+CPOL energy levels taken from Tables 4–6 and we compare the purities obtained in the relativistic jj-coupling to those deduced from the non-relativistic LS-coupling. It is interesting to note that neither of these couplings gives a good general representation of the atomic states, the average purities being found to be very similar when using one or another coupling scheme, namely 35%, 49% and 65% in jj-coupling, in comparison with 36%, 49% and 61% in LS-coupling for the whole set of energy levels considered in Re III, Re IV and Re V, respectively. This shows that the energy levels belonging to the lowest configurations of these three ions are generally as mixed in jj-coupling as in LS-coupling. It is therefore recommended to use as much as possible the LS labeling from Tables 4–6, easier to use and thus better suited than jj-coupling for an unambiguous classification of the levels considered in the present work.

5. Radiative decay parameters

Radiative transition probabilities, gA in s^{-1}, and oscillator strengths in the logarithmic scale, log gf, as computed in our work using the HFR+CPOL and MCDHF methods are reported in Tables 10, 11 and 12 for spectral lines in Re III, Re IV and Re V, respectively. Only the strongest transitions, for which the HFR+CPOL log gf-values are greater than −0.5 for Re III and Re IV and greater than −1.0 for Re V, are listed in these tables. Beyond the fact that it is obviously these intense transitions which are supposed to be most likely observed on the spectra of laboratory and astrophysical plasmas, they are also transitions which were found to be not affected by cancellation effects in our HFR+CPOL calculations, on one hand, and to show a good agreement between the Babushkin and Coulomb gauges in our MCDHF calculations, on the other hand. More precisely, for those transitions, the cancellation factor, CF, as defined by Cowan [26] was found to be systematically greater than 0.05 in the HFR+CPOL computations while the differences between the transition probabilities obtained in the Babushkin and the Coulomb gauges did not exceed 20% in the MCDHF calculations. This represents a guarantee of reliability concerning the results obtained with each of these approaches and listed in Tables 10–12. In the same tables are also given the previously published gA-values for comparison. The latter were obtained by Azarov and Gayasov [6–8] who used, as already mentioned above, the semi-empirical HFR method with rather limited configuration interaction models.

Cross-comparisons between all these sets of results are shown in Figs. 1, 2 and 3 for Re III, Re IV and Re V, respectively. More particularly, in these figures are shown the comparisons between the

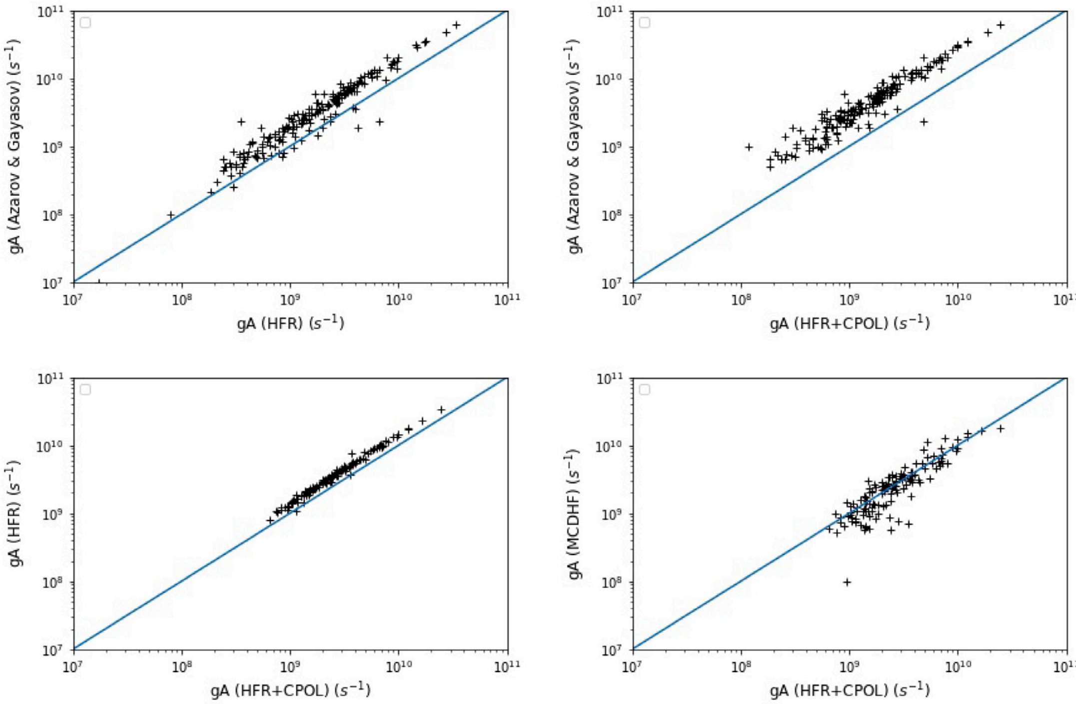

Fig. 2. Comparison between the transition probabilities obtained from different calculations in Re IV.

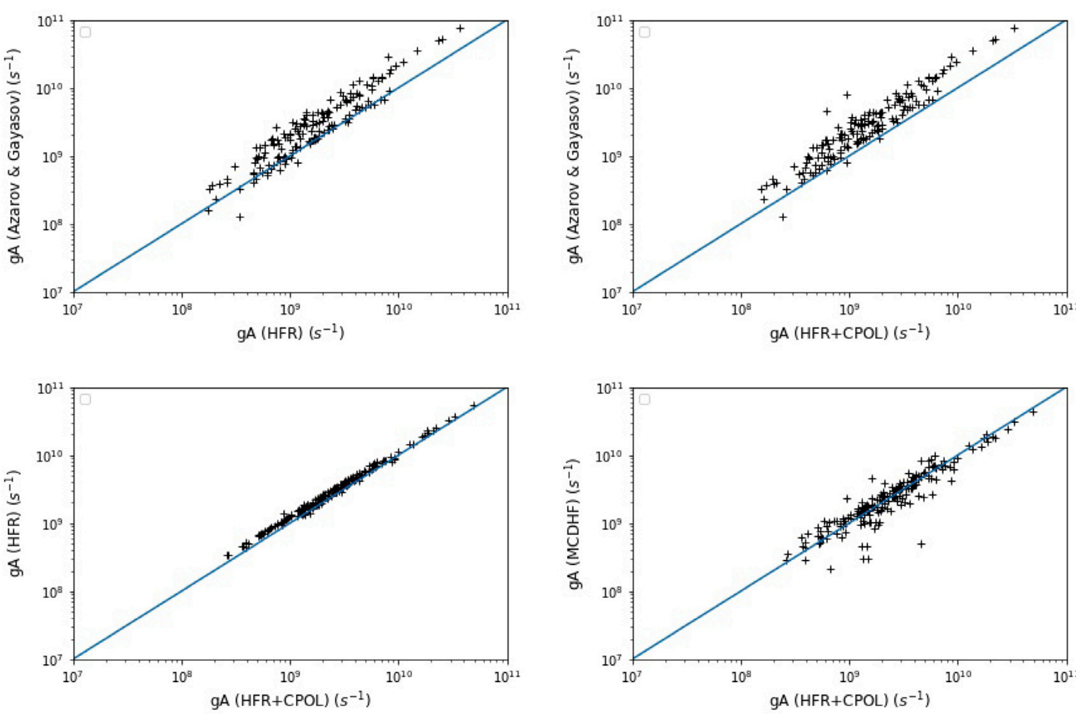

Fig. 3. Comparison between the transition probabilities obtained from different calculations in Re V.

previously published gA-values [6–8] and our HFR and HFR+CPOL values, as well as comparisons between HFR and HFR+CPOL gA-values and comparisons between HFR+CPOL and MCDHF gA-values. After a first look at these figures, we see that the different comparisons present similar behaviors for the three rhenium ions considered. Indeed, for each of these ions, we note that the HFR+CPOL transition probabilities are systematically 15%–20% smaller than the HFR values. This effect was already highlighted in many of our previous studies related to heavy atomic systems when comparing HFR calculations without and with core-polarization contributions, see e.g. [36] and references therein. We also note that both of HFR and HFR+CPOL results are systematically lower than the transition probabilities reported by Azarov and Gayasov [6–8], the latter being however a bit closer to our HFR values obtained without core-polarization effects. In fact, the consideration of such effects in our HFR+CPOL calculations, in addition to much more extended configuration interaction models, led to an average decrease in gA-values of about 25%, 40%, and 30% when compared to the data previously published for Re III [6], Re IV [7], and Re V [8], respectively. Finally, the most important comparisons are those between HFR+CPOL and MCDHF calculations. In fact, we found that the mean ratio gA(HFR+CPOL)/gA(MCDHF) was equal to 1.26 ± 0.33, 1.03 ± 0.26 and 0.94 ± 0.24 for the Re III, Re IV and Re V transitions, respectively. This gives an indication of the accuracy of the decay rates obtained in the present work which can be estimated to be globally of the order of 50% for Re III, 30% for Re IV and 25% for Re V.

Of course, there are transitions for which the differences between our HFR+CPOL and MCDHF calculations are larger than the deviations mentioned above. This is evidenced by the few points that are far from the diagonal line on the bottom right panel of Figs. 1–3. This only concerns a few transitions for which one of the levels (or both levels) is (are) affected by strong mixings in the eigenvector composition. So, for example, for the first Re III line in Table 7 (λ = 1099.606 Å), a discrepancy of a factor of 2.5 is observed between the MCDHF and the HFR+CPOL gA-values. This transition connects the lower even level at 23471 cm^{-1} (J = 4.5) to the upper odd level at 114413 cm^{-1} (J = 3.5). The latter is extremely mixed with its first two components being found to be 20% 5d^{3}6s6p(^{4}P)^{6}P and 11% 5d^{4}6p(^{3}F)^{4}G. A small change in this mixing is likely to generate a significant modification in the line strength characterizing the transition since each component is connected to one of the first two components of the lower even level at 23471 cm^{-1}, namely 76% 5d^{4}6s(^{5}D)^{6}D and 11% 5d^{4}6s(^{3}F)^{4}F by 5d–6p and 6s–6p electric dipole matrix elements that are of the same order of magnitude. More generally, it was verified that all the transitions whose differences between HFP+CPOL and MCDHF gA-values exceed a factor of two in Tables 10–12 involve a lower level and/or an upper level characterized by a very strong mixing in the eigenvector composition.

6. Conclusion

A consistent set of radiative data in Re III–V ions was obtained in this work from calculations carried out using the pseudo-relativistic Hartree–Fock method including core-polarization effects (HFR+CPOL) combined with a semi-empirical adjustment of the radial parameters and the fully relativistic *ab initio* multiconfiguration Dirac–Hartree–Fock (MCDHF) approach. From cross-comparisons between the different theoretical models, the precision of the transition probabilities and oscillator strengths obtained for about 400 intense spectral lines in these ions was estimated to be globally of the order of 50% for Re III, 30% for Re IV and 25% for Re V. These new parameters are likely to be of great interest for the analysis of astrophysical and laboratory plasmas.

CRediT authorship contribution statement

Maxime Brasseur: Investigation. **Sébastien Gamrath:** Investigation. **Pascal Quinet:** Writing – original draft, Supervision, Investigation.

Declaration of competing interest

Pascal Quinet reports financial support was provided by Fund for Scientific Research. Pascal Quinet reports a relationship with Fund for Scientific Research that includes: employment and funding grants. If there are other authors, they declare that they have no known competing financial interests or personal relationships that could have appeared to influence the work reported in this paper.

Data availability

Data will be made available on request.

Acknowledgments

PQ is Research Director of the Belgian National Fund for Scientific Research (F.R.S.-FNRS) whose financial support is greatly appreciated. Part of the atomic calculations were made with computational resources provided by the Consortium des Équipements de Calcul Intensif (CECI), funded by the F.R.S.-FNRS under Grant No. 2.5020.11 and by the Walloon Region of Belgium.

References

[1] R.A. Pitts, S. Carpentier, F. Escourbiac, T. Hirai, V. Komarov, S. Lisgo, A.S. Kukushkin, M. Merola, A. Sashala Naik, R. Mitteau, M. Sugihara, B. Bazylev, P.C. Stangeby, J. Nucl. Mater. 438 (2013) S48.
[2] T. Hirai, S. Panayotis, V. Barabash, C. Amzallag, F. Escourbiac, A. Durocher, M. Merola, J. Linke, Th. Loewenhoff, G. Pintsuk, M. Wirtz, I. Uytdenhouwen, Nucl. Mat. En. 9 (2016) 616.
[3] R.A. Pitts, X. Bonnin, F. Escourbiaca, H. Frerichs, J.P. Gunn, T. Hirai, A.S. Kukushkin, E. Kaveeva, M.A. Miller, D. Moulton, V. Rozhansky, I. Senichenkov, E. Sytova, O. Schmitz, P.C. Stangeby, G. De Temmerman, I. Veselova, S. Wiesen, Nucl. Mat. En. 20 (2019) 100696.
[4] M.R. Gilbert, J.-Ch. Sublet, Nucl. Fusion 51 (2011) 043005.
[5] A. Kramida, Yu. Ralchenko, J. Reader, NIST ASD Team, NIST Atomic Spectra Database, National Institute of Standards and Technology, Gaithersburg, 2023, [https://physics.nist.gov/asd].
[6] V.I. Azarov, R.R. Gayasov, At. Data Nucl. Data Tables 121-122 (2018) 306.
[7] V.I. Azarov, R.R. Gayasov, At. Data Nucl. Data Tables 119 (2018) 218.
[8] V.I. Azarov, R.R. Gayasov, At. Data Nucl. Data Tables 119 (2018) 175.
[9] V.I. Azarov, At. Data Nucl. Data Tables 119 (2018) 193.
[10] V.I. Azarov, W.-Ü.L. Tchang-Brillet, R.R. Gayasov, At. Data Nucl. Data Tables 121-122 (2018) 345.
[11] A.N. Ryabtsev, A.J.J. Raassen, W.-Ü.L. Tchang-Brillet, Y.N. Joshi, P.H.M. Uylings, V.I. Azarov, Phys. Scr. 57 (1998) 82.
[12] V.I. Azarov, A.J.J. Raaseen, Y.N. Joshi, P.H.M. Uylings, A.N. Ryabtsev, Phys. Scr. 56 (1997) 325.
[13] V.I. Azarov, W.-Ü.L. Tchang-Brillet, J.-F. Wyart, F.G. Meijer, Phys. Scr. 67 (2003) 190.
[14] V. Fivet, E. Biémont, L. Engström, H. Lundberg, H. Nilsson, P. Palmeri, P. Quinet, J. Phys. B 41 (2008) 015702.
[15] J. Migdalek, W.E. Baylis, J. Quant. Spectrosc. Radiat. Transfer 37 (1987) 521.
[16] U.I. Safronova, W.R. Johnson, M.S. Safronova, J.R. Albritton, Phys. Rev. A 66 (2002) 022507.
[17] J. Migdalek, W. Siegel, J. Phys. B 45 (2012) 145002.
[18] J. Migdalek, W. Siegel, J. Phys. B 47 (2014) 075003.
[19] M. Tanaka, D. Kato, G. Gaigalas, K. Kawaguchi, Mon. Not. R. Astron. Soc. 496 (2020) 1369.
[20] S. Ben Nasr, H. Carvajal Gallego, J. Deprince, P. Palmeri, P. Quinet, Astron. Astrophys. 678 (2023) A67.
[21] D.S. Leckrone, G.M. Wahlgren, S.G. Johansson, Astrophys. J. 377 (1991) L37.
[22] G.M. Wahlgren, S.G. Johansson, U. Litzén, N.D. Gibson, J.C. Cooper, J.E. Lawler, D.S. Leckrone, R. Engleman Jr., Astrophys. J. 475 (1997) 380.
[23] D.S. Leckrone, C.R. Proffitt, G.M. Wahlgren, S.G. Johansson, T. Brage, Astron. J. 117 (1999) 1454.
[24] V.I. Azarov, A System for the Automatic Processing of Photospectrograms, Preprint of the Institute of Spectroscopy, Russian Academy of Sciences, Troisk, 1991, p. 1.
[25] A. Kramida, Yu. Ralchenko, J. Reader, NIST ASD Team, NIST Atomic Spectra Database (Version 5.4), National Institute of Standards and Technology, Gaithersburg, MD, 2016.
[26] R.D. Cowan, The Theory of Atomic Structure and Spectra, University of California Press, Berkeley, 1981.
[27] P. Quinet, P. Palmeri, E. Biémont, M.M. McCurdy, G. Rieger, E.H. Pinnington, M.E. Wickliffe, J.E. Lawler, Mon. Not. R. Astron. Soc. 307 (1999) 934.
[28] P. Quinet, P. Palmeri, E. Biémont, Z.S. Li, Z.G. Zhang, S. Svanberg, J. Alloys Compd. 344 (2002) 255.
[29] H. Nilsson, L. Engström, H. Lundberg, P. Palmeri, V. Fivet, P. Quinet, E. Biémont, Eur. Phys. J. D 49 (2008) 13.
[30] P. Palmeri, P. Quinet, V. Fivet, E. Biémont, H. Nilsson, L. Engström, H. Lundberg, Phys. Scr. 78 (2008) 015304.
[31] S. Enzonga Yoca, P. Quinet, E. Biémont, J. Phys. B 45 (2012) 035001.
[32] S. Fraga, J. Karwowski, K.M.S. Saxena, Handbook of Atomic Data, Elsevier, Amsterdam, 1976.
[33] I.P. Grant, Relativistic Quantum Theory of Atoms and Molecules: Theory and Computation, Springer, New York, 2007.
[34] C. Froese Fischer, M. Godefroid, T. Brage, P. Jönsson, G. Gaigalas, J. Phys. B 49 (2016) 182004.
[35] C. Froese Fischer, G. Gaigalas, P. Jönsson, J. Bieroń, Comput. Phys. Comm. 237 (2019) 184.
[36] P. Quinet, Can. J. Phys. 95 (2017) 790.

Explanation of Tables

Table 1. Radial parameters adopted for the HFR+CPOL calculations in Re III.

Configuration	Electronic configuration
Parameter	Radial parameter
Ab initio	Numerical value of the radial parameter (in cm^{-1}) as computed using the *ab initio* HFR+CPOL method
Fitted	Numerical value of the radial parameter (in cm^{-1}) as obtained in the semi-empirical least-squares adjustment
Ratio	Ratio between fitted and *ab initio* values of the parameter

Table 2. Radial parameters adopted for the HFR+CPOL calculations in Re IV.

Configuration	Electronic configuration
Parameter	Radial parameter
Ab initio	Numerical value of the radial parameter (in cm^{-1}) as computed using the *ab initio* HFR+CPOL method
Fitted	Numerical value of the radial parameter (in cm^{-1}) as obtained in the semi-empirical least-squares adjustment
Ratio	Ratio between fitted and *ab initio* values of the parameter

Table 3. Radial parameters adopted for the HFR+CPOL calculations in Re V.

Configuration	Electronic configuration
Parameter	Radial parameter
Ab initio	Numerical value of the radial parameter (in cm^{-1}) as computed using the *ab initio* HFR+CPOL method
Fitted	Numerical value of the radial parameter (in cm^{-1}) as obtained in the semi-empirical least-squares adjustment
Ratio	Ratio between fitted and *ab initio* values of the parameter

Table 4. Comparison between the energy levels computed with the HFR+CPOL approach and the available experimental values in Re III.

E_{Exp}	Experimental energy level (in cm^{-1}) taken from [6]
$E_{HFR+CPOL}$	Calculated energy level (in cm^{-1}) obtained in the present work with the semi-empirical HFR+CPOL approach
ΔE	E_{Exp} - $E_{HFR+CPOL}$
J	Total angular momentum
Composition in LS coupling	First three LS-components (in %) of the eigenvector

Table 5. Comparison between the energy levels computed with the HFR+CPOL approach and the available experimental values in Re IV.

E_{Exp}	Experimental energy level (in cm^{-1}) taken from [7]
$E_{HFR+CPOL}$	Calculated energy level (in cm^{-1}) obtained in the present work with the semi-empirical HFR+CPOL approach
ΔE	E_{Exp} - $E_{HFR+CPOL}$
J	Total angular momentum
Composition in LS coupling	First three LS-components (in %) of the eigenvector

Table 6. Comparison between the energy levels computed with the HFR+CPOL approach and the available experimental values in Re V.

E_{Exp}	Experimental energy level (in cm^{-1}) taken from [8]
$E_{HFR+CPOL}$	Calculated energy level (in cm^{-1}) obtained in the present work with the semi-empirical HFR+CPOL approach
ΔE	E_{Exp} - $E_{HFR+CPOL}$
J	Total angular momentum
Composition in LS coupling	First three LS-components (in %) of the eigenvector

Table 7. Comparison between the energy levels computed with the MCDHF and HFR+CPOL approaches and the available experimental values in Re III.

E_{Exp}	Experimental energy level (in cm^{-1}) taken from [6]
E_{MCDHF}	Calculated energy level (in cm^{-1}) obtained in the present work with the MCDHF approach
ΔE_{MCDHF}	E_{Exp} - E_{MCDHF}
$E_{HFR+CPOL}$	Calculated energy level (in cm^{-1}) obtained in the present work with the HFR+CPOL approach
$\Delta E_{HFR+CPOL}$	E_{Exp} - $E_{HFR+CPOL}$
J	Total angular momentum
jj-purity	Main component of the eigenvector in jj-coupling (in %)
LS-purity	Main component of the eigenvector in LS-coupling (in %)

Table 8. Comparison between the energy levels computed with the MCDHF and HFR+CPOL approaches and the available experimental values in Re IV.

E_{Exp}	Experimental energy level (in cm^{-1}) taken from [6]
E_{MCDHF}	Calculated energy level (in cm^{-1}) obtained in the present work with the MCDHF approach
ΔE_{MCDHF}	E_{Exp} - E_{MCDHF}
$E_{HFR+CPOL}$	Calculated energy level (in cm^{-1}) obtained in the present work with the HFR+CPOL approach
$\Delta E_{HFR+CPOL}$	E_{Exp} - $E_{HFR+CPOL}$
J	Total angular momentum
jj-purity	Main component of the eigenvector in jj-coupling (in %)
LS-purity	Main component of the eigenvector in LS-coupling (in %)

Table 9. Comparison between the energy levels computed with the MCDHF and HFR+CPOL approaches and the available experimental values in Re V.

E_{Exp}	Experimental energy level (in cm^{-1}) taken from [6]
E_{MCDHF}	Calculated energy level (in cm^{-1}) obtained in the present work with the MCDHF approach
ΔE_{MCDHF}	E_{Exp} - E_{MCDHF}
$E_{HFR+CPOL}$	Calculated energy level (in cm^{-1}) obtained in the present work with the HFR+CPOL approach
$\Delta E_{HFR+CPOL}$	E_{Exp} - $E_{HFR+CPOL}$

J	Total angular momentum
jj-purity	Main component of the eigenvector in jj-coupling (in %)
LS-purity	Main component of the eigenvector in LS-coupling (in %)

Table 10. Transition probabilities (gA) and oscillator strengths (log gf) for the strongest spectral lines in Re III.

λ_{Ritz}	Ritz wavelength obtained using the experimental energy levels from [6]
Lower even level	Lower energy level of the transition taken from [6]. The value of E (in cm^{-1}) taken from [6] is rounded to the unit for the classification
Upper odd level	Upper energy level of the transition taken from [6]. The value of E (in cm^{-1}) taken from [6] is rounded to the unit for the classification
gA	Weighted transition probability (in 10^8 s^{-1}) taken from previous study [6] and obtained with the HFR+CPOL and the MCDHF calculations carried out in the present work
log gf	Weighted oscillator strength (in the logarithmic scale) obtained with the HFR+CPOL and the MCDHF calculations carried out in the present work

Table 11. Transition probabilities (gA) and oscillator strengths (log gf) for the strongest spectral lines in Re IV.

λ_{Ritz}	Ritz wavelength obtained using the experimental energy levels from [7]
Lower even level	Lower energy level of the transition taken from [7]. The value of E (in cm^{-1}) taken from [6] is rounded to the unit for the classification
Upper odd level	Upper energy level of the transition taken from [7]. The value of E (in cm^{-1}) taken from [6] is rounded to the unit for the classification
gA	Weighted transition probability (in 10^8 s^{-1}) taken from previous study [7] and obtained with the HFR+CPOL and the MCDHF calculations carried out in the present work
log gf	Weighted oscillator strength (in the logarithmic scale) obtained with the HFR+CPOL and the MCDHF calculations carried out in the present work

Table 12. Transition probabilities (gA) and oscillator strengths (log gf) for the strongest spectral lines in Re V.

λ_{Ritz}	Ritz wavelength obtained using the experimental energy levels from [8]
Lower even level	Lower energy level of the transition taken from [8]. The value of E (in cm^{-1}) taken from [6] is rounded to the unit for the classification
Upper odd level	Upper energy level of the transition taken from [8]. The value of E (in cm^{-1}) taken from [6] is rounded to the unit for the classification
gA	Weighted transition probability (in 10^8 s^{-1}) taken from previous study [8] and obtained with the HFR+CPOL and the MCDHF calculations carried out in the present work
log gf	Weighted oscillator strength (in the logarithmic scale) obtained with the HFR+CPOL and the MCDHF calculations carried out in the present work

Table 1
Radial parameters adopted for the HFR+CPOL calculations in Re III

Configuration	Parameter	*Ab initio* (cm^{-1})	Fitted (cm^{-1})	Ratio
Even parity				
5d^5	E_{av}	37 221.2	33 675.5	
	F^2(5d,5d)	58 724.3	47 262.8	0.8048
	F^4(5d,5d)	38 665.3	32 068.7	0.8294
	α	0.0	−0.5	
	β	0.0	−49.8	
	ζ(5d)	3399.2	2827.3	0.8317
5d^{4}6s	E_{av}	54 864.8	49 865.5	
	F^2(5d,5d)	60 858.2	49 153.2	0.8077
	F^4(5d,5d)	40 237.7	33 097.0	0.8225
	α	0.0	14.7	
	β	0.0	−238.7	
	ζ(5d)	3633.7	3054.2	0.8405
	G^2(5d,6s)	21 105.8	18 238.4	0.8641
5d^{3}6s^2	E_{av}	87 308.1	82 525.8	
	F^2(5d,5d)	62 883.6	56 595.2	0.9000
	F^4(5d,5d)	41 737.0	37 563.3	0.9000
	α	0.0	0.0	
	β	0.0	0.0	
	ζ(5d)	3872.2	3872.2	1.0000
5d^5–5d^{4}6s	R^2(5d,5d;5d,6s)	−26147.7	−22546.5	0.8623
5d^5–5d^{3}6s^2	R^2(5d,5d;6s,6s)	23 538.4	20 296.6	0.8623
5d^{4}6s–5d^{3}6s^2	R^2(5d,5d;5d,6s)	−26172.4	−22567.8	0.8623
Odd parity				
5d^{4}6p	E_{av}	107 942.5	105 123.0	
	F^2(5d,5d)	61 348.7	49 294.7	0.8035
	F^4(5d,5d)	40 601.4	34 094.9	0.8397
	α	0.0	−12.0	
	β	0.0	−78.5	
	ζ(5d)	3684.6	3129.3	0.8493
	ζ(6p)	6136.6	6517.1	1.0620
	F^2(5d,6p)	23 759.3	19 104.5	0.8041
	G^1(5d,6p)	11 147.0	9160.9	0.8218
	G^3(5d,6p)	8968.4	8071.6	0.9000
5d^{3}6s6p	E_{av}	136 214.3	133 896.3	
	F^2(5d,5d)	63 296.2	48 467.4	0.7657
	F^4(5d,5d)	42 043.9	33 149.0	0.7884
	α	0.0	17.9	
	β	0.0	−501.4	
	ζ(5d)	3919.1	3366.7	0.8590
	ζ(6p)	7127.9	7585.6	1.064
	F^2(5d,6p)	25 198.0	20 756.3	0.8237
	G^2(5d,6s)	20 994.8	16 750.4	0.7978
	G^1(5d,6p)	11 402.3	9419.6	0.8261
	G^3(5d,6p)	9364.7	8428.2	0.9000
	G^1(6s,6p)	42 037.4	39 955.4	0.9505
5d^{4}6p–5d^{3}6s6p	R^2(5d,5d;5d,6s)	−26113.0	−24568.6	0.9409
	R^2(5d,6p;6s,6p)	−21447.3	−21386.7	0.9972
	R^1(5d,6p;6p,6s)	−20055.9	−16442.4	0.8198

Table 2
Radial parameters adopted for the HFR+CPOL calculations in Re IV

Configuration	Parameter	*Ab initio* (cm^{-1})	Fitted (cm^{-1})	Ratio
Even parity				
$5d^4$	E_{av}	33 136.8	30 508.3	
	F^2(5d,5d)	62 766.4	51 300.8	0.8173
	F^4(5d,5d)	41 665.1	35 531.4	0.8528
	α	0.0	8.4	
	β	0.0	−381.5	
	ζ(5d)	3805.8	3228.8	0.8484
$5d^3 6s$	E_{av}	72 032.2	67 271.5	0.9339
	F^2(5d,5d)	53 088.6	43 649.4	0.8222
	F^4(5d,5d)	43 002.3	35 778.2	0.8320
	α	0.0	14.9	
	β	0.0	−283.3	
	ζ(5d)	4035.3	3413.9	0.8460
	G^2(5d,6s)	21 759.9	18 902.7	0.8687
$5d^2 6s^2$	E_{av}	126 555.3	123 154.0	
	F^2(5d,5d)	66 293.1	59 663.8	0.9000
	F^4(5d,5d)	44 288.0	39 859.2	0.9000
	α	0.0	0.0	
	β	0.0	0.0	
	ζ(5d)	4268.8	4268.8	1.0000
$5d^4$–$5d^3 6s$	R^2(5d,5d;5d,6s)	−26693.0	−22321.9	0.8362
$5d^4$–$5d^2 6s^2$	R^2(5d,5d;6s,6s)	24 070.6	20 128.9	0.8362
$5d^3 6s$–$5d^2 6s^2$	R^2(5d,5d;5d,6s)	−26666.2	−22299.5	0.8362
Odd parity				
$5d^3 6p$	E_{av}	135 267.1	132 061.3	
	F^2(5d,5d)	65 094.2	52 702.1	0.8096
	F^4(5d,5d)	43 398.0	35 979.9	0.8291
	α	0.0	24.8	
	β	0.0	−563.9	
	ζ(5d)	4097.1	3542.3	0.8646
	ζ(6p)	8397.8	8664.3	1.0317
	F^2(5d,6p)	27 471.0	21 179.2	0.7710
	G^1(5d,6p)	12 041.6	9275.4	0.7703
	G^3(5d,6p)	10 127.1	5665.1	0.5594
$5d^2 6s6p$	E_{av}	184 849.8	180 922.4	0.9788
	F^2(5d,5d)	66 757.0	60 081.3	0.9000
	F^4(5d,5d)	44 637.6	40 173.8	0.9000
	α	0.0	0.0	
	β	0.0	0.0	
	ζ(5d)	4327.0	4237.0	1.0000
	ζ(6p)	9382.8	9382.8	1.0000
	F^2(5d,6p)	28 676.6	25 808.9	0.9000
	G^2(5d,6s)	21 630.8	19 467.7	0.9000
	G^1(5d,6p)	12 197.0	10 977.3	0.9000
	G^3(5d,6p)	10 422.9	9380.6	0.9000
	G^1(6s,6p)	46 355.8	41 720.2	0.9000
$5d^3 6p$–$5d^2 6s6p$	R^2(5d,5d;5d,6s)	−26566.9	−19009.2	0.7155
	R^2(5d,6p;6s,6p)	−23270.4	−16650.5	0.7155
	R^1(5d,6p;6p,6s)	−21256.4	−15209.5	0.7155

Table 3
Radial parameters adopted for the HFR+CPOL calculations in Re V

Configuration	Parameter	*Ab initio* (cm^{-1})	Fitted (cm^{-1})	Ratio
Even parity				
5d^3	E_{av}	27 048.9	25 338.9	
	F^2(5d,5d)	66 494.0	56 709.7	0.8529
	F^4(5d,5d)	44 450.9	38 775.6	0.8723
	α	0.0	15.2	
	β	0.0	−699.6	
	ζ(5d)	4255.0	3603.8	0.8470
5d^{2}6s	E_{av}	89 090.3	84 967.5	0.9537
	F^2(5d,5d)	68 039.2	58 364.5	0.8578
	F^4(5d,5d)	45 604.9	40 848.4	0.8957
	α	0.0	−4.4	
	β	0.0	−807.7	
	ζ(5d)	4481.1	3809.8	0.8502
	G^2(5d,6s)	22 155.9	20 800.6	0.9388
5d^3–5d^{2}6s	R^2(5d,5d;5d,6s)	−26897.8	−22009.3	0.8183
Odd parity				
5d^{2}6p	E_{av}	161 901.0	159 712.7	
	F^2(5d,5d)	68 464.4	58 330.1	0.8520
	F^4(5d,5d)	45 925.9	40 242.5	0.8762
	α	0.0	9.6	
	β	0.0	−565.9	
	ζ(5d)	4539.3	3927.4	0.8652
	ζ(6p)	10 672.1	10 774.2	1.0096
	F^2(5d,6p)	30 573.6	27 404.7	0.8964
	G^1(5d,6p)	12 609.8	11 841.4	0.9391
	G^3(5d,6p)	10 990.6	10 599.8	0.9644
5d6s6p	E_{av}	234 376.3	226 925.7	
	ζ(5d)	4763.4	4763.4	1.0000
	ζ(6p)	11 653.8	11 653.8	1.0000
	F^2(5d,6p)	31 639.2	28 475.3	0.9000
	G^2(5d,6s)	22 019.0	19 817.1	0.9000
	G^1(5d,6p)	12 731.6	11 458.4	0.9000
	G^3(5d,6p)	11 238.0	10 114.2	0.9000
	G^1(6s,6p)	49 986.6	44 987.9	0.9000
5d^{2}6p–5d6s6p	R^2(5d,5d;5d,6s)	−26723.4	−26764.5	1.0015
	R^2(5d,6p;6s,6p)	−24536.7	−22083.0	0.9000
	R^1(5d,6p;6s,6p)	−21933.2	−19739.9	0.9000

Table 4
Comparison between the energy levels computed with the HFR+CPOL approach and the available experimental values in Re III.

E_{Exp}	$E_{HFR+CPOL}$	ΔE	J	Composition in LS coupling					
Even parity									
0.00	−32	32	2.5	88.9%	$5d^5(^6S)^6S$	9.5%	$5d^5(^4P)^4P$	0.4%	$5d^5(^4D)^4D$
13614.31	13 575	39	2.5	25.3%	$5d^5(^4G)^4G$	15.9%	$5d^5(^2F)^2F$	8.6%	$5d^5(^2D)^2D$
14396.44	14 346	50	0.5	53.0%	$5d^46s(^5D)^6D$	16.3%	$5d^5(^4P)^4P$	12.6%	$5d^46s(^3P)^4P$
15771.98	15 757	15	1.5	37.6%	$5d^5(^4P)^4P$	28.1%	$5d^5(^4D)^4D$	14.5%	$5d^46s(^5D)^6D$
16890.46	16 921	−31	3.5	63.5%	$5d^5(^4G)^4G$	13.8%	$5d^5(^4D)^4D$	10.7%	$5d^5(^2F)^2F$
17139.88	17 195	−55	2.5	43.0%	$5d^5(^4G)^4G$	22.1%	$5d^5(^4D)^4D$	16.8%	$5d^5(^4P)^4P$
17908.92	17 904	5	1.5	74.0%	$5d^46s(^5D)^6D$	13.7%	$5d^5(^4D)^4D$	4.1%	$5d^5(^4P)^4P$
18020.00	17 954	66	5.5	83.9%	$5d^5(^4G)^4G$	10.8%	$5d^5(^2H)^2H$	2.4%	$5d^46s(^3G)^4G$
18345.56	18 363	−17	4.5	86.2%	$5d^5(^4G)^4G$	5.2%	$5d^5(^4F)^4F$	3.1%	$5d^5(^2H)^2H$
18392.70	18 408	−15	0.5	30.5%	$5d^5(^4P)^4P$	29.2%	$5d^5(^4D)^4D$	28.9%	$5d^46s(^5D)^6D$
19718.84	19 724	−5	2.5	88.7%	$5d^46s(^5D)^6D$	2.1%	$5d^5(^4D)^4D$	1.9%	$5d^46s(^3D)^4D$
20453.27	20 390	63	3.5	50.8%	$5d^5(^4D)^4D$	19.4%	$5d^5(^4G)^4G$	12.2%	$5d^46s(^5D)^6D$
21568.90	21 530	39	2.5	30.1%	$5d^5(^4D)^4D$	18.1%	$5d^5(^2D)^2D$	14.3%	$5d^5(^4P)^4P$
21973.95	22 075	−101	0.5	45.3%	$5d^5(^4D)^4D$	29.2%	$5d^5(^4P)^4P$	11.7%	$5d^46s(^5D)^4D$
22106.24	22 182	−76	3.5	80.0%	$5d^46s(^5D)^6D$	11.2%	$5d^5(^4D)^4D$	2.6%	$5d^5(^4G)^4G$
22936.77	22 991	−54	1.5	32.5%	$5d^5(^4P)^4P$	33.2%	$5d^5(^4D)^4D$	8.9%	$5d^5(^2D)^2D$
23471.28	23 466	5	4.5	75.6%	$5d^46s(^5D)^6D$	10.5%	$5d^46s(^3F)^4F$	4.1%	$5d^5(^4F)^4F$
26128.71	26 195	−66	1.5	38.8%	$5d^5(^4F)^4F$	25.7%	$5d^5(^2D)^2D$	10.8%	$5d^5(^2D)^2D$
26170.06	26 257	−87	5.5	74.4%	$5d^5(^2I)^2I$	16.1%	$5d^5(^2H)^2H$	7.8%	$5d^5(^4G)^4G$
26659.78	26 649	11	2.5	18.1%	$5d^5(^2F)^2F$	16.1%	$5d^5(^4G)^4G$	15.7%	$5d^5(^4P)^4P$
26910.08	26 880	30	3.5	29.4%	$5d^5(^4F)^4F$	22.6%	$5d^5(^2G)^2G$	15.9%	$5d^5(^2F)^2F$
27421.03	27 362	59	4.5	39.2%	$5d^5(^2G)^2G$	25.1%	$5d^5(^4F)^4F$	12.3%	$5d^46s(^5d)^6D$
28587.87	28 614	−26	6.5	99.2%	$5d^5(^2I)^2I$	0.5%	$5d^46s(^1I)^2I$	0.1%	$5d^46d(^3H)^2I$
30255.47	30 182	73	3.5	25.5%	$5d^5(^2F)^2F$	22.4%	$5d^5(^2F)^2F$	16.7%	$5d^5(^2G)^2G$
30302.28	30 422	−120	2.5	55.1%	$5d^5(^4F)^4F$	16.5%	$5d^5(^2F)^2F$	8.6%	$5d^46s(^3F)^4F$
30835.75	30 811	25	0.5	17.9%	$5d^46s(^5D)^4D$	11.7%	$5d^46s(^3P)^2P$	10.3%	$5d^5(^4P)^4P$
31345.29	31 276	69	2.5	35.6%	$5d^5(^2F)^2F$	12.0%	$5d^5(^2D)^2D$	11.9%	$5d^5(^4p)^4P$
31989.54	32 059	−69	1.5	30.5%	$5d^5(^4F)^4F$	28.5%	$5d^5(^2D)^2D$	14.0%	$5d^46s(^3F)^4F$
32068.35	31 981	87	4.5	42.8%	$5d^5(^2H)^2H$	40.3%	$5d^5(^4F)^4F$	7.0%	$5d^5(^2G)^2G$
32832.90	32 906	−73	3.5	28.4%	$5d^5(^2G)^2G$	19.0%	$5d^5(^4F)^4F$	16.9%	$5d^46s(^3H)^4H$
34349.37	34 327	22	3.5	21.6%	$5d^5(^2F)^2F$	15.9%	$5d^5(^4F)^4F$	12.3%	$5d^46s(^3G)^4G$
34641.11	34 574	67	3.5	38.8%	$5d^46s(^3H)^4H$	21.4%	$5d^5(^2F)^2F$	13.5%	$5d^5(^2G)^2G$
34825.68	34 870	−44	1.5	40.6%	$5d^46s(^5D)^4D$	10.0%	$5d^46s(^3P)^4P$	5.8%	$5d^5(^4F)^4F$
35139.99	35 176	−36	4.5	55.6%	$5d^46s(^3H)^4H$	15.3%	$5d^46s(^3G)^4G$	6.3%	$5d^5(^2G)^2G$
36165.95	36 212	−46	0.5	31.5%	$5d^46s(^3P)^4P$	18.5%	$5d^5(^2S)^2S$	17.7%	$5d^46s(^3P)^4P$
36463.97	36 390	74	2.5	26.9%	$5d^46s(^3g)^4G$	19.5%	$5d46s(^3F)^4F$	0.0%	$5d^26s^2(^3F)^2D$
36927.52	36 955	−27	5.5	44.2%	$5d^5(^2H)^2H$	20.7%	$5d^46s(^3H)^4H$	16.5%	$5d^5(^2I)^2I$
37406.55	37 336	71	4.5	39.5%	$5d^5(^2H)^2H$	29.1%	$5d^5(^2G)^2G$	13.0%	$5d^5(^4F)^4F$
38167.85	38 083	85	5.5	60.5%	$5d^46s(^3H)^4H$	20.5%	$5d^5(^2H)^2H$	6.1%	$5d^46s(^3G)^4G$
38656.17	38 568	88	1.5	23.2%	$5d^46s(^3F)^4F$	19.1%	$5d^46s(^3P)^4P$	12.4%	$5d^46s(^3P)^4P$
38752.31	38 710	42	3.5	24.5%	$5d^46s(^5D)^4D$	17.5%	$5d^46s(^3F)^4F$	17.3%	$5d^46s(^3H)^4H$
39300.25	39 400	−100	6.5	87.0%	$5d^46s(^3H)^4H$	12.4%	$5d^46s(^1I)^2I$	0.2%	$5d^5(^2I)^2I$
39595.72	39 574	22	2.5	50.8%	$5d^46s(^5D)^4D$	13.1%	$5d^5(^2F)^2F$	10.0%	$5d^5(^2D)^2D$
39790.02	39 809	−19	1.5	36.7%	$5d^46s(^5D)^4D$	16.5%	$5d^46s(^3P)^4P$	13.6%	$5d^46s(^3D)^4D$
40000.60	39 960	41	2.5	26.2%	$5d^46s(^3G)^4G$	14.6%	$5d^5(^2D)^2D$	8.4%	$5d^46s(^1D)^2D$
40654.99	40 648	7	2.5	17.9%	$5d^5(^2F)^2F$	16.7%	$5d^5(^2F)^2F$	9.4%	$5d^46s(^3G)^4G$
40934.98	40 901	34	4.5	28.4%	$5d^46s(^3F)^4F$	24.3%	$5d^46s(^3H)^4H$	13.3%	$5d^46s(^3G)^4G$
41115.92	41 167	−51	3.5	25.5%	$5d^46s(^5D)^4D$	24.8%	$5d^46s(^3G)^4G$	15.1%	$5d^46s(^3D)^4D$
41210.25	41 275	−65	1.5	60.5%	$5d^5(^2D)^2D$	11.0%	$5d^46s(^3F)^4F$	8.5%	$5d^5(^2D)^2D$
41405.07	41 488	−83	4.5	26.7%	$5d^5(^2G)^2G$	24.2%	$5d^46s(^3G)^4G$	21.2%	$5d^46s(^1G)^2G$
42600.54	42 587	14	2.5	27.4%	$5d^46s(^3F)^4F$	16.3%	$5d^46s(^3P)^4P$	12.1%	$5d^5(^2D)^2D$
43191.67	43 179	13	2.5	23.5%	$5d^5(^2D)^2D$	20.2%	$5d^46s(^3P)^4P$	16.6%	$5d^46s(^3D)^4D$
43750.37	43 795	−45	3.5	26.7%	$5d^46s(^3F)^4F$	13.6%	$5d^46s(^3G)^4G$	13.6%	$5d^5(^2G)^2G$
45256.54	45 212	45	5.5	47.3%	$5d^46s(^3G)^4G$	19.1%	$5d^46s(^1I)^2I$	16.5%	$5d^46s(^3H)^2H$
45608.03	45 563	45	3.5	26.0%	$5d^5(^2G)^2G$	21.6%	$5d^46s(^3G)^2G$	17.8%	$5d^46s(^3G)^4G$
46314.79	46 378	−63	4.5	54.8%	$5d^46s(^3H)^2H$	12.9%	$5d^46s(^3G)^4G$	11.4%	$5d^46s(^3G)^2G$
46718.20	46 808	−90	3.5	50.9%	$5d^46s(^3D)^4D$	11.6%	$5d^46s(^5D)^4D$	8.4%	$5d^5(^4D)^4D$
47011.78	46 863	149	4.5	23.8%	$5d^46s(^3G)^4G$	23.9%	$5d^46s(^3F)^4F$	17.9%	$5d^5(^2G)^2G$
47091.01	47 053	38	1.5	60.1%	$5d^46s(^3D)^4D$	9.7%	$5d^46s(^3P)^2P$	4.9%	$5d^5(^4D)^4D$
47881.45	47 883	−2	5.5	37.0%	$5d^46s(^1I)^2I$	30.8%	$5d^46s(^3G)^4G$	20.3%	$5d^46s(^3H)^2H$
47910.25	47 856	54	2.5	29.5%	$5d^46s(^3D)^4D$	13.9%	$5d^46s(^3P)^4P$	9.2%	$5d^46s(^3F)^4F$
50496.79	50 637	−140	6.5	86.6%	$5d^46s(^1I)^2I$	12.5%	$5d^46s(^3H)^4H$	0.4%	$5d^5(^2I)^2I$
51007.47	51 050	−43	2.5	27.7%	$5d^46s(^3F)^2F$	10.1%	$5d^46s(^3F)^2F$	9.0%	$5d^46s(^3D)^4D$
51668.96	51 765	−96	3.5	26.0%	$5d^46s(^3F)^2F$	17.0%	$5d^5(^2G)^2G$	15.0%	$5d^46s(^1G)^2G$
52444.21	52 501	−57	3.5	32.5%	$5d^46s(^3G)^2G$	13.4%	$5d^5(^2G)^2G$	12.2%	$5d^5(^2G)^2G$
53402.71	53 231	172	5.5	55.3%	$5d^46s(^3H)^2H$	39.5%	$5d^46s(^1I)^2I$	1.4%	$5d^46s(^3G)^4G$
55975.68	55 880	96	4.5	45.3%	$5d^46s(^3G)^2G$	34.4%	$5d^5(^2G)^2G$	11.7%	$5d^46s(^1G)^2G$
57206.89	57 207	0	4.5	25.2%	$5d^46s(^3F)^4F$	22.4%	$5d^46s(^1G)^2G$	13.7%	$5d^46s(^3F)^4F$
58069.32	58 117	−48	3.5	46.5%	$5d^46s(^1F)^2F$	13.4%	$5d^46s(^3F)^2F$	12.0%	$5d^46s(^1G)^2G$
61243.18	61 236	7	4.5	52.8%	$5d^46s(^3F)^4F$	24.0%	$5d^46s(^1G)^2G$	5.2%	$5d^46s(^1G)^2G$
Odd parity									
64709.45	64 797	−88	0.5	36.2%	$5d^46p(^5D)^6F$	11.9%	$5d^46p(^5D)^4P$	10.2%	$5d^46p(^3P)^4D$
67274.27	67 540	−266	0.5	29.5%	$5d^46p(^5D)^6F$	24.8%	$5d^46p(^5D)^4P$	6.9%	$5d^46p(^3P)^4P$
68339.99	68 401	−61	1.5	72.5%	$5d^46p(^5D)^6F$	7.7%	$5d^46p(^3P)^4D$	6.2%	$5d^46p(^5D)^4D$

(*continued on next page*)

Table 4 (*continued*)

E_{Exp}	$E_{HFR+CPOL}$	ΔE	J	Composition in LS coupling					
71230.53	71 322	−91	2.5	77.0%	$5d^46p(^5D)^6F$	5.3%	$5d^46p(^5D)^4F$	4.3%	$5d^46p(^5D)^4D$
71842.35	71 843	−1	1.5	42.0%	$5d^46p(^5D)^6D$	32.6%	$5d^46p(^5D)^4P$	5.3%	$5d^46p(^5D)^6P$
73640.25	73 718	−78	3.5	61.4%	$5d^46p(^5D)^6F$	11.6%	$5d^46p(^5D)^4F$	6.8%	$5d^46p(^5D)^6D$
75517.33	75 603	−86	4.5	32.4%	$5d^46p(^5D)^6F$	18.0%	$5d^46p(^5D)^4F$	11.9%	$5d^46p(^5D)^6D$
75529.07	75 241	288	2.5	34.9%	$5d^46p(^5D)^6D$	28.5%	$5d^46p(^5D)^6P$	19.1%	$5d^46p(^5D)^4P$
77759.84	77 174	586	3.5	53.5%	$5d^46p(^5D)^6P$	11.0%	$5d^46p(^5D)^6D$	8.4%	$5d^46p(^5D)^4D$
77861.59	77 638	224	1.5	61.0%	$5d^46p(^5D)^6P$	5.1%	$5d^46p(^5D)^4F$	4.8%	$5d^46p(^5D)^6D$
78667.43	78 611	56	0.5	23.6%	$5d^46p(^5D)^6F$	20.8%	$5d^46p(^5D)^6D$	12.6%	$5d^46p(^3P)^4D$
79768.95	80 093	−324	1.5	29.5%	$5d^46p(^5D)^4F$	11.7%	$5d^46p(^5D)^6P$	10.0%	$5d^46p(^3F)^4F$
79861.69	79 616	246	2.5	38.4%	$5d^46p(^5D)^6P$	20.5%	$5d^46p(^5D)^6D$	8.9%	$5d^46p(^5D)^4F$
81136.31	81 070	66	0.5	41.5%	$5d^46p(^5D)^6D$	14.6%	$5d^46p(^5D)^4P$	13.3%	$5d^46p(^3P)^4D$
81404.63	81 408	−3	3.5	22.8%	$5d^46p(^5D)^6F$	11.9%	$5d^46p(^5D)^6P$	0.0%	$5d^26s^26p(^3F)^4G$
81957.47	82 057	−100	4.5	35.7%	$5d^46p(^5D)^6F$	23.5%	$5d^46p(^3H)^4I$	8.4%	$5d^46p(^3G)^4H$
82166.83	82 339	−172	2.5	14.0%	$5d^46p(^3F)^4G$	12.7%	$5d^46p(^5D)^6D$	8.8%	$5d^46p(^5D)^4F$
82301.45	82 163	138	3.5	32.0%	$5d^46p(^5D)^6D$	20.2%	$5d^46p(^3H)^4H$	10.1%	$5d^46p(^3H)^2G$
82459.98	82 604	−144	1.5	23.8%	$5d^46p(^3P)^4D$	13.1%	$5d^46p(^3P)^4D$	10.6%	$5d^46p(^5D)^6F$
83386.03	83 343	43	1.5	39.8%	$5d^46p(^5D)^6D$	34.1%	$5d^46p(^5D)^4P$	4.4%	$5d^46p(^5D)^6P$
83605.25	83 472	133	4.5	31.0%	$5d^46p(^5D)^6D$	21.9%	$5d^46p(^5D)^6F$	11.2%	$5d^46p(^3H)^4I$
83950.19	83 533	417	5.5	76.4%	$5d^46p(^5D)^6F$	10.2%	$5d^46p(^3F)^4G$	5.0%	$5d^46p(^3F)^4G$
84453.78	84 682	−228	2.5	30.8%	$5d^46p(^5D)^4P$	12.7%	$5d^46p(^5D)^4F$	9.3%	$5d^46p(^5D)^6P$
84645.51	84 630	16	3.5	16.2%	$5d^46p(^3G)^4H$	12.4%	$5d^46p(^5D)^6D$	10.5%	$5d^46p(^3H)^2G$
85572.52	85 757	−184	2.5	27.2%	$5d^46p(^5D)^4F$	17.9%	$5d^46p(^5D)^6D$	13.7%	$5d^46p(^5D)^4P$
85975.44	86 114	−139	5.5	33.1%	$5d^46p(^3H)^4I$	27.6%	$5d^46p(^3H)^4H$	0.0%	$5d^48p(^1G)^2H$
86678.58	86 450	229	4.5	29.2%	$5d^46p(^3H)^4H$	15.2%	$5d^46p(^5D)^6D$	13.1%	$5d^46p(^3H)^2G$
86723.56	86 924	−200	0.5	54.3%	$5d^46p(^5D)^4D$	9.2%	$5d^46p(^3P)^4D$	3.6%	$5d^46p(^3D)^4D$
87105.75	87 262	−156	1.5	22.8%	$5d^46p(^5D)^4D$	10.7%	$5d^46p(^3F)^4F$	8.7%	$5d^46p(^5D)^4F$
87231.77	87 455	−223	0.5	39.7%	$5d^46p(^5D)^4P$	12.6%	$5d^46p(^3P)^4P$	9.0%	$5d^46p(^3P)^4P$
87251.23	87 623	−372	3.5	35.8%	$5d^46p(^5D)^4F$	20.6%	$5d^46p(^5D)^6D$	12.8%	$5d^46p(^3G)^4H$
87964.10	87 673	291	2.5	9.7%	$5d^46p(^3G)^4G$	8.0%	$5d^46p(^3F)^4F$	7.6%	$5d^46p(^3F)^2F$
88008.10	88 174	−166	1.5	16.0%	$5d^46p(^3P)^4D$	14.8%	$5d^46p(^5D)^4F$	12.0%	$5d^46p(^3D)^4D$
88143.40	88 179	−36	2.5	20.8%	$5d^46p(^5D)^4D$	10.6%	$5d^46p(^3P)^4D$	7.7%	$5d^46p(^3P)^4D$
88157.70	88 290	−132	6.5	33.4%	$5d^46p(^3H)^4H$	23.2%	$5d^46p(^3H)^4I$	18.3%	$5d^46p(^3H)^2I$
88774.45	88 901	−127	4.5	31.0%	$5d^46p(^3H)^4I$	14.8%	$5d^46p(^5D)^6D$	13.3%	$5d^46p(^3G)^4H$
89340.33	89 534	−194	2.5	13.8%	$5d^46p(^3F)^4G$	12.0%	$5d^46p(^5D)^4D$	9.4%	$5d^46p(^3D)^4D$
89903.34	89 726	177	3.5	14.4%	$5d^46p(^3H)^4H$	12.5%	$5d^46p(^3G)^4F$	7.3%	$5d^46p(^3F)^4F$
90066.20	90 172	−106	3.5	30.2%	$5d^46p(^5D)^4D$	8.5%	$5d^46p(^3D)^4D$	5.9%	$5d^46p(^3D)^2F$
90735.64	90 999	−263	1.5	16.5%	$5d^36s6p(^4F)^6G$	15.7%	$5d^46p(^3P)^4P$	7.4%	$5d^46p(^5D)^4F$
90984.35	90 472	512	5.5	33.8%	$5d^46p(^3H)^4G$	12.8%	$5d^46p(^3H)^2H$	9.8%	$5d^46p(^1I)^2H$
91329.97	91 532	−202	4.5	25.6%	$5d^46p(^5D)^4F$	15.8%	$5d^46p(^3G)^4H$	15.6%	$5d^46p(^5D)^6D$
92152.76	92 115	38	3.5	16.3%	$5d^46p(^3F)^4D$	10.9%	$5d^46p(^3G)^4G$	7.5%	$5d^46p(^3G)^4H$
92449.06	92 669	−220	4.5	18.3%	$5d^46p(^5D)^4F$	9.9%	$5d^46p(^3F)^4F$	9.7%	$5d^46p(^3F)^4G$
92567.53	92 715	−147	3.5	14.0%	$5d^46p(^5D)^4D$	12.0%	$5d^46p(^3F)^4G$	0.0%	$5d^36s8p(^2D)^2F$
92617.24	92 745	−128	1.5	23.2%	$5d^46p(^5D)^4D$	14.3%	$5d^46p(^3P)^2P$	9.9%	$5d^46p(^3P)^4S$
92766.60	92 559	208	0.5	14.2%	$5d^46p(^3P)^4P$	9.2%	$5d^36s6p(^4F)^6F$	8.5%	$5d^36s6p(^4F)^4D$
93087.02	93 301	−214	2.5	18.3%	$5d^46p(^5D)^4D$	11.0%	$5d^46p(^3G)^4G$	8.7%	$5d^46p(^1D)^2F$
93504.22	93 496	8	2.5	17.9%	$5d^46p(^3P)^4D$	12.1%	$5d^46p(^5D)^4F$	11.4%	$5d^46p(^3F)^4F$
93849.58	93 881	−31	2.5	10.7%	$5d^46p(^3D)^4D$	9.5%	$5d^36s6p(^4F)^6G$	1.3%	$5d^36s6p(^2D)^4D$
94319.57	94 375	−55	3.5	22.1%	$5d^46p(^3F)^4G$	10.5%	$5d^46p(^3G)^4G$	8.1%	$5d^46p(^3G)^4F$
94398.47	94 581	−183	5.5	30.4%	$5d^46p(^3H)^2I$	18.2%	$5d^46p(^3G)^4H$	7.8%	$5d^46p(^3F)^4G$
94512.00	94 443	69	4.5	24.7%	$5d^46p(^3G)^4F$	21.9%	$5d^46p(^3H)^4H$	16.9%	$5d^46p(^3H)^4G$
94798.31	94 667	131	2.5	16.7%	$5d^46p(^3H)^4G$	12.4%	$5d^36s6p(^4F)^6G$	6.7%	$5d^46p(^5D)^4P$
94829.16	94 851	−22	3.5	13.3%	$5d^46p(^3H)^4G$	11.9%	$5d^46p(^3H)^4H$	10.4%	$5d^46p(^5D)^4F$
94960.97	94 849	112	5.5	35.1%	$5d^46p(^3H)^4I$	20.5%	$5d^46p(^3G)^4G$	15.2%	$5d^46p(^3H)^4G$
95107.85	95 022	86	1.5	17.6%	$5d^46p(^3F)^4D$	9.5%	$5d^36s6p(^4F)^6F$	6.8%	$5d^46p(^1D)^2D$
95215.65	95 169	47	0.5	17.1%	$5d^46p(^3F)^4D$	12.4%	$5d^36s6p(^4F)^6F$	6.7%	$5d^46p(^3P)^2S$
95661.73	95 735	−73	4.5	10.5%	$5d^46p(^3G)^2H$	9.8%	$5d^46p(^5D)^4F$	9.2%	$5d^46p(^3F)^4G$
96004.04	96 130	−126	1.5	20.3%	$5d^46p(^3G)^4F$	16.6%	$5d^46p(^3F)^4F$	8.8%	$5d^46p(^3F)^4F$
96236.36	95 967	269	2.5	22.7%	$5d^46p(^3G)^4G$	8.8%	$5d^46p(^3D)^4P$	6.9%	$5d^46p(^3F)^4D$
96467.39	96 650	−183	6.5	31.3%	$5d^46p(^3H)^4I$	23.8%	$5d^46p(^3G)^4H$	17.8%	$5d^46p(^1I)^2K$
96701.04	96 435	266	1.5	16.8%	$5d^46p(^3D)^4F$	12.5%	$5d^46p(^3G)^4F$	8.6%	$5d^46p(^3P)^4S$
96701.13	96 382	319	2.5	14.9%	$5d^46p(^3D)^4P$	9.4%	$5d^46p(^3H)^4G$	8.2%	$5d^46p(^3F)^4D$
96900.21	96 709	191	0.5	30.3%	$5d^36s6p(^4F)^6F$	25.0%	$5d^46p(^3D)^4D$	10.1%	$5d^46p(^5D)^4D$
97032.95	96 910	123	5.5	38.8%	$5d^46p(^3H)^4H$	18.0%	$5d^46p(^1I)^2H$	16.1%	$5d^46p(^3G)^2H$
97271.85	97 177	95	1.5	17.5%	$5d^46p(^3F)^2D$	13.6%	$5d^46p(^3G)^4F$	8.4%	$5d^46p(^3F)^2D$
97286.84	97 138	149	3.5	25.7%	$5d^36s6p(^4F)^6G$	8.9%	$5d^46p(^3F)^4F$	2.1%	$5d^46p(^1D)^2F$
97476.34	97 176	300	4.5	36.4%	$5d^46p(^3G)^4G$	10.8%	$5d^46p(^3G)^4F$	8.6%	$5d^46p(^3H)^4G$
97815.34	98 016	−201	3.5	16.2%	$5d^46p(^3F)^2G$	14.7%	$5d^46p(^3G)^4F$	1.5%	$5d^36s6p(^4F)^2G$
97826.06	97 565	261	6.5	49.5%	$5d^46p(^3H)^4H$	28.3%	$5d^46p(^3H)^4I$	19.7%	$5d^46p(^1I)^2K$
97860.52	97 931	−70	2.5	16.0%	$5d^46p(^3G)^4F$	7.3%	$5d^46p(^3P)^2D$	6.9%	$5d^46p(^3P)^4P$
98540.51	98 533	8	7.5	82.9%	$5d^46p(^3H)^4I$	16.5%	$5d^46p(^1I)^2K$	0.5%	$5d^36s6p(^2H)^4I$
98596.29	98 428	168	3.5	32.8%	$5d^46p(^3P)^4D$	10.5%	$5d^46p(^3D)^4F$	8.9%	$5d^46p(^3P)^4D$
98926.96	98 696	231	4.5	31.3%	$5d^46p(^3F)^4F$	14.1%	$5d^46p(^3H)^2G$	8.8%	$5d^46p(^3H)^4H$
99277.71	99 133	145	2.5	12.5%	$5d^46p(^3P)^4P$	12.2%	$5d^46p(^3F)^2D$	11.5%	$5d^46p(^3H)^4G$
99528.13	99 385	143	3.5	25.6%	$5d^46p(^3H)^4G$	16.8%	$5d^46p(^3H)^2G$	10.4%	$5d^36s6p(^4F)^6G$
99634.37	99 463	171	1.5	22.2%	$5d^36s6p(^4F)^6F$	10.3%	$5d^46p(^3P)^2P$	8.7%	$5d^46p(^3D)^4D$

(*continued on next page*)

Table 4 (*continued*)

E_{Exp}	$E_{HFR+CPOL}$	ΔE	J	Composition in LS coupling					
99874.56	99 553	322	5.5	37.2%	$5d^46p(^1I)^2I$	16.8%	$5d^46p(^3H)^4G$	13.4%	$5d^46p(^3F)^4G$
99923.09	99 928	−5	2.5	18.5%	$5d^36s6p(^4F)^6F$	12.2%	$5d^46p(^3P)^4P$	0.0%	$5d^36s8p(^2D)^2D$
99993.43	100 002	−9	4.5	20.6%	$5d^36s6p(^4F)^6G$	11.1%	$5d^46p(^3G)^4H$	10.4%	$5d^46p(^3H)^2G$
100309.90	100 317	−7	5.5	34.9%	$5d^46p(^3G)^4H$	11.6%	$5d^46p(^1G)^2H$	11.3%	$5d^46p(^3G)^4G$
100924.02	100 950	−26	1.5	14.8%	$5d^46p(^3D)^4P$	13.9%	$5d^46p(^3D)^4F$	9.1%	$5d^46p(^3P)^2D$
101075.86	100 716	360	3.5	16.8%	$5d^46p(^3G)^4G$	9.0%	$5d^46p(^1G)^2F$	7.4%	$5d^46p(^3F)^4F$
101190.34	101 310	−120	6.5	29.7%	$5d^46p(^3H)^2I$	24.5%	$5d^46p(^3G)^4H$	22.6%	$5d^46p(^1I)^2K$
101331.98	101 209	123	2.5	26.2%	$5d^36s6p(^4F)^6F$	7.7%	$5d^46p(^3G)^4F$	7.0%	$5d^46p(^3H)^4G$
101452.99	101 703	−250	5.5	40.0%	$5d^46p(^3H)^2I$	16.3%	$5d^46p(^3F)^4G$	12.9%	$5d^46p(^1I)^2H$
101524.43	101 794	−270	0.5	36.9%	$5d^36s6p(^4F)^6D$	27.2%	$5d^36s6p(^4P)^6D$	6.6%	$5d^36s6p(^4F)^6F$
101570.09	101 482	88	3.5	17.0%	$5d^46p(^3G)^2G$	10.0%	$5d^46p(^3F)^4F$	9.9%	$5d^46p(^3F)^2F$
101597.24	101 486	111	4.5	20.0%	$5d^36s6p(^4F)^6G$	10.8%	$5d^46p(^3F)^4F$	0.4%	$5d^36s6p(^4F)^4F$
101863.74	101 916	−52	1.5	15.5%	$5d^36s6p(^4P)^6D$	12.6%	$5d^46p(^3P)^4S$	11.2%	$5d^46p(^3P)^4P$
101975.48	102 405	−430	4.5	20.5%	$5d^46p(^3G)^2H$	15.9%	$5d^36s6p(^4F)^6G$	12.5%	$5d^46p(^3H)^2G$
102444.45	102 359	85	1.5	17.4%	$5d^46p(^3D)^4D$	14.2%	$5d^36s6p(^4F)^6D$	0.0%	$5d^36s8p(^2D)^4P$
102504.01	102 383	121	3.5	7.3%	$5d^46p(^3F)^4F$	7.1%	$5d^36s6p(^4F)^6D$	5.7%	$5d^36s6p(^4F)^6F$
102902.38	103 024	−122	3.5	16.6%	$5d^46p(^3D)^4D$	16.4%	$5d^36s6p(^4F)^6D$	11.3%	$5d^46p(^1F)^2G$
102980.06	103 087	−107	2.5	9.2%	$5d^46p(^1F)^2F$	7.5%	$5d^46p(^3H)^4G$	4.7%	$5d^46p(^3F)^2F$
103139.49	103 286	−147	4.5	26.0%	$5d^46p(^3D)^4F$	18.4%	$5d^46p(^3H)^2H$	10.5%	$5d^46p(^3F)^4G$
103629.58	103 581	49	1.5	22.9%	$5d^46p(^3G)^4F$	9.5%	$5d^46p(^3F)^4F$	8.2%	$5d^46p(^3D)^2D$
103880.12	104 064	−184	5.5	19.8%	$5d^46p(^3H)^2H$	19.2%	$5d^46p(^3G)^4G$	13.8%	$5d^36s6p(^4F)^6G$
103908.35	103 856	52	0.5	22.3%	$5d^46p(^3P)^2P$	11.7%	$5d^36s6p(^4F)^6D$	10.6%	$5d^46p(^1S)^2P$
104145.96	103 774	372	2.5	10.1%	$5d^46p(^3G)^4G$	9.4%	$5d^46p(^3D)^4F$	9.1%	$5d^46p(^3D)^4P$
104173.50	104 270	−96	4.5	25.0%	$5d^46p(^3D)^4F$	11.8%	$5d^46p(^1I)^2H$	6.2%	$5d^46p(^3F)^2G$
104365.42	104 253	112	2.5	14.0%	$5d^46p(^3F)^4D$	13.3%	$5d^46p(^3G)^4F$	9.1%	$5d^46p(^3F)^2F$
104552.00	104 360	192	3.5	26.2%	$5d^36s6p(^4F)^6F$	18.2%	$5d^46p(^3D)^4D$	5.6%	$5d^46p(^3F)^4D$
104565.42	104 537	28	1.5	18.4%	$5d^46p(^3D)^4P$	6.8%	$5d^36s6p(^4P)^6D$	6.0%	$5d^46p(^3F)^4D$
104741.39	104 818	−77	0.5	20.9%	$5d^36s6p(^4P)^6D$	14.0%	$5d^36s6p(^4F)^6D$	8.4%	$5d^46p(^3P)^2P$
104843.57	105 126	−282	3.5	15.9%	$5d^46p(^3F)^2G$	15.7%	$5d^46p(^3G)^4F$	13.8%	$5d^46p(^1G)^2G$
105066.16	105 038	28	1.5	38.0%	$5d^36s6p(^4F)^6D$	6.7%	$5d^36s6p(^4F)^6F$	6.0%	$5d^46p(^3P)^4P$
105130.18	105 399	−269	6.5	39.2%	$5d^46p(^3G)^4H$	32.8%	$5d^46p(^3H)^2I$	9.4%	$5d^46p(^3H)^4I$
105231.14	104 914	317	4.5	11.1%	$5d^46p(^3D)^4F$	10.4%	$5d^46p(^1G)^2G$	9.9%	$5d^46p(^1G)^2H$
105448.80	105 545	−96	2.5	43.1%	$5d^36s6p(^4F)^6D$	13.7%	$5d^36s6p(^4F)^6F$	7.3%	$5d^36s6p(^4P)^6D$
105505.83	105 651	−145	4.5	40.0%	$5d^36s6p(^4F)^6D$	19.5%	$5d^36s6p(^4F)^6F$	5.5%	$5d^36s6p(^4F)^6G$
105508.74	105 658	−149	5.5	43.5%	$5d^36s6p(^4F)^6G$	15.2%	$5d^46p(^3H)^2H$	11.8%	$5d^46p(^3G)^4G$
105984.55	105 743	242	3.5	8.5%	$5d^46p(^1F)^2F$	8.4%	$5d^46p(^3F)^2F$	7.1%	$5d^46p(^3G)^2F$
106007.90	106 200	−192	2.5	22.1%	$5d^46p(^3G)^2F$	8.1%	$5d^46p(^1F)^2F$	7.0%	$5d^46p(^3D)^2F$
106211.02	106 250	−39	3.5	17.4%	$5d^46p(^3G)^2G$	13.4%	$5d^46p(^3F)^2F$	7.8%	$5d^46p(^1F)^2F$
106478.75	106 219	260	0.5	48.0%	$5d^46p(^3D)^4P$	12.1%	$5d^36s6p(^4F)^6D$	8.5%	$5d^46p(^3P)^4P$
106669.93	106 846	−176	3.5	23.3%	$5d^46p(^3D)^2F$	9.7%	$5d^46p(^3G)^2F$	8.5%	$5d^46p(^1F)^2G$
106870.05	107 014	−144	2.5	10.0%	$5d^46p(^3P)^2D$	9.8%	$5d^46p(^1F)^2D$	7.7%	$5d^36s6p(^4F)^4G$
107141.42	107 510	−369	2.5	24.0%	$5d^46p(^3P)^2D$	7.1%	$5d^46p(^1D)^2D$	5.6%	$5d^46p(^3P)^4P$
107385.70	107 230	156	6.5	53.6%	$5d^46p(^1I)^2I$	29.4%	$5d^46p(^1I)^2K$	10.4%	$5d^46p(^3H)^4H$
107421.26	107 610	−187	3.5	32.1%	$5d^36s6p(^4F)^6D$	18.9%	$5d^36s6p(^4F)^6F$	12.5%	$5d^46p(^3D)^2F$
107959.22	108 218	−259	5.5	17.1%	$5d^46p(^3H)^2H$	15.6%	$5d^46p(^1I)^2I$	12.8%	$5d^46p(^3G)^2H$
108563.21	108 816	−253	7.5	83.5%	$5d^46p(^1I)^2K$	16.3%	$5d^46p(^3H)^4I$	0.2%	$5d^36s6p(^2H)^4I$
108625.11	108 526	99	4.5	16.4%	$5d^46p(^3G)^2G$	6.7%	$5d^36s6p(^4F)^6D$	5.8%	$5d^46p(^3F)^4G$
108855.91	108 921	−65	3.5	17.5%	$5d^36s6p(^2G)^4H$	8.7%	$5d^36s6p(^4F)^6F$	7.9%	$5d^36s6p(^2G)^4G$
108864.14	109 097	−233	2.5	24.8%	$5d^46p(^3D)^2D$	6.9%	$5d^46p(^3F)^4F$	5.3%	$5d^46p(^3F)^2F$
108924.72	108 690	235	5.5	32.1%	$5d^46p(^3G)^2H$	17.8%	$5d^46p(^1G)^2H$	17.6%	$5d^46p(^1I)^2H$
109014.70	108 905	110	4.5	28.7%	$5d^36s6p(^4F)^6F$	18.6%	$5d^36s6p(^4F)^6D$	9.2%	$5d^36s6p(^4F)^6G$
110134.96	110 125	10	4.5	42.1%	$5d^46p(^1I)^2H$	8.7%	$5d^46p(^1F)^2G$	6.4%	$5d^46p(^3G)^2G$
110180.06	110 294	−114	2.5	38.3%	$5d^36s6p(^4P)^6P$	9.9%	$5d^36s6p(^4P)^6D$	5.5%	$5d^36s6p(^4P)^6S$
110812.23	110 992	−180	4.5	14.1%	$5d^46p(^1G)^2H$	11.0%	$5d^46p(^1G)^2G$	8.0%	$5d^46p(^1G)^2G$
110994.14	111 334	−340	2.5	17.2%	$5d^46p(^3F)^4F$	7.8%	$5d^46p(^3F)^4G$	5.3%	$5d^46p(^3F)^4G$
111037.21	110 803	234	5.5	35.7%	$5d^36s6p(^4F)^6F$	22.5%	$5d^36s6p(^4F)^6G$	8.7%	$5d^36s6p(^2G)^4G$
111151.60	111 412	−260	3.5	14.2%	$5d^46p(^1F)^2F$	7.3%	$5d^46p(^3G)^2F$	4.4%	$5d^46p(^1G)^2F$
111235.52	111 325	−89	4.5	17.4%	$5d^36s6p(^4F)^6F$	15.6%	$5d^36s6p(^2G)^4H$	15.2%	$5d^36s6p(^2H)^4I$
111868.40	111 738	130	2.5	17.6%	$5d^36s6p(^4P)^6P$	8.7%	$5d^46p(^3P)^2D$	0.7%	$5d^36s6p(^4F)^4F$
112826.67	113 114	−287	5.5	30.2%	$5d^46p(^1G)^2H$	10.5%	$5d^46p(^3F)^4G$	8.8%	$5d^46p(^3H)^2H$
113012.11	112 842	170	3.5	8.6%	$5d^46p(^3P)^4D$	6.7%	$5d^46p(^3F)^2G$	1.1%	$5d^36s6p(^2D)^4F$
113888.11	113 682	206	2.5	16.4%	$5d^36s6p(^4P)^6P$	9.8%	$5d^46p(^1G)^2F$	3.4%	$5d^46p(^3P)^4P$
114220.18	114 229	−9	4.5	15.7%	$5d^46p(^1F)^2G$	13.4%	$5d^46p(^3F)^4G$	7.7%	$5d^46p(^1I)^2H$
114296.66	114 322	−25	2.5	16.0%	$5d^46p(^3P)^2D$	14.5%	$5d^46p(^3D)^2F$	8.4%	$5d^46p(^1D)^2F$
114412.98	114 220	193	3.5	20.0%	$5d^36s6p(^4P)^6P$	11.0%	$5d^46p(^3F)^4G$	7.2%	$5d^46p(^3G)^2F$
114549.19	114 697	−148	5.5	25.5%	$5d^36s6p(^4F)^6F$	24.2%	$5d^36s6p(^2H)^4I$	15.8%	$5d^36s6p(^2G)^4H$
115167.44	114 737	430	3.5	22.8%	$5d^36s6p(^4P)^6P$	11.4%	$5d^36s6p(^4F)^4G$	4.7%	$5d^46p(^1G)^2F$
115336.80	115 363	−26	4.5	26.6%	$5d^46p(^3F)^4F$	12.0%	$5d^46p(^1F)^2G$	7.5%	$5d^46p(^1G)^2G$
117929.36	117 612	317	4.5	24.3%	$5d^36s6p(^2H)^4H$	11.1%	$5d^36s6p(^2H)^4G$	10.4%	$5d^36s6p(^2G)^4F$
118701.09	118 492	209	3.5	24.0%	$5d^46p(^3P)^4D$	8.8%	$5d^36s6p(^4P)^6P$	6.9%	$5d^46p(^3F)^4D$
119243.60	119 396	−152	5.5	25.0%	$5d^46p(^3F)^4G$	24.5%	$5d^46p(^1G)^2H$	14.6%	$5d^36s6p(^2H)^4H$
120153.36	119 744	409	3.5	18.6%	$5d^36s6p(^2H)^4H$	9.0%	$5d^46p(^3F)^4D$	5.9%	$5d^46p(^3F)^4D$
120845.21	120 679	166	6.5	48.0%	$5d^36s6p(^2H)^4H$	35.0%	$5d^36s6p(^2H)^4I$	7.1%	$5d^36s6p(^2G)^4H$
120943.64	120 957	−13	5.5	39.1%	$5d^46p(^3F)^4G$	15.2%	$5d^36s6p(^2H)^4H$	8.8%	$5d^46p(^3F)^4G$
121263.59	121 517	−253	3.5	16.1%	$5d^46p(^3F)^4F$	11.2%	$5d^36s6p(^2G)^4G$	4.0%	$5d^46p(^1G)^2F$

(*continued on next page*)

Table 4 (*continued*)

E_{Exp}	$E_{HFR+CPOL}$	ΔE	J	Composition in LS coupling					
123649.48	123 601	48	4.5	20.2%	$5d^3 6s6p(^2G)^4H$	14.3%	$5d^3 6s6p(^2G)^4G$	12.9%	$5d^3 6s6p(^2H)^4H$
123818.07	123 948	−130	5.5	27.4%	$5d^3 6s6p(^2H)^4I$	22.0%	$5d^3 6s6p(^2G)^4G$	19.3%	$5d^3 6s6p(^2H)^4H$
124290.98	124 313	−22	4.5	11.9%	$5d^3 6s6p(^2H)^4G$	10.7%	$5d^3 6s6p(^4F)^4G$	1.5%	$5d^3 6s6p(^4F)^4F$
124643.76	124 683	−39	4.5	24.6%	$5d^4 6p(^3F)^2G$	6.8%	$5d^3 6s6p(^2G)^4H$	6.1%	$5d^3 6s6p(^2H)^4H$
125116.00	125 211	−95	5.5	21.3%	$5d^3 6s6p(^4F)^4G$	18.3%	$5d^3 6s6p(^4F)^4G$	16.1%	$5d^3 6s6p(^2H)^4G$
126252.50	126 296	−43	3.5	18.4%	$5d^3 6s6p(^2D)^4D$	16.2%	$5d^3 6s6p(^2F)^4D$	14.0%	$5d^3 6s6p(^2F)^4F$
126545.18	126 528	17	6.5	30.8%	$5d^3 6s6p(^2H)^4H$	29.7%	$5d^3 6s6p(^2G)^4H$	14.4%	$5d^3 6s6p(^2H)^4I$
137911.82	138 100	−188	6.5	48.9%	$5d^3 6s6p(^2H)^2I$	22.4%	$5d^3 6s6p(^2H)^2I$	21.1%	$5d^3 6s6p(^2G)^4H$

Table 5
Comparison between the energy levels computed with the HFR+CPOL approach and the available experimental values in Re IV.

E_{Exp}	$E_{HFR+CPOL}$	ΔE	J	Composition in LS coupling					
Even parity									
0.00	−73	73	0	66.5%	$5d^4(^5D)^5D$	15.9%	$5d^4(^3P)^3P$	14.4%	$5d^4(^3P)^3P$
3084.09	3093	−9	1	84.9%	$5d^4(^5D)^5D$	8.0%	$5d^4(^3P)^3P$	6.4%	$5d^4(^3P)^3P$
5978.67	6017	−38	2	92.6%	$5d^4(^5D)^5D$	2.6%	$5d^4(^3P)^3P$	1.7%	$5d^4(^3D)^3D$
8350.18	8358	−8	3	89.2%	$5d^4(^5D)^5D$	3.6%	$5d^4(^3F)^3F$	3.4%	$5d^4(^3D)^3D$
10121.14	10 059	62	4	74.4%	$5d^4(^5D)^5D$	14.1%	$5d^4(^3F)^3F$	5.3%	$5d^4(^3F)^3F$
14503.47	14 580	−77	0	34.1%	$5d^4(^3P)^3P$	32.4%	$5d^4(^5D)^5D$	19.6%	$5d^4(^3P)^3P$
16946.38	16 994	−48	4	57.2%	$5d^4(^3H)^3H$	15.2%	$5d^4(^3G)^3G$	11.3%	$5d^4(^5D)^5D$
19339.89	19 378	−38	1	52.8%	$5d^4(^3P)^3P$	22.5%	$5d^4(^3P)^3P$	12.1%	$5d^4(^5D)^5D$
19817.09	19 823	−6	3	57.9%	$5d^4(^3G)^3G$	17.7%	$5d^4(^3F)^3F$	12.6%	$5d^4(^3F)^3F$
19850.51	19 855	−4	2	50.4%	$5d^4(^3F)^3F$	18.1%	$5d^4(^3F)^3F$	13.8%	$5d^4(^1D)^1D$
20929.53	20 958	−28	5	76.9%	$5d^4(^3H)^3H$	22.5%	$5d^4(^3G)^3G$	0.3%	$5d^36s(^2H)^3H$
22895.90	22 886	10	6	77.8%	$5d^4(^3H)^3H$	21.9%	$5d^4(^1I)^1I$	0.3%	$5d^36s(^2H)^3H$
24323.66	24 350	−26	4	37.5%	$5d^4(^3G)^3G$	26.8%	$5d^4(^3H)^3H$	19.3%	$5d^4(^3F)^3F$
24352.16	24 318	34	2	47.7%	$5d^4(^3P)^3P$	31.6%	$5d^4(^3D)^3D$	10.8%	$5d^4(^3P)^3P$
26044.01	26 046	−2	4	30.7%	$5d^4(^3G)^3G$	29.8%	$5d^4(^3F)^3F$	20.9%	$5d^4(^1G)^1G$
26475.63	26 473	3	3	54.7%	$5d^4(^3F)^3F$	17.7%	$5d^4(^3D)^3D$	13.4%	$5d^4(^3G)^3G$
28526.28	28 465	61	3	56.8%	$5d^4(^3D)^3D$	20.5%	$5d^4(^3G)^3G$	8.1%	$5d^4(^3F)^3F$
29200.98	29 260	−59	2	21.9%	$5d^4(^3D)^3D$	21.7%	$5d^4(^1D)^1D$	16.5%	$5d^4(^3P)^3P$
30051.68	30 030	22	5	75.7%	$5d^4(^3G)^3G$	22.5%	$5d^4(^3H)^3H$	1.3%	$5d^36s(^2G)^3G$
31542.72	31 554	−11	1	86.1%	$5d^4(^3D)^3D$	5.1%	$5d^4(^3P)^3P$	2.4%	$5d^36s(^2D)^3D$
32395.83	32 430	−34	6	78.1%	$5d^4(^1I)^1I$	21.7%	$5d^4(^3H)^3H$	0.1%	$5d^36s(^2H)^3H$
35596.79	35 562	35	2	27.3%	$5d^4(^3D)^3D$	25.6%	$5d^4(^3P)^3P$	21.9%	$5d^4(^1D)^1D$
36034.31	35 961	73	4	46.2%	$5d^4(^1G)^1G$	25.0%	$5d^4(^3F)^3F$	8.6%	$5d^4(^3H)^3H$
36484.41	36 505	−21	0	59.8%	$5d^4(^1S)^1S$	19.7%	$5d^4(^3P)^3P$	17.2%	$5d^4(^1S)^1S$
38457.74	38 385	73	3	66.1%	$5d^4(^1F)^1F$	16.9%	$5d^4(^3D)^3D$	6.8%	$5d^4(^3F)^3F$
39117.76	39 095	23	1	89.6%	$5d^36s(^4F)^5F$	4.4%	$5d^36s(^2D)^3D$	3.0%	$5d^36s(^2D)^3D$
41099.59	41 108	−8	2	67.4%	$5d^36s(^4F)^5F$	12.4%	$5d^4(^3P)^3P$	3.2%	$5d^36s(^2D)^3D$
41601.56	41 536	66	2	45.7%	$5d^4(^3P)^3P$	22.0%	$5d^36s(^4F)^5F$	11.8%	$5d^4(^3P)^3P$
44328.51	44 350	−21	3	93.7%	$5d^36s(^4F)^5F$	1.7%	$5d^36s(^4F)^3F$	1.5%	$5d^36s(^2D)^3D$
44725.81	44 587	139	4	63.2%	$5d^4(^3F)^3F$	27.2%	$5d^4(^1G)^1G$	2.4%	$5d^4(^3G)^3G$
45502.44	45 602	−100	2	47.6%	$5d^4(^3F)^3F$	23.7%	$5d^4(^3F)^3F$	12.8%	$5d^4(^1D)^1D$
45947.27	45 979	−32	1	56.0%	$5d^4(^3P)^3P$	30.6%	$5d^4(^3P)^3P$	5.5%	$5d^36s(^4P)^3P$
46525.20	46 542	−17	3	64.9%	$5d^4(^3F)^3F$	14.3%	$5d^4(^3F)^3F$	12.7%	$5d^4(^1F)^1F$
47703.16	47 714	−11	4	89.2%	$5d^36s(^4F)^5F$	5.7%	$5d^36s(^2G)^3G$	1.6%	$5d^4(^3F)^3F$
48745.80	48 777	−31	0	54.8%	$5d^4(^3P)^3P$	23.1%	$5d^4(^3P)^3P$	12.6%	$5d^4(^1S)^1S$
49208.90	49 243	−34	4	43.0%	$5d^4(^1G)^1G$	18.6%	$5d^4(^1G)^1G$	17.7%	$5d^4(^3F)^3F$
50820.82	50 840	−19	5	82.5%	$5d^36s(^4F)^5F$	15.0%	$5d^36s(^2G)^3G$	1.3%	$5d^36s(^2H)^3H$
52384.70	52 368	17	2	49.4%	$5d^36s(^4P)^5P$	19.7%	$5d^36s(^2P)^3P$	10.2%	$5d^36s(^4F)^3F$
53222.25	53 233	−11	1	78.1%	$5d^36s(^4P)^5P$	15.1%	$5d^36s(^2P)^3P$	3.2%	$5d^4(^3P)^3P$
55502.70	55 533	−30	2	62.6%	$5d^36s(^4F)^3F$	20.0%	$5d^36s(^4P)^5P$	3.7%	$5d^4(^1D)^1D$
57931.16	57 898	33	3	42.1%	$5d^36s(^2G)^3G$	28.5%	$5d^36s(^4F)^3F$	19.9%	$5d^36s(^4P)^5P$
58757.85	58 739	19	3	74.5%	$5d^36s(^4P)^5P$	15.3%	$5d^36s(^2G)^3G$	6.2%	$5d^36s(^4F)^3F$
59116.79	59 056	61	4	42.4%	$5d^36s(^2G)^3G$	37.6%	$5d^36s(^2H)^3H$	11.5%	$5d^36s(^4F)^3F$
60858.33	60 839	19	1	29.5%	$5d^36s(^2D)^3D$	19.2%	$5d^36s(^2P)^1P$	12.8%	$5d^36s(^2D)^3D$
61519.13	61 551	−32	0	81.1%	$5d^36s(^2P)^3P$	12.2%	$5d^36s(^4P)^3P$	2.5%	$5d^4(^3P)^3P$
61557.12	61 676	−119	5	45.4%	$5d^36s(^2H)^3H$	31.8%	$5d^36s(^2G)^3G$	12.7%	$5d^36s(^4F)^5F$
63119.85	63 060	60	3	52.3%	$5d^36s(^4F)^3F$	37.1%	$5d^36s(^2G)^3G$	3.2%	$5d^36s(^4F)^5F$
63934.66	63 910	25	4	33.4%	$5d^36s(^2G)^3G$	28.7%	$5d^36s(^2G)^1G$	11.0%	$5d^36s(^4F)^3F$
64843.35	64 857	−14	2	27.0%	$5d^36s(^2D)^3D$	25.0%	$5d^36s(^2P)^3P$	24.9%	$5d^36s(^4P)^5P$
65907.48	65 821	86	4	52.3%	$5d^36s(^4F)^3F$	40.4%	$5d^36s(^2H)^3H$	4.2%	$5d^36s(^2G)^3G$
66323.75	66 341	−17	1	57.2%	$5d^36s(^2P)^3P$	22.3%	$5d^36s(^2P)^1P$	10.9%	$5d^36s(^4P)^5P$
67802.22	67 935	−133	6	99.3%	$5d^36s(^2H)^3H$	0.4%	$5d^4(^3H)^3H$	0.2%	$5d^26p^2(^3F)^3H$
69982.88	69 913	70	5	52.6%	$5d^36s(^2H)^3H$	35.0%	$5d^36s(^2G)^3G$	8.1%	$5d^36s(^2H)^1H$
70710.10	70 741	−31	3	79.0%	$5d^36s(^2d)^3D$	8.7%	$5d^36s(^2D)^3D$	5.5%	$5d^36s(^4F)^3F$
70811.30	70 775	36	2	25.4%	$5d^36s(^4P)^3P$	24.4%	$5d^36s(^2D)^3D$	15.8%	$5d^36s(^2P)^3P$
71331.28	71 333	−2	1	44.9%	$5d^36s(^4P)^3P$	26.3%	$5d^36s(^2D)^3D$	9.3%	$5d^36s(^2D)^3D$
72990.87	73 096	−105	0	75.4%	$5d^36s(^4P)^3P$	10.9%	$5d^36s(^2P)^3P$	5.4%	$5d^4(^1S)^1S$
74604.60	74 617	−12	5	81.9%	$5d^36s(^2H)^1H$	16.4%	$5d^36s(^2G)^3G$	1.0%	$5d^36s(^4F)^5F$
75318.37	75 251	67	2	61.4%	$5d^36s(^2F)^3F$	12.5%	$5d^36s(^2D)^3D$	10.7%	$5d^36s(^2P)^3P$
75421.36	75 400	21	3	87.4%	$5d^36s(^2F)^3F$	3.9%	$5d^36s(^2D)^3D$	3.2%	$5d^36s(^2D)^3D$
75722.03	75 707	15	4	52.2%	$5d^36s(^2F)^3F$	14.5%	$5d^36s(^4F)^3F$	12.9%	$5d^36s(^2G)^1G$
76466.25	76 427	39	4	41.9%	$5d^36s(^2G)^1G$	37.8%	$5d^36s(^2F)^3F$	6.9%	$5d^36s(^4F)^3F$
76798.48	76 781	17	2	57.3%	$5d^36s(^4P)^3P$	21.2%	$5d^36s(^2F)^3F$	8.4%	$5d^36s(^2P)^3P$
78474.88	78 523	−48	2	53.9%	$5d^36s(^2D)^1D$	11.8%	$5d^36s(^2D)^1D$	10.8%	$5d^36s(^2P)^3P$
83520.75	83 536	−15	3	79.2%	$5d^36s(^2F)^1F$	11.3%	$5d^36s(^2D)^3D$	3.6%	$5d^4(^1F)^1F$
Odd parity									
95642.75	95 822	−179	2	65.4%	$5d^36p(^4F)^5G$	11.8%	$5d^36p(^4F)^3F$	8.7%	$5d^36p(^2D)^3F$
99039.24	98 665	374	1	42.5%	$5d^36p(^4F)^3D$	35.4%	$5d^36p(^4F)^5F$	4.7%	$5d^36p(^4F)^5D$
101184.06	101 378	−194	3	77.5%	$5d^36p(^4F)^5G$	8.8%	$5d^36p(^4F)^3F$	3.5%	$5d^36p(^2D)^3F$
102740.89	102 872	−131	2	32.7%	$5d^36p(^4F)^3D$	32.1%	$5d^36p(^4F)^5F$	10.2%	$5d^36p(^4F)^5D$
105653.00	105 821	−168	4	59.3%	$5d^36p(^4F)^5G$	10.7%	$5d^36p(^4F)^3G$	8.7%	$5d^36p(^2G)^3H$
108147.80	107 964	184	3	33.4%	$5d^36p(^4F)^5F$	23.6%	$5d^36p(^4F)^5D$	18.9%	$5d^36p(^4F)^3D$
108261.46	108 544	−283	1	33.2%	$5d^36p(^4P)^5D$	16.3%	$5d^36p(^2P)^3D$	13.0%	$5d^36p(^2P)^3P$
108440.86	109 055	−614	0	42.6%	$5d^36p(^4P)^5D$	19.6%	$5d^36p(^2P)^3P$	18.4%	$5d^36p(^4F)^5D$

(continued on next page)

Table 5 (*continued*)

E_{Exp}	$E_{HFR+CPOL}$	ΔE	J	Composition in LS coupling					
108572.85	108 542	31	2	17.9%	$5d^36p(^4P)^5D$	14.7%	$5d^36p(^4F)^5F$	7.3%	$5d^36p(^2P)^1D$
108664.39	108 775	−111	5	23.8%	$5d^36p(^4F)^5G$	16.6%	$5d^36p(^4F)^3G$	14.5%	$5d^36p(^2G)^3H$
111271.09	111 362	−91	0	48.3%	$5d^36p(^4F)^5D$	19.3%	$5d^36p(^2P)^1S$	11.6%	$5d^36p(^4P)^3P$
111284.25	111 167	117	1	37.7%	$5d^36p(^4F)^5F$	15.7%	$5d^36p(^4F)^5D$	9.4%	$5d^36p(^2P)^3D$
111928.65	111 612	316	4	33.7%	$5d^36p(^4F)^5D$	13.1%	$5d^36p(^2G)^3F$	11.8%	$5d^36p(^4F)^5F$
113073.16	113 194	−121	3	34.6%	$5d^36p(^4F)^3G$	17.2%	$5d^36p(^4F)^5D$	10.6%	$5d^36p(^2G)^3G$
113169.81	113 267	−97	2	34.9%	$5d^36p(^4F)^5D$	32.6%	$5d^36p(^4F)^5F$	8.5%	$5d^36p(^4F)^3F$
114013.68	113 387	627	1	32.4%	$5d^36p(^4P)^5P$	25.4%	$5d^36p(^4F)^5D$	7.0%	$5d^36p(^2P)^3S$
114377.71	114 521	−143	4	33.1%	$5d^36p(^2G)^3H$	25.5%	$5d^36p(^4F)^5G$	11.0%	$5d^36p(^4F)^5D$
116093.40	116 158	−65	3	34.6%	$5d^36p(^4F)^5F$	16.0%	$5d^36p(^2G)^3G$	9.0%	$5d^36p(^4F)^5D$
116539.61	116 670	−130	5	51.5%	$5d^36p(^4F)^5G$	22.3%	$5d^36p(^2H)^3I$	7.2%	$5d^36p(^2H)^1H$
117141.27	117 032	109	3	26.5%	$5d^36p(^4P)^5D$	16.9%	$5d^36p(^4F)^5F$	9.1%	$5d^36p(^4F)^3D$
117144.08	117 053	91	1	38.1%	$5d^36p(^4F)^5D$	21.6%	$5d^36p(^4F)^3D$	13.8%	$5d^36p(^4F)^5F$
117146.54	117 120	27	4	42.1%	$5d^36p(^4F)^5F$	13.6%	$5d^36p(^2H)^3H$	12.4%	$5d^36p(^2G)^3H$
117565.57	117 457	109	2	38.7%	$5d^36p(^4P)^5P$	20.6%	$5d^36p(^4P)^3P$	12.6%	$5d^36p(^4P)^5S$
117952.85	118 051	−98	2	18.6%	$5d^36p(^4F)^3F$	15.3%	$5d^36p(^4P)^5D$	13.1%	$5d^36p(^2D)^3F$
119416.52	119 350	67	5	34.4%	$5d^36p(^4F)^5F$	17.2%	$5d^36p(^4F)^5G$	15.5%	$5d^36p(^4F)^3G$
119970.09	120 189	−219	3	29.1%	$5d^36p(^4F)^3G$	14.8%	$5d^36p(^2G)^1F$	11.6%	$5d^36p(^4F)^5D$
120179.98	120 299	−119	1	28.0%	$5d^36p(^4P)^5D$	24.9%	$5d^36p(^2P)^3D$	6.4%	$5d^36p(^2D)^3P$
120284.01	119 837	447	4	22.9%	$5d^36p(^4F)^5D$	19.0%	$5d^36p(^2H)^3H$	0.2%	$5d^26s6p(^1G)^1G$
120418.94	120 289	130	2	27.9%	$5d^36p(^4F)^5D$	25.5%	$5d^36p(^4F)^3D$	14.4%	$5d^36p(^4P)^5P$
120439.96	120 304	136	6	69.8%	$5d^36p(^4F)^5G$	21.5%	$5d^36p(^2G)^3H$	5.8%	$5d^36p(^2H)^3I$
121577.29	121 809	−232	2	36.1%	$5d^36p(^4F)^3F$	11.6%	$5d^36p(^4P)^5D$	9.9%	$5d^36p(^2D)^3F$
122276.03	122 264	12	3	30.0%	$5d^36p(^4F)^3F$	11.4%	$5d^36p(^4F)^5D$	10.6%	$5d^36p(^4P)^5P$
122592.46	122 416	176	0	39.8%	$5d^36p(^2P)^3P$	20.2%	$5d^36p(^4F)^5D$	19.3%	$5d^36p(^4P)^3P$
123169.82	123 374	−204	4	48.0%	$5d^36p(^4F)^3G$	28.8%	$5d^36p(^4F)^5F$	7.4%	$5d^36p(^2G)^1G$
123550.38	123 050	500	3	36.0%	$5d^36p(^4P)^5P$	16.4%	$5d^36p(^2P)^3D$	10.8%	$5d^36p(^4F)^3D$
123838.92	123 463	376	1	28.0%	$5d^36p(^2P)^3D$	25.3%	$5d^36p(^4P)^5P$	11.7%	$5d^36p(^2P)^3P$
124007.37	123 925	82	2	21.3%	$5d^36p(^4P)^5P$	14.8%	$5d^36p(^4P)^5D$	11.2%	$5d^36p(^2P)^3D$
124629.23	124 652	−23	6	38.3%	$5d^36p(^2H)^3H$	37.4%	$5d^36p(^2H)^3I$	13.1%	$5d^36p(^2H)^1I$
124849.98	124 811	39	5	41.5%	$5d^36p(^2H)^3H$	19.8%	$5d^36p(^2H)^3G$	11.0%	$5d^36p(^4F)^5F$
124923.63	124 997	−73	4	36.0%	$5d^36p(^4F)^3F$	14.3%	$5d^36p(^2G)^3F$	7.5%	$5d^36p(^4F)^5D$
125064.02	125 028	36	3	28.6%	$5d^36p(^4P)^5D$	20.6%	$5d^36p(^4F)^3D$	15.9%	$5d^36p(^2G)^3F$
126012.61	126 332	−319	1	47.1%	$5d^36p(^4P)^3P$	13.6%	$5d^36p(^4P)^5D$	13.0%	$5d^36p(^2P)^3S$
126510.33	126 589	−79	2	26.5%	$5d^36p(^2D)^3D$	17.9%	$5d^36p(^2D)^3P$	14.9%	$5d^36p(^2P)^3P$
127611.60	127 647	−35	5	31.5%	$5d^36p(^2G)^3H$	23.3%	$5d^36p(^2H)^3I$	20.7%	$5d^36p(^4F)^5F$
127867.69	128 071	−203	4	53.9%	$5d^36p(^2G)^3G$	10.0%	$5d^36p(^2G)^3F$	8.9%	$5d^36p(^2H)^3H$
128587.37	128 680	−93	3	16.2%	$5d^36p(^4F)^3F$	12.5%	$5d^36p(^2F)^3G$	0.0%	$5d^26s7s(^1D)^1F$
128917.62	129 142	−224	5	28.6%	$5d^36p(^4F)^3G$	26.3%	$5d^36p(^2G)^3G$	14.4%	$5d^36p(^2H)^3I$
129151.61	128 974	178	1	21.8%	$5d^36p(^4P)^3D$	27.1%	$5d^36p(^2P)^1P$	3.9%	$5d^36p(^2D)^3P$
129345.74	129 329	17	2	27.8%	$5d^36p(^2F)^3F$	18.9%	$5d^36p(^2F)^1D$	9.6%	$5d^36p(^4P)^5P$
129514.45	129 639	−125	2	25.9%	$5d^36p(^2G)^3F$	13.6%	$5d^36p(^2P)^1D$	9.6%	$5d^36p(^2D)^3F$
129824.96	129 847	−22	4	25.4%	$5d^36p(^2G)^3F$	16.0%	$5d^36p(^2H)^3H$	12.4%	$5d^36p(^2G)^3H$
129879.97	129 784	96	3	18.5%	$5d^36p(^2D)^3F$	13.8%	$5d^36p(^2F)^3G$	10.9%	$5d^36p(^2G)^3G$
130501.89	130 617	−115	2	22.6%	$5d^36p(^4P)^3D$	16.3%	$5d^36p(^2D)^3P$	14.7%	$5d^36p(^2P)^3D$
130600.98	130 497	104	4	55.2%	$5d^36p(^4P)^5D$	7.9%	$5d^36p(^2H)^1G$	7.4%	$5d^36p(^2F)^3G$
130800.63	130 706	95	5	35.1%	$5d^36p(^2G)^3H$	18.9%	$5d^36p(^2H)^3H$	14.4%	$5d^36p(^4F)^5F$
131638.02	131 449	189	3	14.0%	$5d^36p(^2F)^3D$	9.9%	$5d^36p(^4P)^3D$	7.5%	$5d^36p(^2G)^3G$
131729.72	131 700	30	6	33.1%	$5d^36p(^2H)^1I$	31.7%	$5d^36p(^2G)^3H$	14.4%	$5d^36p(^4F)^5G$
132053.22	132 122	−69	1	41.7%	$5d^36p(^2P)^3P$	9.7%	$5d^36p(^2D)^3P$	9.7%	$5d^36p(^2D)^1P$
132120.22	132 038	82	4	21.2%	$5d^36p(^2F)^1G$	13.8%	$5d^36p(^4P)^5D$	11.6%	$5d^36p(^2F)^3G$
133152.54	133 343	−190	3	14.0%	$5d^36p(^2F)^3D$	10.9%	$5d^36p(^2D)^3D$	7.5%	$5d^36p(^4P)^5P$
133503.65	133 332	172	4	23.9%	$5d^36p(^2G)^1G$	19.0%	$5d^36p(^2H)^3G$	10.7%	$5d^36p(^2H)^1G$
133523.38	133 472	51	1	31.4%	$5d^36p(^2P)^3S$	21.0%	$5d^36p(^2D)^3D$	9.0%	$5d^36p(^4P)^5P$
133535.92	133 647	−111	2	39.5%	$5d^36p(^2G)^3F$	23.3%	$5d^36p(^4P)^5S$	9.2%	$5d^36p(^4P)^3P$
133918.71	133 735	183	3	21.9%	$5d^36p(^2G)^3G$	21.1%	$5d^36p(^2F)^3G$	18.2%	$5d^36p(^2G)^3F$
134058.65	134 041	18	2	28.9%	$5d^36p(^4P)^5S$	16.5%	$5d^36p(^2P)^3D$	8.8%	$5d^36p(^2G)^3F$
134147.73	133 895	253	5	40.9%	$5d^36p(^2G)^1H$	22.2%	$5d^36p(^2H)^3G$	13.1%	$5d^36p(^4F)^3G$
134853.68	134 728	126	2	18.9%	$5d^36p(^2F)^3F$	15.2%	$5d^36p(^2P)^1D$	14.7%	$5d^36p(^4P)^3P$
135091.82	134 999	93	3	25.0%	$5d^36p(^2H)^3G$	16.6%	$5d^36p(^2F)^3F$	9.4%	$5d^36p(^4P)^5D$
135884.40	135 804	80	6	43.5%	$5d^36p(^2H)^3H$	36.0%	$5d^36p(^2H)^3I$	9.3%	$5d^36p(^2G)^3H$
136397.49	136 616	−219	1	41.5%	$5d^36p(^4P)^3D$	16.3%	$5d^36p(^2D)^3D$	13.7%	$5d^36p(^2P)^3S$
137293.23	137 321	−28	3	42.0%	$5d^36p(^4P)^3D$	11.8%	$5d^36p(^4F)^3D$	9.9%	$5d^36p(^4P)^5P$
137793.42	137 871	−78	7	100.0%	$5d^36p(^2H)^3I$				
138006.35	138 028	−22	2	26.4%	$5d^36p(^4P)^3D$	20.0%	$5d^36p(^2D)^3D$	10.7%	$5d^36p(^2D)^3D$
138653.23	138 746	−93	5	37.9%	$5d^36p(^2H)^1H$	35.2%	$5d^36p(^2G)^3G$	10.9%	$5d^36p(^2H)^3I$
138802.64	138 487	316	1	31.7%	$5d^36p(^4P)^3S$	21.8%	$5d^36p(^2D)^1P$	11.8%	$5d^36p(^2D)^1P$
139168.53	139 296	−127	4	61.7%	$5d^36p(^2D)^3F$	7.9%	$5d^36p(^2D)^3F$	6.1%	$5d^36p(^2F)^3G$
141076.46	141 044	32	3	30.6%	$5d^36p(^2D)^3D$	18.8%	$5d^36p(^2P)^3D$	9.9%	$5d^36p(^4P)^3D$
141109.65	141 232	−122	2	35.4%	$5d^36p(^2P)^3P$	8.3%	$5d^36p(^2D)^1D$	8.0%	$5d^36p(^2D)^3D$
141129.13	141 118	11	4	34.7%	$5d^36p(^2H)^3G$	24.5%	$5d^36p(^2F)^3F$	20.0%	$5d^36p(^2H)^1G$
141593.79	141 864	−270	5	34.6%	$5d^36p(^2H)^3G$	20.9%	$5d^36p(^2G)^1H$	18.2%	$5d^36p(^2H)^1H$
142133.17	142 323	−190	6	44.5%	$5d^36p(^2H)^1I$	36.5%	$5d^36p(^2G)^3H$	8.2%	$5d^36p(^2H)^3I$
142521.11	142 450	71	2	63.5%	$5d^26s6p(^3F)^5G$	4.6%	$5d^26s6p(^1D)^3F$	4.1%	$5d^36p(^2D)^3F$
142532.77	142 406	127	3	26.5%	$5d^36p(^2H)^3G$	17.4%	$5d^36p(^2D)^3D$	12.0%	$5d^36p(^2D)^1F$

(*continued on next page*)

Table 5 (*continued*)

E_{Exp}	$E_{HFR+CPOL}$	ΔE	J	Composition in LS coupling					
143103.32	143 015	88	4	22.7%	$5d^36p(^2G)^1G$	15.8%	$5d^36p(^2G)^3F$	11.3%	$5d^36p(^2F)^3G$
143117.78	143 493	−375	1	43.1%	$5d^36p(^4P)^3S$	21.1%	$5d^36p(^2D)^3P$	9.6%	$5d^36p(^2D)^1P$
143638.09	143 707	−69	3	29.2%	$5d^36p(^2F)^3F$	17.8%	$5d^36p(^2F)^3G$	15.4%	$5d^36p(^2F)^3D$
146089.18	146 128	−39	5	86.3%	$5d^36p(^2F)^3G$	4.3%	$5d^36p(^2G)^1H$	4.0%	$5d^36p(^2H)^3G$
146125.28	146 019	106	4	35.1%	$5d^36p(^2F)^3F$	31.0%	$5d^36p(^2F)^3G$	13.1%	$5d^36p(^2H)^3G$
146134.95	146 199	−64	3	35.4%	$5d^26s6p(^3F)^5G$	10.0%	$5d^36p(^2P)^3D$	9.3%	$5d^36p(^2D)^1F$
146492.11	146 712	−220	2	51.4%	$5d^36p(^2F)^3D$	6.7%	$5d^36p(^4P)^3D$	4.8%	$5d^36p(^2F)^3F$
147743.52	147 474	270	1	31.7%	$5d^36p(^2P)^1P$	15.5%	$5d^36p(^2F)^3D$	10.5%	$5d^36p(^2D)^3D$
148137.51	147 988	150	4	49.5%	$5d^36p(^2F)^1G$	24.7%	$5d^36p(^2H)^1G$	6.1%	$5d^36p(^2F)^3G$
148896.66	149 005	−108	3	49.1%	$5d^36p(^2F)^1F$	21.8%	$5d^36p(^2F)^3D$	8.1%	$5d^36p(^2F)^3G$
151682.85	151 675	8	1	37.1%	$5d^36p(^2D)^3D$	16.8%	$5d^36p(^2D)^3D$	14.1%	$5d^36p(^2D)^3P$
153491.32	153 629	−138	3	22.0%	$5d^36p(^2D)^3F$	20.4%	$5d^36p(^2D)^1F$	13.6%	$5d^36p(^2D)^3D$
161105.96	161 014	92	3	51.1%	$5d^36p(^2D)^3D$	21.7%	$5d^36p(^2D)^3F$	8.2%	$5d^36p(^2D)^3F$

Table 6
Comparison between the energy levels computed with the HFR+CPOL approach and the available experimental values in Re V.

E_{Exp}	$E_{HFR+CPOL}$	ΔE	J	Composition in LS coupling					
Even parity									
0.00	12	−12	1.5	84.2%	$5d^3(^4F)^4F$	8.4%	$5d^3(^2D)^2D$	4.8%	$5d^3(^2D)^2D$
4852.98	4889	−36	2.5	95.1%	$5d^3(^4F)^4F$	3.2%	$5d^3(^2D)^2D$	1.2%	$5d^3(^2D)^2D$
8972.90	8984	−11	3.5	87.7%	$5d^3(^4F)^4F$	10.5%	$5d^3(^2G)^2G$	1.6%	$5d^3(^2F)^2F$
11913.86	11 873	41	4.5	63.7%	$5d^3(^4F)^4F$	28.3%	$5d^3(^2G)^2G$	7.7%	$5d^3(^2H)^2H$
12402.68	12 353	50	1.5	45.1%	$5d^3(^4P)^4P$	35.7%	$5d^3(^2P)^2P$	7.4%	$5d^3(^4F)^4F$
14325.42	14 348	−23	0.5	66.2%	$5d^3(^4P)^4P$	33.0%	$5d^3(^2P)^2P$	0.6%	$5d^26s(^3P)^2P$
19012.90	19 001	12	3.5	85.1%	$5d^3(^2G)^2G$	11.7%	$5d^3(^4F)^4F$	2.7%	$5d^3(^2F)^2F$
19966.76	19 994	−27	4.5	55.9%	$5d^3(^2H)^2H$	27.8%	$5d^3(^4F)^4F$	16.0%	$5d^3(^2G)^2G$
20922.06	20 868	54	2.5	89.9%	$5d^3(^4P)^4P$	6.1%	$5d^3(^2D)^2D$	2.1%	$5d^3(^2D)^2D$
23201.41	23 207	−6	1.5	43.2%	$5d^3(^4P)^4P$	33.3%	$5d^3(^2D)^2D$	10.0%	$5d^3(^2D)^2D$
23668.85	23 750	−81	0.5	64.7%	$5d^3(^2P)^2P$	33.6%	$5d^3(^4P)^4P$	1.5%	$5d^26s(^3P)^2P$
27076.87	27 092	−15	5.5	99.8%	$5d^3(^2H)^2H$	0.1%	$5d6p5f(^3G)^2H$		
28738.78	28 660	79	2.5	81.0%	$5d^3(^2D)^2D$	7.4%	$5d^3(^2D)^2D$	5.7%	$5d^3(^4P)^4P$
30365.54	30 339	27	4.5	55.0%	$5d^3(^2G)^2G$	36.2%	$5d^3(^2H)^2H$	8.3%	$5d^3(^4F)^4F$
32766.42	32 801	−35	1.5	53.3%	$5d^3(^2P)^2P$	18.9%	$5d^3(^2D)^2D$	13.3%	$5d^3(^2D)^2D$
34161.81	34 158	4	2.5	86.0%	$5d^3(^2F)^2F$	6.1%	$5d^3(^2D)^2D$	4.5%	$5d^3(^2D)^2D$
34625.26	34 631	−6	3.5	94.2%	$5d^3(^2F)^2F$	3.9%	$5d^3(^2G)^2G$	1.1%	$5d^26s(^3F)^2F$
52051.89	52 090	−38	1.5	66.9%	$5d^3(^2D)^2D$	31.3%	$5d^3(^2D)^2D$	0.5%	$5d^3(^4P)^4P$
52467.07	52 440	27	2.5	77.9%	$5d^3(^2D)^2D$	9.6%	$5d^3(^2F)^2F$	8.1%	$5d^3(^2D)^2D$
63506.40	63 471	35	1.5	92.4%	$5d^26s(^3F)^4F$	6.9%	$5d^26s(^1D)^2D$	0.1%	$5d^26s(^3P)^2P$
66188.65	66 226	−37	2.5	83.6%	$5d^26s(^3F)^4F$	8.0%	$5d^26s(^3F)^2F$	7.0%	$5d^26s(^1D)^2D$
71889.06	71 928	−39	3.5	95.8%	$5d^26s(^3F)^4F$	3.4%	$5d^26s(^3F)^2F$	0.4%	$5d^26s(^1G)^2G$
77307.49	77 331	−24	4.5	92.6%	$5d^26s(^3F)^4F$	7.0%	$5d^26s(^1G)^2G$	0.1%	$5d6p5f(^3G)^4F$
77994.60	77 990	5	2.5	50.9%	$5d^26s(^3F)^2F$	20.1%	$5d^26s(^1D)^2D$	15.2%	$5d^26s$(3F)4F
78208.65	78 164	45	0.5	92.7%	$5d^26s(^3P)^4P$	5.0%	$5d^26s(^1S)^2S$	1.8%	$5d^26s(^3P)^2P$
81246.07	81 199	47	1.5	86.9%	$5d^26s(^3P)^4P$	11.0%	$5d^26s(^1D)^2D$	1.5%	$5d^26s(^3F)^4F$
82122.71	82 157	−34	2.5	50.8%	$5d^26s(^3P)^4P$	33.0%	$5d^26s(^3F)^2F$	14.8%	$5d^26s(^1D)^2D$
85741.64	85 740	2	1.5	65.8%	$5d^26s(^1D)^2D$	16.0%	$5d^26s(^3P)^2p$	11.1%	$5d^26s(^3P)^4P$
86161.85	86 084	78	3.5	64.1%	$5d^26s(^3F)^2F$	32.9%	$5d^26s(^1G)^2G$	1.3%	$5d^26s(^3F)^4F$
91992.45	91 997	−5	2.5	56.1%	$5d^26s(^1D)^2D$	36.2%	$5d^26s(^3P)^4P$	5.5%	$5d^26s(^3F)^2F$
92004.47	92 086	−82	4.5	92.0%	$5d^26s(^1G)^2G$	7.1%	$5d^26s(^3F)^4F$	0.3%	$5d^3(^2G)^2G$
92326.67	92 398	−71	0.5	90.9%	$5d^26s(^3P)^2P$	3.2%	$5d^26s(^3P)^4P$	3.1%	$5d^26s(^1S)^2S$
93707.66	93 630	78	3.5	65.8%	$5d^26s(^1G)^2G$	30.6%	$5d^26s(^3F)^2F$	2.6%	$5d^26s(^3F)^4F$
99336.07	99 329	7	1.5	80.8%	$5d^26s(^3P)^2P$	14.5%	$5d^26s(^1D)^2D$	1.7%	$5d^3(^2P)^2P$
Odd parity									
126234.59	126 465	−230	2.5	63.3%	$5d^26p(^3F)^4G$	18.6%	$5d^26p(^3F)^2F$	11.6%	$5d^26p(^1D)^2F$
131236.56	130 943	294	1.5	49.7%	$5d^26p(^3F)^4F$	30.7%	$5d^26p(^3F)^2D$	8.5%	$5d^26p(^3F)^4D$
135906.77	135 929	−22	3.5	75.0%	$5d^26p(^3F)^4G$	10.4%	$5d^26p(^3F)^2F$	7.1%	$5d^26p(^3F)^4F$
137538.54	137 662	−123	2.5	43.3%	$5d^26p(^3F)^4F$	19.7%	$5d^26p(^3F)^2D$	18.2%	$5d^26p(^3F)^4D$
141022.57	140 940	83	0.5	48.1%	$5d^26p(^3P)^4D$	16.5%	$5d^26p(^3P)^2S$	10.8%	$5d^26p(^3F)^4D$
143230.54	143 181	50	4.5	43.4%	$5d^26p(^3F)^4G$	20.5%	$5d^26p(^3F)^4F$	17.4%	$5d^26p(^3F)^2G$
143475.48	143 437	38	2.5	25.8%	$5d^26p(^3F)^4F$	22.5%	$5d^26p(^3F)^4G$	14.1%	$5d^26p(^1D)^2D$
143927.51	144 114	−187	1.5	26.0%	$5d^26p(^3P)^4D$	21.1%	$5d^26p(^1D)^2P$	16.1%	$5d^26p(^1D)^2D$
144702.76	144 602	101	3.5	37.5%	$5d^26p(^3F)^4F$	28.7%	$5d^26p(^3F)^4D$	12.0%	$5d^26p(^3F)^2F$
144946.32	145 296	−350	0.5	40.9%	$5d^26p(^3P)^2S$	30.4%	$5d^26p(^3P)^4P$	19.5%	$5d^26p(^3P)^4D$
145311.00	145 329	−18	1.5	35.2%	$5d^26p(^3F)^4F$	19.3%	$5d^26p(^3F)^2D$	23.0%	$5d^26p(^3F)^4D$
147749.65	147 621	129	2.5	24.0%	$5d^26p(^3F)^4D$	17.8%	$5d^26p(^3F)^2F$	17.3%	$5d^26p(^3P)^4D$
148097.20	148 090	7	3.5	28.7%	$5d^26p(^3F)^2G$	18.8%	$5d^26p(^3F)^4D$	18.6%	$5d^26p(^3F)^2F$
148143.95	147 761	383	1.5	39.7%	$5d^26p(^3P)^4D$	21.8%	$5d^26p(^3P)^4S$	11.5%	$5d^26p(^3P)^2P$
149049.99	149 130	−80	0.5	63.9%	$5d^26p(^3F)^4D$	17.9%	$5d^26p(^3P)^4D$	11.6%	$5d^26p(^1D)^2P$
151877.34	151 800	77	4.5	55.2%	$5d^26p(^3F)^4G$	13.8%	$5d^26p(^1G)^2G$	12.0%	$5d^26p(^3F)^4F$
153294.64	153 514	−219	3.5	37.5%	$5d^26p(^3F)^4F$	30.6%	$5d^26p(^1G)^2G$	20.1%	$5d^26p(^3F)^2G$
153832.45	153 904	−72	2.5	28.7%	$5d^26p(^3F)^2F$	16.5%	$5d^26p(^3F)^4D$	12.2%	$5d^26p(^3P)^2D$
155597.70	155 590	8	3.5	27.4%	$5d^26p(^1D)^2F$	21.1%	$5d^26p(^1G)^2F$	16.3%	$5d^26p(^3F)^2F$
155990.14	156 031	−41	1.5	38.5%	$5d^26p(^3P)^4S$	17.3%	$5d^26p(^1D)^2D$	15.1%	$5d^26p(^3P)^4D$
156212.54	156 288	−75	1.5	50.9%	$5d^26p(^3F)^4D$	19.7%	$5d^26p(^3F)^2D$	8.7%	$5d^26p(^3P)^4D$
156490.63	156 367	124	4.5	43.8%	$5d^26p(^1G)^2H$	37.9%	$5d^26p(^3F)^4F$	13.5%	$5d^26p(^1G)^2G$
157152.26	157 051	101	2.5	38.2%	$5d^26p(^1D)^2F$	19.9%	$5d^26p(^3F)^4D$	19.5%	$5d^26p(^3F)^2F$
157629.21	157 336	293	5.5	92.3%	$5d^26p(^3F)^4G$	7.2%	$5d^26p(^1G)^2H$	0.2%	$5d6s5f(^3G)^4G$
158442.87	158 529	−86	3.5	30.4%	$5d^26p(^3F)^4D$	20.9%	$5d^26p(^3F)^2G$	17.4%	$5d^26p(^1G)^2G$
160580.69	160 512	69	0.5	39.0%	$5d^26p(^3P)^4P$	30.1%	$5d^26p(^1D)^2P$	17.5%	$5d^26p(^3P)^2S$
160748.37	160 555	193	1.5	62.7%	$5d^26p(^3P)^4P$	11.0%	$5d^26p(^3P)^4S$	6.4%	$5d^26p(^1D)^2P$
162092.97	162 142	−49	2.5	28.2%	$5d^26p(^3P)^2D$	28.0%	$5d^26p(^3F)^4D$	20.3%	$5d^26p(^3F)^4D$
163341.12	163 528	−187	4.5	63.5%	$5d^26p(^3F)^2G$	19.8%	$5d^26p(^3F)^4F$	15.0%	$5d^26p(^1G)^2G$
164068.22	164 013	55	2.5	38.9%	$5d^26p(^3P)^4P$	30.7%	$5d^26p(^1D)^2D$	16.4%	$5d^26p(^3P)^4D$
164424.89	164 501	−76	3.5	36.8%	$5d^26p(^3P)^4D$	17.1%	$5d^26p(^3F)^2F$	14.3%	$5d^26p(^3F)^4D$
165156.79	165 241	−84	1.5	30.2%	$5d^26p(^1D)^2D$	27.1%	$5d^26p(^1D)^2P$	17.8%	$5d^26p(^3P)^2P$
166967.38	166 898	69	0.5	35.4%	$5d^26p(^1D)^2P$	23.6%	$5d^26p(^3P)^4P$	15.3%	$5d^26p(^3P)^2S$
167335.17	167 424	−89	1.5	54.8%	$5d^26p(^3P)^2D$	12.8%	$5d^26p(^3P)^2P$	10.0%	$5d^26p(^3F)^2D$
168014.04	167 944	70	2.5	28.2%	$5d^26p(^1D)^2D$	23.6%	$5d^26p(^3P)^2D$	15.8%	$5d^26p(^3P)^4P$
168691.51	168 719	−27	4.5	47.7%	$5d^26p(^1G)^2G$	38.0%	$5d^26p(^1G)^2H$	9.5%	$5d^26p(^3F)^4F$
171185.93	171 331	−145	0.5	46.6%	$5d^26p(^3P)^2P$	24.6%	$5d^26p(^1S)^2P$	12.4%	$5d^26p(^3P)^4D$
172562.67	172 441	122	5.5	91.7%	$5d^26p(^1G)^2H$	7.2%	$5d^26p(^3F)^4G$	0.4%	$5d6s5f(^1H)^2H$
173725.21	173 757	−32	2.5	28.7%	$5d^26p(^3P)^4P$	25.2%	$5d^26p(^1G)^2F$	22.8%	$5d^26p(^3P)^2D$

(*continued on next page*)

Table 6 (*continued*)

E_{Exp}	$E_{HFR+CPOL}$	ΔE	J	Composition in LS coupling					
174120.53	174 213	−92	3.5	54.3%	$5d^26p(^1G)^2F$	21.7%	$5d^26p(^1G)^2G$	6.6%	$5d^26p(^3F)^4D$
177193.54	177 079	115	1.5	50.3%	$5d^26p(^3P)^2P$	15.2%	$5d^26p(^1D)^2D$	13.3%	$5d^26p(^3P)^2d$
178243.69	178 254	−10	2.5	64.1%	$5d^26p(^1G)^2F$	12.1%	$5d^26p(^3F)^2D$	8.2%	$5d^26p(^3P)^2D$
183498.82	183 542	−43	0.5	61.4%	$5d^26p(^1S)^2P$	22.6%	$5d^26p(^3P)^2P$	11.4%	$5d^26p(^1D)^2P$
195575.77	195 524	52	1.5	87.4%	$5d^26p(^1S)^2P$	2.8%	$5d^26p(^3P)^2D$	2.3%	$5d^26p(^3P)^4P$

Table 7
Comparison between the energy levels computed with the MCDHF approach and the available experimental values in Re III.

E_{Exp}	E_{MCDHF}	ΔE_{MCDHF}	$E_{HFR+CPOL}$	$\Delta E_{HFR+CPOL}$	J	jj-purity	LS-purity
Even parity							
0.00	0	0	−32	32	2.5	89%	89%
13614.31	16 445	−2831	13 575	39	2.5	25%	25%
14396.44	15 229	−833	14 346	50	0.5	40%	53%
15771.98	16 933	−1161	15 757	15	1.5	38%	38%
16890.46	19 712	−2822	16 921	−31	3.5	64%	64%
17139.88	19 329	−2189	17 195	−55	2.5	43%	43%
17908.92	18 864	−955	17 904	5	1.5	46%	74%
18020.00	20 750	−2730	17 954	66	5.5	84%	84%
18345.56	20 949	−2603	18 363	−17	4.5	86%	86%
18392.70	19 626	−1233	18 408	−15	0.5	31%	31%
19718.84	19 765	−46	19 724	−5	2.5	71%	89%
20453.27	21 540	−1087	20 390	63	3.5	51%	51%
21568.90	23 499	−1930	21 530	39	2.5	30%	30%
21973.95	23 204	−1230	22 075	−101	0.5	45%	45%
22106.24	23 123	−1017	22 182	−76	3.5	79%	80%
22936.77	24 167	−1230	22 991	−54	1.5	33%	33%
23471.28	23 399	72	23 466	5	4.5	76%	76%
26128.71	28 054	−1925	26 195	−66	1.5	39%	39%
26170.06	30 081	−3911	26 257	−87	5.5	74%	74%
26659.78	28 548	−1888	26 649	11	2.5	18%	18%
26910.08	30 329	−3419	26 880	30	3.5	29%	29%
27421.03	30 588	−3167	27 362	59	4.5	39%	39%
28587.87	32 435	−3847	28 614	−26	6.5	99%	99%
30255.47	32 827	−2572	30 182	73	3.5	22%	26%
30302.28	32 131	−1829	30 422	−120	2.5	55%	55%
30835.75	32 137	−1301	30 811	25	0.5	23%	18%
31345.29	33 838	−2493	31 276	69	2.5	36%	36%
31989.54	33 449	−1459	32 059	−69	1.5	31%	31%
32068.35	34 879	−2811	31 981	87	4.5	40%	43%
32832.90	35 560	−2727	32 906	−73	3.5	28%	28%
34349.37	36 481	−2132	34 327	22	3.5	22%	22%
34641.11	37 190	−2549	34 574	67	3.5	39%	39%
34825.68	35 895	−1069	34 870	−44	1.5	37%	41%
35139.99	37 657	−2517	35 176	−36	4.5	36%	56%
36165.95	36 760	−594	36 212	−46	0.5	19%	32%
36463.97	38 085	−1621	36 390	74	2.5	27%	27%
36927.52	40 520	−3592	36 955	−27	5.5	44%	44%
37406.55	40 121	−2714	37 336	71	4.5	40%	40%
38167.85	39 296	−1128	38 083	85	5.5	39%	61%
38656.17	39 439	−783	38 568	88	1.5	23%	23%
38752.31	40 090	−1338	38 710	42	3.5	20%	25%
39300.25	41 439	−2139	39 400	−100	6.5	87%	87%
39595.72	40 428	−832	39 574	22	2.5	46%	51%
39790.02	40 659	−869	39 809	−19	1.5	23%	37%
40000.60	42 027	−2026	39 960	41	2.5	26%	26%
40654.99	42 682	−2027	40 648	7	2.5	18%	18%
40934.98	42 383	−1448	40 901	34	4.5	28%	28%
41115.92	43 025	−1909	41 167	−51	3.5	26%	26%
41210.25	44 108	−2898	41 275	−65	1.5	61%	61%
41405.07	43 739	−2334	41 488	−83	4.5	28%	27%
42600.54	43 434	−833	42 587	14	2.5	20%	27%
43191.67	44 990	−1798	43 179	13	2.5	24%	24%
43750.37	45 027	−1277	43 795	−45	3.5	24%	27%
45256.54	47 261	−2004	45 212	45	5.5	47%	47%
45608.03	47 836	−2228	45 563	45	3.5	39%	26%
46314.79	48 684	−2369	46 378	−63	4.5	41%	55%
46718.20	48 680	−1962	46 808	−90	3.5	51%	51%
47011.78	48 881	−1869	46 863	149	4.5	24%	24%
47091.01	48 357	−1266	47 063	38	1.5	49%	60%
47881.45	50 352	−2471	47 883	−2	5.5	37%	37%
47910.25	49 274	−1364	47 856	54	2.5	22%	30%
50496.79	53 294	−2797	50 637	−140	6.5	87%	87%
51007.47	52 518	−1511	51 050	−43	2.5	19%	28%
51668.96	53 624	−1955	51 765	−96	3.5	19%	26%
52444.21	55 296	−2852	52 501	−57	3.5	19%	33%
53402.71	55 611	−2208	53 231	172	5.5	47%	55%
55975.68	58 756	−2780	55 880	96	4.5	41%	45%
57206.89	59 696	−2489	57 207	0	4.5	25%	25%
58069.32	57 340	729	58 117	−48	3.5	47%	47%
61243.18	60 643	600	61 236	7	4.5	53%	53%
Odd parity							
64709.45	63 540	1169	64 797	−88	0.5	58%	36%
67274.27	65 604	1670	67 540	−266	0.5	74%	30%
68339.99	66 544	1796	68 401	−61	1.5	66%	73%

(continued on next page)

Table 7 (*continued*)

E_{Exp}	E_{MCDHF}	ΔE_{MCDHF}	$E_{HFR+CPOL}$	$\Delta E_{HFR+CPOL}$	J	jj-purity	LS-purity
71230.53	69 209	2022	71 322	−91	2.5	66%	77%
71842.35	70 008	1834	71 843	−1	1.5	77%	42%
73640.25	71 669	1971	73 718	−78	3.5	64%	61%
75517.33	73 922	1595	75 603	−86	4.5	57%	32%
75529.07	73 619	1910	75 241	288	2.5	72%	35%
77759.84	76 028	1732	77 174	586	3.5	59%	54%
77861.59	76 175	1687	77 638	224	1.5	42%	61%
78667.43	76 868	1799	78 611	56	0.5	21%	24%
79768.95	78 019	1750	80 093	−324	1.5	43%	30%
79861.69	77 896	1966	79 616	246	2.5	55%	38%
81136.31	78 973	2163	81 070	66	0.5	31%	42%
81404.63	79 577	1828	81 408	−3	3.5	45%	23%
81957.47	80 572	1385	82 057	−100	4.5	32%	36%
82166.83	80 626	1541	82 339	−172	2.5	29%	14%
82301.45	81 764	537	82 163	138	3.5	30%	32%
82459.98	80 740	1720	82 604	−144	1.5	31%	24%
83386.03	81 036	2350	83 343	43	1.5	33%	40%
83605.25	82 402	1203	83 472	133	4.5	53%	31%
83950.19	81 349	2601	83 533	417	5.5	76%	76%
84453.78	82 486	1968	84 682	−228	2.5	32%	31%
84645.51	83 849	797	84 630	16	3.5	26%	16%
85572.52	83 875	1698	85 757	−184	2.5	35%	27%
85975.44	85 971	4	86 114	−139	5.5	55%	33%
86678.58	85 933	746	86 450	229	4.5	50%	29%
86723.56	85 261	1463	86 924	−200	0.5	40%	54%
87105.75	86 079	1027	87 262	−156	1.5	19%	23%
87231.77	85 436	1796	87 455	−223	0.5	20%	40%
87251.23	85 737	1514	87 623	−372	3.5	51%	36%
87964.10	86 133	1831	87 673	291	2.5	19%	10%
88008.10	86 568	1440	88 174	−166	1.5	20%	16%
88143.40	87 566	577	88 179	−36	2.5	16%	21%
88157.70	88 430	−272	88 290	−132	6.5	71%	33%
88774.45	88 078	696	88 901	−127	4.5	19%	31%
89340.33	88 857	483	89 534	−194	2.5	13%	14%
89903.34	88 805	1098	89 726	177	3.5	27%	14%
90066.20	89 261	805	90 172	−106	3.5	32%	30%
90735.64	89 254	1482	90 999	−263	1.5	16%	17%
90984.35	91 287	−303	90 472	512	5.5	53%	34%
91329.97	90 059	1271	91 532	−202	4.5	39%	26%
92152.76	91 558	595	92 115	38	3.5	17%	16%
92449.06	92 302	147	92 669	−220	4.5	15%	18%
92567.53	92 319	249	92 715	−147	3.5	22%	14%
92617.24	91 408	1209	92 745	−128	1.5	11%	23%
92766.60	90 956	1811	92 559	208	0.5	25%	14%
93087.02	91 845	1242	93 301	−214	2.5	14%	18%
93504.22	92 461	1043	93 496	8	2.5	17%	18%
93849.58	92 958	892	93 881	−31	2.5	15%	11%
94319.57	93 064	1256	94 375	−55	3.5	23%	22%
94398.47	93 918	480	94 581	−183	5.5	21%	30%
94512.00	94 256	256	94 443	69	4.5	28%	25%
94798.31	94 079	719	94 667	131	2.5	17%	17%
94829.16	93 978	851	94 851	−22	3.5	33%	13%
94960.97	94 920	41	94 849	112	5.5	36%	35%
95107.85	93 535	1573	95 022	86	1.5	12%	18%
95215.65	93 536	1680	95 169	47	0.5	18%	17%
95661.73	95 048	614	95 735	−73	4.5	15%	11%
96004.04	94 850	1154	96 130	−126	1.5	20%	20%
96236.36	95 795	441	95 967	269	2.5	12%	23%
96467.39	96 458	9	96 650	−183	6.5	42%	31%
96701.04	95 689	1012	96 435	266	1.5	24%	17%
96701.13	96 438	263	96 382	319	2.5	19%	15%
96900.21	96 013	887	96 709	191	0.5	23%	30%
97032.95	96 938	95	96 910	123	5.5	26%	39%
97271.85	96 717	555	97 177	95	1.5	14%	18%
97286.84	96 305	982	97 138	149	3.5	12%	26%
97476.34	96 853	623	97 176	300	4.5	32%	36%
97815.34	96 997	818	98 016	−201	3.5	24%	16%
97826.06	97 545	281	97 565	261	6.5	51%	50%
97860.52	97 286	575	97 931	−70	2.5	21%	16%
98540.51	98 283	258	98 533	8	7.5	83%	83%
98596.29	97 158	1438	98 428	168	3.5	33%	33%
98926.96	97 509	1418	98 696	231	4.5	34%	31%
99277.71	98 130	1148	99 133	145	2.5	11%	13%
99528.13	98 933	595	99 385	143	3.5	45%	26%
99634.37	98 410	1224	99 463	171	1.5	13%	22%

(*continued on next page*)

Table 7 (*continued*)

E_{Exp}	E_{MCDHF}	ΔE_{MCDHF}	$E_{HFR+CPOL}$	$\Delta E_{HFR+CPOL}$	J	jj-purity	LS-purity
99874.56	99 261	614	99 553	322	5.5	19%	37%
99923.09	99 260	663	99 928	−5	2.5	22%	19%
99993.43	99 398	595	100 002	−9	4.5	19%	21%
100309.90	99 806	504	100 317	−7	5.5	38%	35%
100924.02	99 832	1092	100 950	−26	1.5	20%	15%
101075.86	99 996	1080	100 716	360	3.5	13%	17%
101190.34	101 499	−309	101 310	−120	6.5	37%	30%
101331.98	100 330	1002	101 209	123	2.5	12%	26%
101452.99	101 524	−71	101 703	−250	5.5	31%	40%
101524.43	99 653	1871	101 794	−270	0.5	40%	37%
101570.09	101 185	385	101 482	88	3.5	21%	17%
101597.24	101 097	500	101 486	111	4.5	17%	20%
101863.74	100 515	1349	101 916	−52	1.5	17%	16%
101975.48	101 501	474	102 405	−430	4.5	20%	21%
102444.45	101 796	648	102 359	85	1.5	11%	17%
102504.01	101 624	880	102 383	121	3.5	12%	7%
102902.38	102 462	440	103 024	−122	3.5	23%	17%
102980.06	102 394	586	103 087	−107	2.5	12%	9%
103139.49	102 991	148	103 286	−147	4.5	26%	26%
103629.58	102 896	734	103 581	49	1.5	22%	23%
103880.12	104 752	−872	104 064	−184	5.5	22%	20%
103908.35	102 692	1216	103 856	52	0.5	12%	22%
104145.96	102 973	1173	103 774	372	2.5	11%	10%
104173.50	103 258	916	104 270	−96	4.5	25%	25%
104365.42	104 664	−299	104 253	112	2.5	19%	14%
104552.00	103 896	656	104 360	192	3.5	20%	26%
104565.42	103 548	1017	104 537	28	1.5	13%	18%
104741.39	103 630	1111	104 818	−77	0.5	22%	21%
104843.57	104 325	519	105 126	−282	3.5	20%	16%
105066.16	104 291	775	105 038	28	1.5	26%	38%
105130.18	104 513	617	105 399	−269	6.5	39%	39%
105231.14	104 323	908	104 914	317	4.5	19%	11%
105448.80	103 385	2064	105 545	−96	2.5	15%	43%
105505.83	105 311	195	105 651	−145	4.5	54%	40%
105508.74	102 331	3178	105 658	−149	5.5	21%	44%
105984.55	105 046	939	105 743	242	3.5	12%	9%
106007.90	105 481	527	106 200	−192	2.5	20%	22%
106211.02	105 549	662	106 250	−39	3.5	14%	17%
106478.75	106 235	244	106 219	260	0.5	46%	48%
106669.93	106 761	−91	106 846	−176	3.5	15%	23%
106870.05	106 085	785	107 014	−144	2.5	9%	10%
107141.42	106 814	327	107 510	−369	2.5	24%	24%
107385.70	107 712	−326	107 230	156	6.5	82%	54%
107421.26	106 927	494	107 610	−189	3.5	18%	32%
107959.22	107 308	651	108 218	−259	5.5	31%	17%
108563.21	108 910	−347	108 816	−253	7.5	84%	84%
108625.11	106 800	1825	108 526	99	4.5	22%	16%
108855.91	108 002	854	108 921	−65	3.5	15%	18%
108864.14	108 563	301	109 097	−233	2.5	17%	25%
108924.72	109 215	−290	108 690	235	5.5	23%	32%
109014.70	108 271	744	108 905	110	4.5	30%	29%
110134.96	110 028	107	110 125	10	4.5	42%	42%
110180.06	109 172	1008	110 294	−114	2.5	52%	38%
110812.23	110 211	601	110 992	−180	4.5	23%	14%
110994.14	110 830	164	111 334	−340	2.5	18%	17%
111037.21	108 525	2512	110 803	234	5.5	47%	36%
111151.60	111 375	−223	111 412	−260	3.5	14%	14%
111235.52	112 885	−1649	111 325	−89	4.5	19%	17%
111868.40	111 349	519	111 738	130	2.5	12%	18%
112826.67	112 685	142	113 114	−287	5.5	30%	30%
113012.11	112 582	430	112 842	170	3.5	11%	9%
113888.11	112 940	948	113 682	206	2.5	21%	16%
114220.18	114 456	−236	114 229	−9	4.5	16%	16%
114296.66	113 584	713	114 322	−25	2.5	10%	16%
114412.98	113 518	895	114 220	193	3.5	8%	20%
114549.19	113 592	957	114 697	−148	5.5	30%	26%
115167.44	114 397	770	114 737	430	3.5	15%	23%
115336.80	114 840	497	115 363	−26	4.5	28%	27%
117929.36	116 823	1106	117 612	317	4.5	28%	24%
118701.09	117 837	864	118 492	209	3.5	24%	24%
119243.60	118 743	501	119 396	−152	5.5	25%	25%
120153.36	120 181	−28	119 744	409	3.5	18%	19%
120845.21	120 225	620	120 679	166	6.5	60%	48%
120943.64	120 796	148	120 957	−13	5.5	39%	39%
121263.59	120 881	383	121 517	−253	3.5	17%	16%

(*continued on next page*)

Table 7 (*continued*)

E_{Exp}	E_{MCDHF}	ΔE_{MCDHF}	$E_{HFR+CPOL}$	$\Delta E_{HFR+CPOL}$	J	jj-purity	LS-purity
123649.48	123 483	166	123 601	48	4.5	19%	20%
123818.07	123 293	525	123 948	−130	5.5	28%	27%
124290.98	124 053	238	124 313	−22	4.5	16%	12%
124643.76	124 691	−47	124 683	−39	5.5	18%	25%
125116.00	124 674	442	125 211	−95	6.5	18%	21%
126252.50	125 872	381	126 296	−43	4.5	10%	18%
126545.18	126 458	87	126 528	17	6.5	39%	31%
137911.82	137 921	−9	138 100	−188	6.5	49%	49%

Table 8
Comparison between the energy levels computed with the MCDHF approach and the available experimental values in Re IV.

E_{Exp}	E_{MCDHF}	ΔE_{MCDHF}	$E_{HFR+CPOL}$	$\Delta E_{HFR+CPOL}$	J	jj-purity	LS-purity
Even parity							
0.00	0	0	−73	73	0	66%	67%
3084.09	2446	638	3093	−9	1	85%	85%
5978.67	4975	1004	6017	−38	2	93%	93%
8350.18	7218	1132	8358	−8	3	89%	89%
10121.14	9124	997	10 059	62	4	74%	74%
14503.47	13 808	695	14 580	−77	0	34%	34%
16946.38	18 082	−1136	16 994	−48	4	57%	57%
19339.89	18 522	818	19 378	−38	1	53%	53%
19817.09	20 616	−799	19 823	−6	3	58%	58%
19850.51	20 282	−431	19 855	−4	2	50%	50%
20929.53	21 993	−1063	20 958	−28	5	77%	77%
22895.90	24 017	−1121	22 886	10	6	78%	78%
24323.66	24 537	−213	24 350	−26	4	37%	37%
24352.16	24 061	291	24 318	34	2	48%	48%
26044.01	26 767	−723	26 046	−2	4	30%	31%
26475.63	27 060	−584	26 473	3	3	55%	55%
28526.28	29 666	−1140	28 465	61	3	57%	57%
29200.98	29 448	−247	29 260	−59	2	22%	22%
30051.68	30 470	−418	30 030	22	5	76%	76%
31542.72	32 196	−653	31 554	−11	1	86%	86%
32395.83	33 804	−1408	32 430	−34	6	78%	78%
35596.79	35 925	−329	35 562	35	2	27%	27%
36034.31	36 506	−472	35 961	73	4	46%	46%
36484.41	36 173	311	36 505	−21	0	60%	60%
38457.74	40 136	−1678	38 385	73	3	66%	66%
39117.76	38 173	945	39 095	23	1	90%	90%
41099.59	40 036	1064	41 108	−8	2	35%	67%
41601.56	42 731	−1129	41 536	66	2	46%	46%
44328.51	42 781	1548	44 350	−21	3	73%	94%
44725.81	45 586	−860	44 587	139	4	63%	63%
45502.44	46 690	−1188	45 602	−100	2	48%	48%
45947.27	46 922	−975	45 979	−32	1	56%	56%
46525.20	47 754	−1229	46 542	−17	3	65%	65%
47703.16	46 115	1588	47 714	−11	4	79%	89%
48745.80	49 650	−904	48 777	−31	0	55%	55%
49208.90	50 873	−1664	49 243	−34	4	43%	43%
50820.82	48 955	1866	50 840	−19	5	83%	83%
52384.70	51 915	470	52 368	17	2	47%	49%
53222.25	52 505	717	53 233	−11	1	61%	78%
55502.70	54 744	759	55 533	−30	2	35%	63%
57931.16	57 088	843	57 898	33	3	42%	42%
58757.85	57 857	901	58 739	19	3	75%	75%
59116.79	59 203	−86	59 056	61	4	38%	42%
60858.33	60 163	695	60 839	19	1	29%	29%
61519.13	60 666	853	61 551	−32	0	81%	81%
61557.12	61 560	−3	61 676	−119	5	32%	45%
63119.85	61 950	1170	63 060	60	3	47%	52%
63934.66	63 619	316	63 910	25	4	62%	33%
64843.35	65 682	−839	64 857	−14	2	23%	27%
65907.48	65 461	446	65 821	86	4	46%	52%
66323.75	65 155	1169	66 341	−17	1	79%	57%
67802.22	68 258	−456	67 935	−133	6	99%	99%
69982.88	69 693	290	69 913	70	5	49%	53%
70710.10	69 285	1425	70 741	−31	3	79%	79%
70811.30	69 620	1191	70 775	36	2	15%	25%
71331.28	70 464	867	71 333	−2	1	36%	45%
72990.87	72 685	306	73 096	−105	0	75%	75%
74604.60	74 835	−230	74 617	−12	5	37%	82%
75318.37	74 849	469	75 251	67	2	61%	61%
75421.36	75 830	−409	75 400	21	3	51%	87%
75722.03	75 055	667	75 707	15	4	52%	52%
76466.25	76 296	170	76 427	39	4	32%	42%
76798.48	76 065	733	76 781	17	2	49%	57%
78474.88	77 250	1225	78 523	−48	2	41%	54%
83520.75	84 784	−1263	83 536	−15	3	55%	79%
Odd parity							
95642.75	92 471	3172	95 822	−179	2	77%	65%
99039.24	96 128	2911	98 665	374	1	83%	43%
101184.06	97 452	3732	101 378	−194	3	83%	78%
102740.89	99 447	3294	102 872	−131	2	83%	33%
105653.00	101 913	3740	105 821	−168	4	72%	59%
108147.80	104 641	3507	107 964	184	3	78%	33%
108261.46	105 668	2593	108 544	−283	1	33%	33%
108440.86	105 636	2805	109 055	−614	0	50%	43%

(continued on next page)

Table 8 (*continued*)

E_{Exp}	E_{MCDHF}	ΔE_{MCDHF}	$E_{HFR+CPOL}$	$\Delta E_{HFR+CPOL}$	J	jj-purity	LS-purity
108572.85	105 637	2936	108 542	31	2	26%	18%
108664.39	105 502	3162	108 775	−111	5	49%	24%
111271.09	108 069	3202	111 362	−91	0	48%	48%
111284.25	107 802	3482	111 167	117	1	55%	38%
111928.65	108 652	3277	111 612	316	4	51%	34%
113073.16	109 624	3449	113 194	−121	3	56%	35%
113169.81	109 510	3660	113 267	−97	2	69%	35%
114013.68	111 535	2479	113 387	627	1	34%	32%
114377.71	111 137	3241	114 521	−143	4	44%	33%
116093.40	112 653	3440	116 158	−65	3	39%	35%
116539.61	113 038	3502	116 670	−130	5	35%	52%
117141.27	113 593	3548	117 032	109	3	43%	27%
117144.08	113 549	3595	117 053	91	1	72%	38%
117146.54	113 787	3360	117 120	27	4	36%	42%
117565.57	114 154	3412	117 457	109	2	72%	39%
117952.85	114 609	3344	118 051	−98	2	35%	19%
119416.52	115 855	3562	119 350	67	5	47%	34%
119970.09	116 998	2972	120 189	−219	3	32%	29%
120179.98	117 226	2954	120 299	−119	1	21%	28%
120284.01	118 222	2062	119 837	447	4	31%	23%
120418.94	116 817	3602	120 289	130	2	47%	28%
120439.96	115 994	4446	120 304	136	6	70%	70%
121577.29	118 262	3315	121 809	−232	2	12%	36%
122276.03	118 521	3755	122 264	12	3	41%	30%
122592.46	119 646	2946	122 416	176	0	24%	40%
123169.82	118 977	4193	123 374	−204	4	72%	48%
123550.38	120 589	2961	123 050	500	3	17%	36%
123838.92	120 819	3020	123 463	376	1	39%	28%
124007.37	120 935	3072	123 925	82	2	40%	21%
124629.23	122 562	2067	124 652	−23	6	84%	38%
124849.98	122 107	2743	124 811	39	5	61%	42%
124923.63	121 319	3605	124 997	−73	4	38%	36%
125064.02	121 757	3307	125 028	36	3	24%	29%
126012.61	122 933	3080	126 332	−319	1	32%	47%
126510.33	123 747	2763	126 589	−79	2	44%	27%
127611.60	124 278	3334	127 647	−35	5	34%	32%
127867.69	124 994	2874	128 071	−203	4	37%	54%
128587.37	125 798	2789	128 680	−93	3	27%	16%
128917.62	126 223	2695	129 142	−224	5	22%	29%
129151.61	126 109	3043	128 974	178	1	24%	22%
129345.74	125 952	3394	129 329	17	2	50%	28%
129514.45	127 407	2107	129 639	−125	2	13%	26%
129824.96	127 258	2567	129 847	−22	4	15%	25%
129879.97	127 596	2284	129 784	96	3	21%	19%
130501.89	127 959	2543	130 617	−115	2	17%	23%
130600.98	127 775	2826	130 497	104	4	55%	55%
130800.63	127 976	2824	130 706	95	5	43%	35%
131638.02	129 237	2401	131 449	189	3	30%	14%
131729.72	129 188	2542	131 700	30	6	46%	33%
132053.22	128 756	3297	132 122	−69	1	26%	41%
132120.22	129 756	2364	132 038	82	4	32%	21%
133152.54	129 958	3195	133 343	−190	3	18%	14%
133503.65	131 168	2336	133 332	172	4	22%	24%
133523.38	129 939	3584	133 472	51	1	15%	31%
133535.92	130 452	3084	133 647	−111	2	40%	40%
133918.71	131 976	1943	133 735	183	3	44%	22%
134058.65	130 890	3169	134 041	18	2	25%	29%
134147.73	131 680	2468	133 895	253	5	26%	41%
134853.68	132 197	2657	134 728	126	2	26%	19%
135091.82	133 177	1915	134 999	93	3	25%	25%
135884.40	133 272	2612	135 804	80	6	75%	44%
136397.49	133 336	3061	136 616	−219	1	31%	42%
137293.23	134 357	2936	137 321	−28	3	46%	42%
137793.42	135 409	2384	137 871	−78	7	100%	100%
138006.35	134 703	3303	138 028	−22	2	26%	26%
138653.23	135 584	3069	138 746	−93	5	38%	38%
138802.64	135 630	3173	138 487	316	1	34%	32%
139168.53	135 556	3613	139 296	−127	4	62%	62%
141076.46	137 593	3483	141 044	32	3	36%	31%
141109.65	137 546	3564	141 232	−122	2	28%	35%
141129.13	139 201	1928	141 118	11	4	52%	35%
141593.79	144 541	−2947	141 864	−270	5	62%	35%
142133.17	139 301	2832	142 323	−190	6	37%	45%
142521.11	139 551	2970	142 450	71	2	58%	64%
142532.77	140 130	2403	142 406	127	3	29%	27%

(*continued on next page*)

Table 8 (*continued*)

E_{Exp}	E_{MCDHF}	ΔE_{MCDHF}	$E_{HFR+CPOL}$	$\Delta E_{HFR+CPOL}$	J	jj-purity	LS-purity
143103.32	139 918	3185	143 015	88	4	47%	23%
143117.78	140 100	3018	143 493	−375	1	45%	43%
143638.09	141 276	2362	143 707	−69	3	51%	29%
146089.18	139 034	7055	146 128	−39	5	86%	86%
146125.28	144 406	1719	146 019	106	4	38%	35%
146134.95	142 945	3190	146 199	−64	3	21%	35%
146492.11	144 259	2233	146 712	−220	2	27%	51%
147743.52	145 428	2316	147 474	270	1	41%	32%
148137.51	147 042	1096	147 988	150	4	38%	50%
148896.66	147 247	1650	149 005	−108	3	73%	49%
151682.85	150 521	1162	151 675	8	1	46%	37%
153491.32	151 677	1814	153 629	−138	3	56%	22%
161105.96	158 856	2250	161 014	92	3	54%	51%

Table 9
Comparison between the energy levels computed with the MCDHF approach and the available experimental values in Re V.

E_{Exp}	E_{MCDHF}	ΔE_{MCDHF}	$E_{HFR+CPOL}$	$\Delta E_{HFR+CPOL}$	J	jj-purity	LS-purity
Even parity							
0.00	0	0	12	−12	1.5	84%	84%
4852.98	4343	510	4889	−36	2.5	95%	95%
8972.90	8351	622	8984	−11	3.5	88%	88%
11913.86	11 622	292	11 873	41	4.5	64%	64%
12402.68	13 043	−640	12 353	50	1.5	45%	45%
14325.42	14 925	−600	14 348	−23	0.5	66%	66%
19012.90	19 716	−703	19 001	12	3.5	85%	85%
19966.76	20 907	−940	19 994	−27	4.5	56%	56%
20922.06	21 137	−215	20 868	54	2.5	90%	90%
23201.41	23 130	71	23 207	−6	1.5	33%	43%
23668.85	23 563	106	23 750	−81	0.5	65%	65%
27076.87	28 692	−1615	27 092	−15	5.5	100%	100%
28738.78	28 931	−192	28 660	79	2.5	81%	81%
30365.54	30 839	−473	30 339	27	4.5	55%	55%
32766.42	31 943	823	32 801	−35	1.5	53%	53%
34161.81	36 491	−2329	34 158	4	2.5	86%	86%
34625.26	36 757	−2132	34 631	−6	3.5	94%	94%
52051.89	53 955	−1903	52 090	−38	1.5	67%	67%
52467.07	53 659	−1192	52 440	27	2.5	78%	78%
63506.40	60 261	3245	63 471	35	1.5	92%	92%
66188.65	62 929	3260	66 226	−37	2.5	67%	84%
71889.06	68 147	3742	71 928	−39	3.5	88%	96%
77307.49	73 391	3916	77 331	−24	4.5	93%	93%
77994.60	75 077	2918	77 990	5	2.5	59%	51%
78208.65	75 172	3037	78 164	45	0.5	74%	93%
81246.07	77 894	3352	81 199	47	1.5	71%	87%
82122.71	78 962	3161	82 157	−34	2.5	51%	51%
85741.64	82 559	3183	85 740	2	1.5	66%	66%
86161.85	83 513	2649	86 084	78	3.5	56%	64%
91992.45	88 212	3780	91 997	−5	2.5	56%	56%
92004.47	90 127	1877	92 086	−82	4.5	92%	92%
92326.67	90 109	2218	92 398	−71	0.5	78%	91%
93707.66	91 391	2317	93 630	78	3.5	66%	66%
99336.07	96 469	2867	99 329	7	1.5	76%	81%
Odd parity							
126234.59	125 490	745	126 465	−230	2.5	84%	63%
131236.56	130 897	340	130 943	294	1.5	88%	50%
135906.77	134 508	1399	135 929	−22	3.5	90%	75%
137538.54	136 583	956	137 662	−123	2.5	90%	43%
141022.57	141 296	−273	140 940	83	0.5	74%	48%
143230.54	141 976	1255	143 181	50	4.5	75%	43%
143475.48	142 385	1090	143 437	38	2.5	45%	26%
143927.51	143 724	204	144 114	−187	1.5	37%	26%
144702.76	143 617	1086	144 602	101	3.5	73%	38%
144946.32	144 937	9	145 296	−350	0.5	85%	41%
145311.00	144 206	1105	145 329	−18	1.5	74%	35%
147749.65	147 048	702	147 621	129	2.5	22%	24%
148097.20	146 785	1312	148 090	7	3.5	62%	29%
148143.95	147 766	378	147 761	383	1.5	66%	40%
149049.99	148 339	711	149 130	−80	0.5	64%	64%
151877.34	150 268	1609	151 800	77	4.5	74%	55%
153294.64	152 074	1221	153 514	−219	3.5	57%	38%
153832.45	152 103	1729	153 904	−72	2.5	61%	29%
155597.70	154 951	647	155 590	8	3.5	36%	27%
155990.14	155 237	753	156 031	−41	1.5	39%	39%
156212.54	154 798	1415	156 288	−75	1.5	70%	51%
156490.63	156 022	469	156 367	124	4.5	57%	44%
157152.26	156 006	1146	157 051	101	2.5	37%	38%
157629.21	155 162	2467	157 336	293	5.5	92%	92%
158442.87	157 293	1150	158 529	−86	3.5	32%	30%
160580.69	159 706	875	160 512	69	0.5	36%	39%
160748.37	160 182	566	160 555	193	1.5	42%	63%
162092.97	160 620	1473	162 142	−49	2.5	47%	28%
163341.12	161 480	1861	163 528	−187	4.5	65%	64%
164068.22	162 966	1102	164 013	55	2.5	35%	39%
164424.89	163 308	1117	164 501	−76	3.5	37%	37%
165156.79	164 213	944	165 241	−84	1.5	57%	30%
166967.38	165 671	1296	166 898	69	0.5	35%	35%
167335.17	166 562	773	167 424	−89	1.5	59%	55%
168014.04	166 806	1208	167 944	70	2.5	30%	28%
168691.51	168 358	334	168 719	−27	4.5	83%	48%
171185.93	170 231	955	171 331	−145	0.5	29%	47%
172562.67	172 230	333	172 441	122	5.5	92%	92%
173725.21	172 645	1080	173 757	−32	2.5	53%	29%

(continued on next page)

Table 9 (*continued*)

E_{Exp}	E_{MCDHF}	ΔE_{MCDHF}	$E_{HFR+CPOL}$	$\Delta E_{HFR+CPOL}$	J	jj-purity	LS-purity
174120.53	173 909	212	174 213	−92	3.5	69%	54%
177193.54	175 537	1657	177 079	115	1.5	66%	50%
178243.69	178 004	240	178 254	−10	2.5	64%	64%
183498.82	182 737	762	183 542	−43	0.5	61%	61%
195575.77	194 022	1553	195 524	52	1.5	87%	87%

Table 10
Transition probabilities (gA) and oscillator strengths (log gf) for the strongest spectral lines in Re III.

λ_{Ritz} (Å)	Lower even level		Upper odd level		gA (10^8 s^{-1})			log gf	
	E (cm^{-1})	J	E (cm^{-1})	J	Previous	HFR+CPOL	MCDHF	HFR+CPOL	MCDHF
1099.606	23 471	4.5	114 413	3.5	70.00	17.50	42.30	−0.50	−0.12
1196.729	35 140	4.5	118 701	3.5	33.00	17.80	12.10	−0.42	−0.59
1202.161	19 719	2.5	102 902	3.5	50.30	23.00	10.10	−0.30	−0.66
1252.165	0	2.5	79 862	2.5	58.60	23.50	23.70	−0.26	−0.25
1256.895	17 140	2.5	96 701	1.5	6.30	23.50	15.20	−0.25	−0.44
1258.339	20 453	3.5	99 923	2.5	43.40	35.40	25.50	−0.08	−0.22
1263.731	18 346	4.5	97 476	4.5	153.00	52.60	38.30	0.10	−0.04
1265.254	32 833	3.5	111 868	2.5	20.10	15.80	8.98	1.00	−0.67
1284.330	0	2.5	77 862	1.5	60.00	26.00	25.30	−0.19	−0.20
1286.011	0	2.5	77 760	3.5	132.00	45.40	47.50	0.06	0.07
1287.690	17 140	2.5	94 798	2.5	41.30	15.80	23.30	−0.41	−0.24
1300.628	30 255	3.5	107 141	2.5	29.60	48.60	35.60	0.09	−0.04
1312.914	18 346	4.5	94 512	4.5	66.40	25.60	10.70	−0.18	−0.56
1323.994	0	2.5	75 529	2.5	51.30	18.40	17.60	−0.31	−0.34
1344.994	13 614	2.5	87 964	2.5	26.90	15.60	11.70	−0.37	−0.50
1347.310	18 346	4.5	92 568	3.5	31.30	15.20	4.92	−0.39	−0.87
1369.485	31 345	2.5	104 365	2.5	49.90	20.30	10.30	−0.24	−0.54
1374.094	32 068	4.5	104 844	3.5	52.80	16.00	24.30	−0.35	−0.16
1374.316	17 140	2.5	89 903	3.5	33.90	22.70	9.01	−0.19	−0.59
1376.675	18 346	4.5	90 984	5.5	40.40	14.30	11.70	−0.39	−0.48
1388.970	20 453	3.5	92 449	4.5	13.60	11.00	5.50	−0.50	−0.80
1407.832	13 614	2.5	84 646	3.5	34.30	11.90	14.20	−0.45	−0.37
1417.084	22 937	1.5	93 504	2.5	17.10	10.70	9.75	−0.49	−0.53
1432.909	16 890	3.5	86 679	4.5	44.70	19.50	13.60	−0.22	−0.38
1446.287	32 833	3.5	101 975	4.5	18.50	11.90	4.10	−0.43	−0.89
1478.636	18 346	4.5	85 975	5.5	22.00	9.82	8.55	−0.49	−0.55
1514.809	40 655	2.5	106 670	3.5	13.70	10.40	4.38	−0.45	−0.82
1528.906	30 255	3.5	95 662	4.5	31.80	12.10	11.00	−0.37	−0.41
1535.037	22 106	3.5	87 251	3.5	31.30	15.80	3.00	−0.26	−0.98
1560.313	15 772	1.5	79 862	2.5	16.80	11.50	19.70	−0.38	−0.14
1570.668	19 719	2.5	83 386	1.5	17.10	10.40	11.50	−0.41	−0.37
1573.234	27 421	4.5	90 984	5.5	33.20	13.30	18.90	−0.30	−0.15
1575.668	14 396	0.5	77 862	1.5	22.10	16.40	15.30	−0.21	−0.24
1584.109	34 349	3.5	97 476	4.5	15.40	10.90	4.60	−0.38	−0.76
1597.888	19 719	2.5	82 301	3.5	29.10	15.50	4.13	−0.23	−0.80
1598.995	22 106	3.5	84 646	3.5	14.00	9.96	9.63	−0.42	−0.43
1614.133	17 909	1.5	79 862	2.5	20.90	16.80	4.69	−0.18	−0.74
1615.693	35 140	4.5	97 033	5.5	26.00	11.40	12.20	−0.35	−0.32
1621.119	19 719	2.5	81 405	3.5	25.40	24.10	26.20	−0.02	0.01
1626.042	22 106	3.5	83 605	4.5	64.20	37.30	42.50	0.17	0.23
1630.993	34 349	3.5	95 662	4.5	14.20	8.33	7.57	−0.48	−0.52
1653.469	23 471	4.5	83 950	5.5	118.00	85.00	87.60	0.55	0.55
1661.829	38 752	3.5	98 927	4.5	14.90	10.10	5.84	−0.38	−0.62
1662.708	19 719	2.5	79 862	2.5	7.00	8.39	8.75	−0.46	−0.44
1670.809	22 106	3.5	81 957	4.5	19.00	20.80	7.35	−0.06	−0.51
1671.654	35 140	4.5	94 961	5.5	32.80	35.80	23.10	0.18	−0.01
1675.029	61 243	4.5	120 944	5.5	41.70	34.20	14.10	0.16	−0.23
1684.295	35 140	4.5	94 512	4.5	22.80	18.80	15.70	−0.10	−0.18
1702.022	43 750	3.5	102 504	3.5	12.80	9.57	20.40	−0.38	−0.05
1709.024	46 718	3.5	105 231	4.5	12.00	7.61	14.90	−0.48	−0.19
1729.514	43 750	3.5	101 570	3.5	14.20	9.96	2.36	−0.35	−0.97
1759.798	46 315	4.5	103 139	4.5	12.80	15.00	3.76	−0.16	−0.76
1765.482	47 910	2.5	104 552	3.5	8.30	7.02	5.93	−0.48	−0.56
1772.381	46 718	3.5	103 139	4.5	18.70	18.40	10.20	−0.06	−0.32
1774.295	41 116	3.5	97 476	4.5	12.10	8.28	5.89	−0.41	−0.56
1777.997	43 750	3.5	99 993	4.5	5.70	6.98	9.87	−0.48	−0.33
1790.691	35 140	4.5	90 984	5.5	18.80	10.70	12.60	−0.29	−0.22
1838.729	45 608	3.5	99 993	4.5	14.90	7.83	6.29	−0.40	−0.50
1842.009	23 471	4.5	77 760	3.5	39.80	29.90	33.10	0.18	0.23
1854.551	19 719	2.5	73 640	3.5	15.50	11.90	12.40	−0.21	−0.19
1857.490	51 007	2.5	104 844	3.5	13.40	7.77	6.01	−0.40	−0.51
1870.435	40 935	4.5	94 398	5.5	32.40	33.00	28.90	0.24	0.18
1871.859	22 106	3.5	75 529	2.5	27.70	20.50	14.20	0.03	−0.13
1918.520	19 719	2.5	71 842	1.5	11.80	9.52	5.37	−0.28	−0.53
1940.466	22 106	3.5	73 640	3.5	17.30	13.80	18.20	−0.11	0.01
1941.217	40 935	4.5	92 449	4.5	4.70	6.45	3.87	−0.44	−0.66
1941.307	19 719	2.5	71 231	2.5	20.00	14.50	13.00	−0.09	−0.13
1942.859	51 669	3.5	103 139	4.5	9.80	7.42	3.90	−0.38	−0.66
1967.131	35 140	4.5	85 975	5.5	18.40	13.10	14.00	−0.12	−0.09
1982.905	17 909	1.5	68 340	1.5	10.80	7.54	3.57	−0.35	−0.68
1987.557	14 396	0.5	64 709	0.5	8.00	5.95	5.71	−0.45	−0.47
1991.474	41 116	3.5	91 330	4.5	11.90	8.84	6.85	−0.28	−0.39
2041.479	40 935	4.5	89 903	3.5	6.30	10.50	5.77	−0.18	−0.44
2042.234	41 116	3.5	90 066	3.5	6.80	8.61	3.74	−0.27	−0.63

(*continued on next page*)

Table 10 (*continued*)

λ_{Ritz} (Å)	Lower even level		Upper odd level		gA (10^8 s^{-1})			log gf	
	E (cm^{-1})	J	E (cm^{-1})	J	Previous	HFR+CPOL	MCDHF	HFR+CPOL	MCDHF
2074.822	36 464	2.5	84 646	3.5	7.00	5.98	3.18	−0.41	−0.69
2135.719	51 007	2.5	97 815	3.5	7.10	5.32	4.64	−0.44	−0.50

Table 11
Transition probabilities (gA) and oscillator strengths (log gf) for the strongest spectral lines in Re IV.

λ_{Ritz} (Å)	Lower even level		Upper odd level		gA (10^8 s^{-1})			log gf	
	E (cm^{-1})	J	E (cm^{-1})	J	Previous	HFR+CPOL	MCDHF	HFR+CPOL	MCDHF
881.607	10 121	4	123 550	3	201.70	48.70	85.50	−0.24	0.00
885.476	16 946	4	129 880	3	101.00	49.70	46.10	−0.23	−0.27
886.035	36 034	4	148 897	3	102.00	27.00	35.80	−0.50	−0.37
900.273	30 052	5	141 129	4	145.00	55.20	33.20	−0.17	−0.39
908.260	36 034	4	146 135	3	95.30	37.10	17.70	−0.34	−0.66
910.157	20 930	5	130 801	5	235.00	76.10	125.00	−0.02	0.19
911.267	32 396	6	142 133	6	350.00	124.00	149.00	0.19	0.27
914.952	10 121	4	119 417	5	83.40	29.00	33.10	−0.44	−0.38
916.449	30 052	5	139 169	4	336.00	123.00	131.00	0.19	0.22
918.874	24 324	4	133 153	3	190.00	66.50	57.20	−0.08	−0.14
929.335	36 034	4	143 638	3	132.00	52.20	111.00	−0.17	0.16
930.725	26 476	3	133 919	3	132.00	31.20	36.80	−0.39	−0.32
933.977	36 034	4	143 103	4	265.00	88.60	94.70	0.06	0.09
934.875	46 525	3	153 491	3	69.80	24.50	23.50	−0.50	−0.51
935.120	20 930	5	127 868	4	190.00	70.70	63.20	−0.04	−0.08
941.111	32 396	6	138 653	5	311.00	99.30	92.10	0.12	0.09
941.793	45 502	2	151 683	1	99.50	44.10	28.40	−0.23	−0.42
943.203	22 896	6	128 918	5	611.00	244.00	180.00	0.51	0.38
947.752	35 597	2	141 110	2	64.90	26.90	29.00	−0.44	−0.41
947.856	24 324	4	129 825	4	200.00	68.90	50.70	−0.03	−0.17
954.203	24 352	2	129 152	1	55.60	23.80	19.70	−0.49	−0.57
958.934	49 209	4	153 491	3	141.00	70.10	59.00	−0.02	−0.09
959.172	10 121	4	114 378	4	107.00	32.00	47.60	−0.36	−0.18
960.651	30 052	5	134 148	5	207.00	79.20	53.30	0.04	−0.13
961.646	19 851	2	123 839	1	69.10	27.70	20.30	−0.41	−0.55
962.275	20 930	5	124 850	5	173.00	63.30	45.60	−0.06	−0.20
963.057	26 044	4	129 880	3	115.00	37.30	30.70	−0.28	−0.37
963.568	26 044	4	129 825	4	62.30	24.00	15.10	−0.48	−0.68
965.452	8350	3	111 929	4	117.00	40.50	53.50	−0.24	−0.13
965.773	24 324	4	127 868	4	101.00	37.40	28.70	−0.28	−0.40
966.290	32 396	6	135 884	6	124.00	43.10	30.80	−0.22	−0.37
967.702	16 946	4	120 284	4	292.00	98.60	124.00	0.14	0.24
970.650	16 946	4	119 970	3	183.00	60.00	70.10	−0.07	0.00
978.874	24 352	2	126 510	2	100.00	37.20	40.00	−0.27	−0.24
979.319	26 476	3	128 587	3	90.00	30.60	31.20	−0.36	−0.35
982.246	10 121	4	111 929	4	162.00	58.20	55.20	−0.07	−0.10
982.783	32 396	6	134 148	5	201.00	70.30	91.40	0.01	0.12
982.962	22 896	6	124 629	6	178.00	65.80	57.80	−0.02	−0.08
983.025	19 851	2	121 577	2	81.70	26.80	25.10	−0.41	−0.44
989.325	19 340	1	120 419	2	67.50	26.40	22.00	−0.41	−0.49
996.875	29 201	2	129 514	2	19.10	32.00	34.10	−0.32	−0.29
1003.132	49 209	4	148 897	3	84.00	23.20	33.50	−0.46	−0.30
1003.444	3084	1	102 741	2	65.60	25.40	26.60	−0.42	−0.40
1012.085	26 044	4	124 850	5	74.70	26.20	25.80	−0.40	−0.40
1014.783	10 121	4	108 664	5	59.50	21.30	21.20	−0.49	−0.49
1016.492	44 726	4	143 103	4	82.50	35.00	6.98	−0.27	−0.97
1030.606	45 502	2	142 533	3	44.90	21.50	13.10	−0.46	−0.68
1034.188	26 476	3	123 170	4	41.10	20.10	21.90	−0.50	−0.45
1039.038	19 851	2	116 093	3	48.30	20.00	19.70	−0.49	−0.50
1057.039	46 525	3	141 129	4	88.10	31.70	23.50	−0.28	−0.41
1314.226	44 329	3	120 419	2	22.80	16.60	14.20	−0.37	−0.44
1337.290	58 758	3	133 536	2	14.20	13.20	9.38	−0.45	−0.60
1345.335	67 802	6	142 133	6	24.00	16.10	20.10	−0.36	−0.26
1366.594	75 722	4	148 897	3	19.50	11.50	7.50	−0.49	−0.68
1373.286	44 329	3	117 147	4	51.00	33.00	26.20	−0.03	−0.13
1374.651	65 907	4	138 653	5	23.20	15.90	21.50	−0.35	−0.22
1375.907	52 385	2	125 064	3	26.50	20.10	29.30	−0.24	−0.08
1385.685	39 118	1	111 284	1	31.70	19.80	25.20	−0.24	−0.14
1385.996	69 983	5	142 133	6	36.20	22.00	25.10	−0.20	−0.14
1387.536	41 100	2	113 170	2	24.60	17.00	26.70	−0.31	−0.11
1389.399	41 100	2	113 073	3	20.80	15.30	20.80	−0.35	−0.22
1390.941	57 931	3	129 825	4	23.10	18.40	9.77	−0.27	−0.55
1393.439	44 329	3	116 093	3	37.80	24.60	34.40	−0.15	0.00
1395.015	59 117	4	130 801	5	42.60	29.60	35.70	−0.06	0.02
1405.172	52 385	2	123 550	3	31.00	16.90	13.10	−0.30	−0.41
1405.555	69 983	5	141 129	4	27.60	23.30	8.74	−0.16	−0.59
1412.452	63 120	3	133 919	3	16.50	24.00	5.75	−0.14	−0.76
1414.264	59 117	4	129 825	4	17.30	13.80	5.75	−0.38	−0.76
1414.349	75 421	3	146 125	4	67.80	46.90	54.50	0.15	0.21
1423.519	64 843	2	135 092	3	19.20	15.20	5.89	−0.34	−0.75
1427.568	44 329	3	114 378	4	26.60	22.50	27.60	−0.16	−0.07
1428.751	67 802	6	137 793	7	251.10	163.00	162.00	0.70	0.69
1429.868	57 931	3	127 868	4	22.80	14.10	6.23	−0.36	−0.72
1434.851	76 798	2	146 492	2	15.70	11.60	10.90	−0.45	−0.47

(continued on next page)

Table 11 (*continued*)

λ_{Ritz} (Å)	Lower even level		Upper odd level		gA (10^8 s^{-1})			log gf	
	E (cm^{-1})	J	E (cm^{-1})	J	Previous	HFR+CPOL	MCDHF	HFR+CPOL	MCDHF
1440.022	47 703	4	117 147	4	21.50	16.00	12.00	−0.30	−0.43
1444.179	61 557	5	130 801	5	24.40	20.90	23.50	−0.18	−0.13
1445.241	52 385	2	121 577	2	15.30	10.30	9.38	−0.49	−0.53
1460.740	70 710	3	139 169	4	105.50	71.90	73.40	0.36	0.37
1463.932	64 843	2	133 153	3	49.50	30.00	38.00	−0.02	0.09
1465.916	75 421	3	143 638	3	21.30	18.60	13.50	−0.22	−0.36
1468.813	67 802	6	135 884	6	45.50	37.50	36.20	0.08	0.07
1470.776	70 811	2	138 803	1	16.60	13.20	10.70	−0.37	−0.46
1477.499	75 421	3	143 103	4	20.70	12.60	6.65	−0.38	−0.66
1480.855	74 605	5	142 133	6	140.30	95.40	84.10	0.50	0.44
1484.092	75 722	4	143 103	4	11.30	14.70	29.60	−0.31	−0.01
1484.550	61 557	5	128 918	5	32.90	21.30	21.80	−0.15	−0.14
1488.205	70 811	2	138 006	2	14.10	10.60	8.62	−0.45	−0.54
1495.529	63 935	4	130 801	5	51.20	35.40	30.50	0.07	0.01
1500.666	76 466	4	143 103	4	42.60	28.50	7.71	−0.02	−0.58
1504.168	70 811	2	137 293	3	24.10	14.90	10.90	−0.30	−0.43
1507.261	67 802	6	134 148	5	17.70	13.80	17.60	−0.33	−0.22
1516.364	59 117	4	125 064	3	13.40	10.60	7.59	−0.44	−0.58
1520.725	75 318	2	141 076	3	17.90	15.30	14.20	−0.28	−0.31
1529.615	83 521	3	148 897	3	44.20	35.90	32.10	0.10	0.05
1547.586	83 521	3	148 138	4	54.80	39.60	37.00	0.15	0.12
1551.172	55 503	2	119 970	3	23.10	13.70	11.50	−0.31	−0.38
1585.487	61 557	5	124 629	6	23.70	15.30	23.20	−0.24	−0.06
1600.313	57 931	3	120 419	2	10.30	9.49	14.70	−0.44	−0.25
1601.277	55 503	2	117 953	2	11.80	10.10	10.40	−0.41	−0.40
1630.670	44 329	3	105 653	4	29.20	20.50	25.70	−0.09	0.01
1636.249	67 802	6	128 918	5	11.80	9.75	8.97	−0.41	−0.44
1640.387	47 703	4	108 664	5	15.30	10.90	14.00	−0.36	−0.25
1653.036	76 798	2	137 293	3	18.40	14.00	17.30	−0.24	−0.15
1664.324	41 100	2	101 184	3	26.20	17.50	23.80	−0.14	0.00
1665.280	63 120	3	123 170	4	31.60	21.70	26.20	−0.04	0.04
1688.901	57 931	3	117 141	3	12.30	10.10	12.90	−0.36	−0.26
1700.457	58 758	3	117 566	2	19.40	15.10	8.94	−0.18	−0.41
1711.576	75 722	4	134 148	5	26.80	25.00	37.40	0.04	0.22
1711.966	44 329	3	102 741	2	17.70	13.90	14.00	−0.21	−0.21
1725.630	47 703	4	105 653	4	28.80	20.70	12.70	−0.03	−0.25
1727.794	70 710	3	128 587	3	13.20	11.80	12.30	−0.28	−0.26
1728.801	50 821	5	108 664	5	36.10	26.50	29.60	0.07	0.12
1737.002	55 503	2	113 073	3	11.60	8.31	8.53	−0.42	−0.41
1741.468	59 117	4	116 540	5	19.90	14.00	10.70	−0.20	−0.31
1752.917	67 802	6	124 850	5	19.70	17.60	8.36	−0.09	−0.41
1758.843	44 329	3	101 184	3	20.60	14.30	14.90	−0.18	−0.16
1759.727	67 802	6	124 629	6	50.40	37.40	40.40	0.24	0.27
1764.095	76 466	4	133 153	3	5.00	7.71	5.30	−0.44	−0.61
1771.587	57 931	3	114 378	4	19.30	13.90	6.46	−0.18	−0.52
1779.735	52 385	2	108 573	2	10.00	8.16	7.47	−0.41	−0.45
1792.107	70 710	3	126 510	2	16.80	12.80	15.70	−0.21	−0.12
1807.121	64 843	2	120 180	1	8.20	6.44	5.90	−0.50	−0.54
1822.586	69 983	5	124 850	5	13.10	11.30	8.27	−0.25	−0.39
1850.937	63 120	3	117 147	4	10.50	7.38	10.10	−0.42	−0.29
2017.610	59 117	4	108 664	5	12.70	8.89	6.53	−0.27	−0.40

Table 12
Transition probabilities (gA) and oscillator strengths (log gf) for the strongest spectral lines in Re V.

λ_{Ritz} (Å)	Lower even level		Upper odd level		gA (10^8 s^{-1})			log gf	
	E (cm^{-1})	J	E (cm^{-1})	J	Previous	HFR+CPOL	MCDHF	HFR+CPOL	MCDHF
655.690	11 914	4.5	164 425	3.5	67.00	30.50	32.20	−0.71	−0.68
658.881	19 967	4.5	171 739	3.5	30.20	15.90	23.70	−0.99	−0.81
660.383	11 914	4.5	163 341	4.5	63.10	29.40	30.70	−0.72	−0.70
674.858	8973	3.5	157 152	2.5	42.00	18.90	22.70	−0.89	−0.81
675.746	23 201	1.5	171 186	0.5	56.10	25.70	24.40	−0.76	−0.78
682.459	11 914	4.5	158 443	3.5	43.30	19.40	16.10	−0.87	−0.95
686.269	11 914	4.5	157 629	5.5	89.30	33.50	32.50	−0.63	−0.64
687.352	27 077	5.5	172 563	5.5	412.00	184.00	176.00	0.12	0.10
689.720	28 739	2.5	173 725	2.5	58.10	26.40	28.20	−0.73	−0.70
691.674	11 914	4.5	156 491	4.5	84.00	27.00	25.80	−0.71	−0.73
692.391	32 766	1.5	177 194	1.5	105.00	29.80	18.50	−0.67	−0.88
692.896	8973	3.5	153 295	3.5	70.00	28.00	34.00	−0.70	−0.61
694.050	34 162	2.5	178 244	2.5	137.00	60.40	66.00	−0.36	−0.32
695.628	30 366	4.5	174 121	3.5	170.00	91.80	62.40	−0.18	−0.34
695.972	11 914	4.5	155 598	3.5	110.00	45.70	81.70	−0.48	−0.23
696.850	20 922	2.5	164 425	3.5	77.60	37.40	32.40	−0.56	−0.63
698.587	20 922	2.5	164 068	2.5	162.00	72.30	61.80	−0.28	−0.34
698.770	52 467	2.5	195 576	1.5	27.10	91.20	79.60	−0.18	−0.23
699.146	34 162	2.5	177 194	1.5	23.60	18.40	14.50	−0.87	−0.97
706.142	27 077	5.5	168 692	4.5	157.00	61.60	99.20	−0.34	−0.13
707.065	12 403	1.5	153 832	2.5	30.30	15.00	14.90	−0.95	−0.95
707.345	30 366	4.5	171 739	3.5	708.00	284.00	245.00	0.33	0.26
709.106	0	1.5	141 023	0.5	139.00	61.50	69.40	−0.33	−0.28
711.956	4853	2.5	145 311	1.5	163.00	53.80	84.80	−0.39	−0.19
714.472	11 914	4.5	151 877	4.5	285.00	126.00	139.00	−0.02	0.03
716.870	34 625	3.5	174 121	3.5	184.00	73.40	84.00	−0.25	−0.19
718.908	34 625	3.5	173 725	2.5	98.90	43.60	43.60	−0.47	−0.47
719.039	4853	2.5	143 928	1.5	109.00	48.10	24.70	−0.43	−0.72
719.986	23 201	1.5	162 093	2.5	31.90	16.00	46.20	−0.91	−0.44
721.384	4853	2.5	143 475	2.5	184.00	69.30	72.80	−0.27	−0.25
722.146	19 967	4.5	158 443	3.5	770.00	332.00	309.00	0.41	0.38
722.442	32 766	1.5	171 186	0.5	40.90	30.50	23.10	−0.62	−0.74
722.930	30 366	4.5	168 692	4.5	422.00	187.00	161.00	0.17	0.10
723.907	19 013	3.5	157 152	2.5	493.00	208.00	185.00	0.21	0.16
727.163	20 922	2.5	158 443	3.5	43.30	16.70	17.30	−0.88	−0.86
730.397	23 669	0.5	160 581	0.5	89.40	39.00	36.00	−0.51	−0.54
732.473	19 967	4.5	156 491	4.5	413.00	175.00	181.00	0.15	0.16
733.041	28 739	2.5	165 157	1.5	218.00	100.00	90.50	−0.09	−0.14
733.868	27 077	5.5	163 341	4.5	1160.00	487.00	441.00	0.59	0.55
734.304	11 914	4.5	148 097	3.5	527.00	223.00	183.00	0.26	0.17
736.696	12 403	1.5	148 144	1.5	112.00	34.00	35.80	−0.56	−0.54
740.367	20 922	2.5	155 990	1.5	44.90	19.20	15.20	−0.80	−0.90
742.255	14 325	0.5	149 050	0.5	68.40	29.00	25.60	−0.62	−0.67
744.703	19 013	3.5	153 295	3.5	382.00	165.00	131.00	0.14	0.04
744.837	8973	3.5	143 231	4.5	102.00	40.20	39.70	−0.48	−0.48
745.151	32 766	1.5	166 967	0.5	140.00	49.80	57.20	−0.38	−0.32
745.900	34 625	3.5	168 692	4.5	67.40	22.40	16.70	−0.73	−0.86
745.938	30 366	4.5	164 425	3.5	147.00	56.90	87.30	−0.32	−0.14
747.281	14 325	0.5	148 144	1.5	59.80	17.90	15.90	−0.82	−0.87
749.688	34 625	3.5	168 014	2.5	361.00	137.00	121.00	0.06	0.01
749.883	28 739	2.5	162 093	2.5	156.00	56.50	46.20	−0.32	−0.41
751.817	23 201	1.5	156 213	1.5	286.00	85.50	42.30	−0.14	−0.45
752.018	30 366	4.5	163 341	4.5	103.00	39.10	47.00	−0.48	−0.40
752.398	12 403	1.5	145 311	1.5	111.00	45.70	47.80	−0.41	−0.39
755.342	32 766	1.5	165 157	1.5	58.10	24.50	23.90	−0.68	−0.69
755.736	23 669	0.5	155 990	1.5	128.00	43.60	25.50	−0.43	−0.66
760.763	52 052	1.5	183 499	0.5	186.00	76.10	69.70	−0.18	−0.22
763.045	4853	2.5	135 907	3.5	88.60	34.80	33.10	−0.52	−0.54
763.388	34 162	2.5	165 157	1.5	30.10	12.90	14.60	−0.95	−0.89
765.515	23 201	1.5	153 832	2.5	83.40	32.80	26.30	−0.54	−0.64
770.418	34 625	3.5	164 425	3.5	183.00	83.60	67.70	−0.13	−0.22
771.592	14 325	0.5	143 928	1.5	62.10	29.10	35.60	−0.59	−0.50
772.715	27 077	5.5	156 491	4.5	128.00	58.50	26.60	−0.28	−0.62
773.236	32 766	1.5	162 093	2.5	84.40	36.80	33.00	−0.48	−0.53
778.734	28 739	2.5	157 152	2.5	41.20	14.80	18.00	−0.87	−0.79
780.455	19 967	4.5	148 097	3.5	73.80	34.50	53.70	−0.50	−0.31
785.846	28 739	2.5	155 990	1.5	29.60	21.10	25.00	−0.71	−0.63
788.277	28 739	2.5	155 598	3.5	83.80	39.70	44.40	−0.43	−0.38
788.472	20 922	2.5	147 750	2.5	33.60	12.60	12.40	−0.93	−0.94
792.176	0	1.5	126 235	2.5	54.90	22.70	21.10	−0.67	−0.70
792.445	52 052	1.5	178 244	2.5	77.30	28.20	31.60	−0.57	−0.53
795.060	52 467	2.5	178 244	2.5	148.00	63.30	44.70	−0.22	−0.37
799.094	52 052	1.5	177 194	1.5	51.50	20.00	17.40	−0.72	−0.78
799.131	12 403	1.5	137 539	2.5	95.40	39.40	37.60	−0.42	−0.44

(continued on next page)

Table 12 (*continued*)

λ_{Ritz} (Å)	Lower even level		Upper odd level		gA (10^8 s^{-1})			log gf	
	E (cm^{-1})	J	E (cm^{-1})	J	Previous	HFR+CPOL	MCDHF	HFR+CPOL	MCDHF
801.754	52 467	2.5	177 194	1.5	140.00	53.60	49.30	−0.29	−0.32
807.880	20 922	2.5	144 703	3.5	104.00	41.00	36.80	−0.40	−0.44
821.873	52 052	1.5	173 725	2.5	59.90	23.90	15.30	−0.62	−0.81
822.007	52 467	2.5	174 121	3.5	142.00	54.10	46.80	−0.26	−0.32
823.480	34 162	2.5	155 598	3.5	41.20	13.80	13.60	−0.86	−0.86
825.996	32 766	1.5	153 832	2.5	42.10	20.00	21.40	−0.69	−0.66
839.399	34 162	2.5	153 295	3.5	18.10	19.00	10.30	−0.70	−0.96
860.928	27 077	5.5	143 231	4.5	20.90	11.60	13.00	−0.89	−0.84
1108.599	71 889	3.5	162 093	2.5	20.90	16.00	17.00	−0.53	−0.50
1110.816	66 189	2.5	156 213	1.5	16.60	20.30	24.10	−0.43	−0.35
1140.982	66 189	2.5	153 832	2.5	18.20	14.00	17.70	−0.56	−0.46
1142.030	86 162	3.5	173 725	2.5	27.60	19.90	22.20	−0.41	−0.36
1147.876	77 307	4.5	164 425	3.5	27.10	21.10	19.50	−0.38	−0.41
1150.111	78 209	0.5	165 157	1.5	13.10	7.66	11.00	−0.82	−0.66
1155.351	71 889	3.5	158 443	3.5	31.70	27.20	21.00	−0.27	−0.38
1157.002	77 995	2.5	164 425	3.5	16.90	12.00	16.80	−0.62	−0.47
1161.796	77 995	2.5	164 068	2.5	17.60	13.50	15.30	−0.56	−0.51
1168.995	63 506	1.5	149 050	0.5	33.70	25.90	25.40	−0.28	−0.28
1172.839	71 889	3.5	157 152	2.5	9.60	8.15	9.21	−0.77	−0.72
1211.538	78 209	0.5	160 748	1.5	49.70	36.40	42.10	−0.09	−0.03
1215.035	82 123	2.5	164 425	3.5	83.80	54.20	68.30	0.08	0.18
1217.610	91 992	2.5	174 121	3.5	19.80	8.69	11.60	−0.72	−0.59
1220.323	82 123	2.5	164 068	2.5	19.60	15.10	13.60	−0.47	−0.52
1221.714	86 162	3.5	168 014	2.5	24.40	17.20	18.20	−0.41	−0.39
1222.425	63 506	1.5	145 311	1.5	57.90	42.70	49.70	−0.02	0.05
1226.076	66 189	2.5	147 750	2.5	33.00	25.30	24.50	−0.24	−0.26
1228.417	71 889	3.5	153 295	3.5	47.20	31.60	40.60	−0.15	−0.04
1232.508	77 307	4.5	158 443	3.5	24.90	19.10	21.90	−0.36	−0.30
1243.582	93 708	3.5	174 121	3.5	57.70	48.20	53.40	0.05	0.09
1244.993	77 307	4.5	157 629	5.5	260.00	181.00	202.00	0.63	0.67
1250.465	82 123	2.5	162 093	2.5	0.00	12.00	16.70	−0.55	−0.41
1250.483	63 506	1.5	143 475	2.5	0.00	24.70	34.00	−0.24	−0.10
1257.825	81 246	1.5	160 748	1.5	16.60	11.70	13.90	−0.56	−0.48
1259.206	85 742	1.5	165 157	1.5	48.40	34.40	41.10	−0.09	−0.01
1260.484	81 246	1.5	160 581	0.5	22.20	16.00	18.70	−0.42	−0.35
1263.302	77 995	2.5	157 152	2.5	17.60	13.30	11.00	−0.50	−0.58
1263.865	66 189	2.5	145 311	1.5	7.90	5.16	8.77	−0.91	−0.68
1267.305	99 336	1.5	178 244	2.5	15.20	9.09	7.40	−0.66	−0.75
1268.082	92 327	0.5	171 186	0.5	12.60	6.51	10.30	−0.81	−0.60
1273.656	66 189	2.5	144 703	3.5	19.90	11.90	15.40	−0.54	−0.43
1277.742	86 162	3.5	164 425	3.5	25.30	20.10	17.40	−0.31	−0.37
1278.479	77 995	2.5	156 213	1.5	20.30	22.00	25.10	−0.27	−0.21
1281.533	93 708	3.5	171 739	3.5	24.60	13.30	15.80	−0.49	−0.41
1284.398	99 336	1.5	177 194	1.5	64.10	40.80	51.20	0.01	0.10
1288.608	77 995	2.5	155 598	3.5	54.20	32.20	20.10	−0.10	−0.30
1295.685	86 162	3.5	163 341	4.5	103.00	62.60	64.80	0.20	0.21
1304.001	92 004	4.5	168 692	4.5	68.10	57.50	67.10	0.17	0.23
1310.270	82 123	2.5	158 443	3.5	51.60	36.20	19.20	−0.03	−0.31
1312.196	71 889	3.5	148 097	3.5	11.40	10.30	13.40	−0.58	−0.46
1315.416	91 992	2.5	168 014	2.5	28.80	19.70	23.90	−0.29	−0.21
1318.603	77 995	2.5	153 832	2.5	18.20	12.50	13.60	−0.49	−0.45
1328.021	77 995	2.5	153 295	3.5	25.40	21.20	39.50	−0.25	0.02
1333.182	92 327	0.5	167 335	1.5	46.90	29.40	36.20	−0.11	−0.02
1333.621	93 708	3.5	168 692	4.5	88.10	59.80	70.20	0.20	0.27
1333.930	81 246	1.5	156 213	1.5	6.20	3.92	5.19	−0.98	−0.86
1336.201	85 742	1.5	160 581	0.5	6.90	6.22	9.02	−0.78	−0.62
1344.282	99 336	1.5	173 725	2.5	27.40	19.30	26.80	−0.28	−0.14
1361.007	82 123	2.5	155 598	3.5	7.90	9.37	23.30	−0.58	−0.19
1394.511	82 123	2.5	153 832	2.5	18.30	13.00	17.50	−0.42	−0.29
1396.913	71 889	3.5	143 475	2.5	5.70	3.72	4.51	−0.96	−0.88
1401.544	66 189	2.5	137 539	2.5	8.30	6.32	7.62	−0.73	−0.65
1401.709	71 889	3.5	143 231	4.5	26.90	20.20	28.80	−0.22	−0.07
1401.804	92 004	4.5	163 341	4.5	11.90	7.22	10.80	−0.67	−0.50
1412.635	77 307	4.5	148 097	3.5	13.80	9.02	10.90	−0.57	−0.49
1425.530	77 995	2.5	148 144	1.5	9.50	5.86	10.80	−0.74	−0.48
1434.347	66 189	2.5	135 907	3.5	39.10	29.00	35.50	−0.05	0.04
1436.091	93 708	3.5	163 341	4.5	24.00	13.00	20.00	−0.40	−0.21
1456.071	99 336	1.5	168 014	2.5	9.80	4.16	7.04	−0.88	−0.65
1476.447	63 506	1.5	131 237	1.5	13.50	9.59	12.30	−0.50	−0.39
1483.784	77 307	4.5	144 703	3.5	51.20	38.30	48.00	0.10	0.20
1485.522	77 995	2.5	145 311	1.5	4.10	3.60	6.10	−0.92	−0.69
1489.585	86 162	3.5	153 295	3.5	16.70	14.50	15.00	−0.32	−0.30
1494.816	81 246	1.5	148 144	1.5	16.20	13.60	17.10	−0.34	−0.24
1514.664	82 123	2.5	148 144	1.5	6.70	3.94	4.39	−0.86	−0.82

(*continued on next page*)

Table 12 (*continued*)

λ_{Ritz} (Å)	Lower even level		Upper odd level		gA (10^8 s^{-1})			log gf	
	E (cm^{-1})	J	E (cm^{-1})	J	Previous	HFR+CPOL	MCDHF	HFR+CPOL	MCDHF
1516.920	77 307	4.5	143 231	4.5	56.80	41.30	50.00	0.16	0.24
1523.241	71 889	3.5	137 539	2.5	35.30	27.00	32.00	−0.03	0.05
1523.764	82 123	2.5	147 750	2.5	18.50	13.20	16.30	−0.34	−0.25
1534.688	91 992	2.5	157 152	2.5	18.20	12.90	15.20	−0.34	−0.27
1537.328	66 189	2.5	131 237	1.5	24.70	18.10	21.90	−0.19	−0.11
1550.720	92 004	4.5	156 491	4.5	38.70	28.60	37.90	0.02	0.14
1562.068	71 889	3.5	135 907	3.5	33.00	23.50	27.80	−0.07	0.01
1562.556	91 992	2.5	155 990	1.5	17.50	19.80	25.80	−0.14	−0.02
1569.853	81 246	1.5	144 946	0.5	7.40	5.52	6.10	−0.70	−0.65
1592.004	78 209	0.5	141 023	0.5	13.10	10.20	11.80	−0.41	−0.35
1594.180	63 506	1.5	126 235	2.5	34.30	25.10	29.50	−0.02	0.05
1606.957	81 246	1.5	143 475	2.5	4.90	3.87	2.89	−0.83	−0.95
1615.769	93 708	3.5	155 598	3.5	16.90	13.50	15.20	−0.28	−0.22
1617.997	82 123	2.5	143 928	1.5	17.60	14.60	18.60	−0.24	−0.14
1679.432	77 995	2.5	137 539	2.5	11.10	8.19	10.10	−0.46	−0.37
1689.056	85 742	1.5	144 946	0.5	3.20	2.64	2.89	−0.95	−0.91
1726.753	77 995	2.5	135 907	3.5	11.30	7.58	6.97	−0.47	−0.51
1732.086	85 742	1.5	143 475	2.5	6.40	5.27	4.92	−0.63	−0.66
1834.984	99 336	1.5	153 832	2.5	6.30	5.38	5.20	−0.57	−0.58